Journal of Paleontology, 90(5), 2016, p. 815–853

0022-3360/16/0088-0906
doi: 10.1017/jpa.2016.57

Journal of PALEONTOLOGY
A JOURNAL OF THE PALEONTOLOGICAL SOCIETY

Systematics of organic-walled microfossils from the ca. 780–740 Ma Chuar Group, Grand Canyon, Arizona

Susannah M. Porter[1] and Leigh Anne Riedman[1,2]

[1]Department of Earth Science, University of California at Santa Barbara, Santa Barbara, California 93106, USA ⟨porter@geol.ucsb.edu⟩, ⟨lriedman@umail.ucsb.edu⟩
[2]New address: Department of Earth and Planetary Sciences, Harvard University, Cambridge, Massachusetts 02138, USA ⟨lriedman@fas.harvard.edu⟩

Abstract.—The ca. 780–740 Ma Chuar Group, Grand Canyon, Arizona, provides an exceptional record of life during the diversification of crown-group eukaryotes, just prior to the first Cryogenian glaciation. We document in detail the assemblage of organic-walled microfossils preserved in fine-grained siliciclastics throughout the unit. In contrast with earlier studies, we primarily used SEM to document fossil morphologies, augmented by transmitted light microscopy, FIB-SEM, and TEM. This resulted in the discovery of new species and the recognition of broad-ranging, intraspecific biological and taphonomic variation in other species. Twenty-two species and five unnamed morphotypes are described, including three new species: *Kaibabia gemmulella*, *Microlepidopalla mira*, and *Volleyballia dehlerae*; two new combinations: *Galerosphaera walcottii* and *Lanulatisphaera laufeldii*; and 17 previously described forms. The possible colonial green alga *Palaeastrum dyptocranum* Butterfield in Butterfield, Knoll, and Swett, 1994 and the index fossil *Cerebrosphaera globosa* (Ogurtsova and Sergeev, 1989) Sergeev and Schopf, 2010 (= *C. buickii* Butterfield, 1994) are described for the first time from Chuar rocks. *Lanulatisphaera laufeldii*, a locally abundant and globally widespread species characterized by submicrometer filamentous processes that form a reticulate network, may be a useful marker for the time interval just before the appearance of vase-shaped microfossils (VSMs) ca. 740 Ma.

Organic-walled microfossil assemblages decline in diversity upsection, coincident with the appearance of VSMs and intermittent euxinia within the basin. Whether this pattern is due to preservational bias related to greater water depth or the higher TOC of upper Chuar rocks or instead reflects biotic turnover related to the spread of euxinic water masses in the basin is unknown.

Introduction

The ca. 780–740 Ma Chuar Group provides an exceptional glimpse of life during a time when eukaryotic organisms were becoming an increasingly important part of the biosphere. Although stromatolites and prokaryotic body fossils occur throughout the succession (Ford and Breed, 1973a; Schopf et al., 1973), the Chuar Group is best known for its eukaryotic fossils, including *Chuaria circularis*, the first Precambrian body fossil to be described (Walcott, 1899; Ford and Breed, 1973b); vase-shaped microfossils, interpreted as the remains of amoebozoan and possibly rhizarian testate amoebae (Bloeser et al., 1977; Bloeser, 1985; Porter and Knoll, 2000; Porter et al., 2003); and eukaryotic steranes, most notably gammacerane—thought to be derived from ciliates (Summons et al., 1988)—and cryostane, a newly discovered biomarker possibly derived from toxin-producing sponges or protists (Brocks et al., 2016).

Organic-walled microfossils also occur throughout the Chuar Group, in shales, mudstones, and siltstones. These were first reported by Downie (in an appendix to Ford and Breed, 1969) and subsequently described by Vidal and Ford (1985), who documented the presence of about a dozen species. Here we describe 27 species and unnamed morphotypes of acritarchs, colonial forms, and filaments from 38 samples spanning most of the Chuar succession. Descriptions are based primarily on scanning electron microscopy (SEM), supported by transmitted light microscopy (TLM), focused ion beam (FIB)-SEM, and transmission electron microscopy (TEM). This approach has resulted in a host of new information about these fossils, including evidence for wide-ranging biological and taphonomic variation, submicrometer details of fossil morphology, and the recognition of new species. In addition, this approach has provided evidence that systematic studies of these fossils based solely on TLM can be misleading: some forms that might be assigned to different genera or species under TLM, for example, have been found under SEM to be conspecific. These results bode well for the future of Proterozoic paleontology and biostratigraphy as they suggest that there is much left to be discovered in Proterozoic shales and that the existing thicket of taxonomic names may be pruned.

Geologic setting

The Chuar Group is exposed in several valleys within a 150 km^2 area in the eastern Grand Canyon, Arizona (Fig. 1). The exposure is bounded to the east by the Butte Fault and on all other sides by the Great Unconformity with the overlying Cambrian Tapeats Sandstone. Chuar sediments were deposited

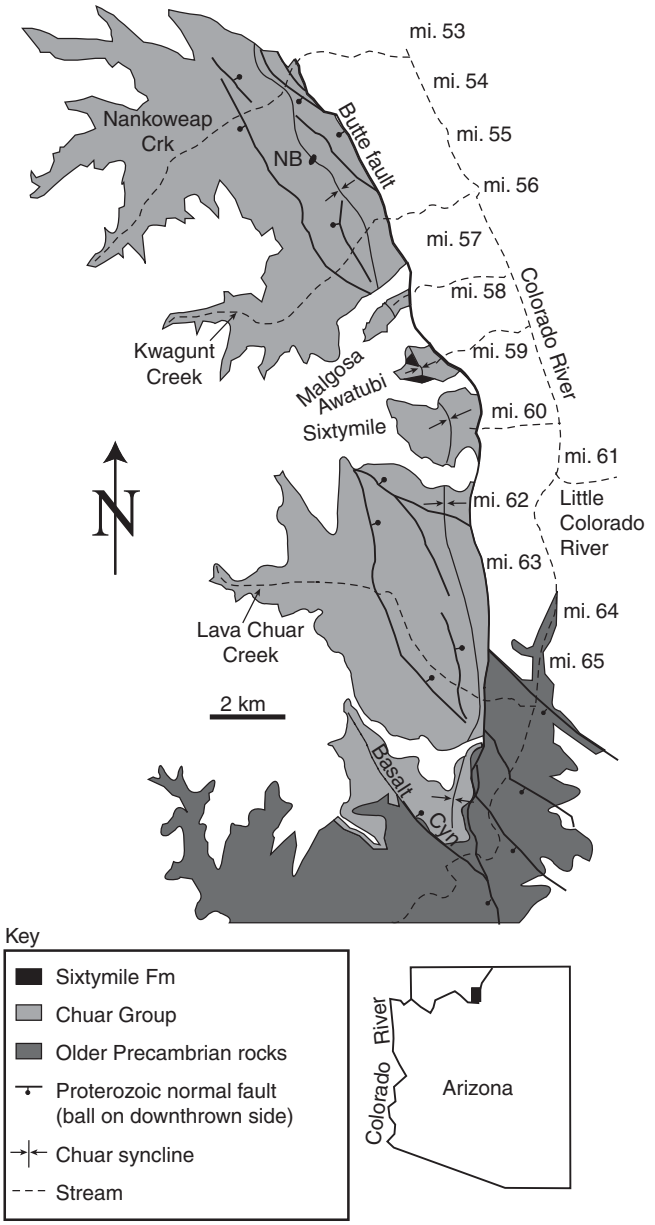

Figure 1. Geologic map showing the exposure of the Chuar Group, Grand Canyon, Arizona (modified from Timmons et al., 2001). River miles measured downstream from Lee's Ferry, Arizona. NB = Nankoweap Butte.

in an intracratonic basin of unknown original extent that formed as a result of east–west extension possibly related to the initial breakup of Rodinia and incipient formation of the Cordilleran rift margin (Dehler et al., 2001b; Timmons et al., 2001). Stratigraphic thinning toward the Butte Fault zone in the east, thickness changes across intraformational faults, and thickening of strata toward the hingeline of the Chuar syncline all suggest that extension occurred contemporaneously with Chuar deposition, accommodated by normal slip across the Butte Fault and associated north–south trending structures (Fig. 1, Dehler et al., 2001b; Timmons et al., 2001; Dehler et al., 2012).

The Chuar Group consists of ~1,600 meters of relatively conformable, predominantly mudrock facies (>85%) with subordinate sandstone and dolomite beds (Dehler et al., 2001b). Together with the underlying Nankoweap Formation and Unkar Group and the overlying Sixtymile Formation, it forms the ~4,000 m thick Grand Canyon Supergroup, the oldest suite of sedimentary rocks in the Grand Canyon (Elston, 1989). The Chuar Group is subdivided into the Galeros Formation (comprising in ascending order the Tanner, Jupiter, Carbon Canyon, and Duppa members) and the overlying Kwagunt Formation (comprising in ascending order the Carbon Butte, Awatubi, and Walcott members; Fig. 2; Ford and Breed, 1973a). Fossils have been found in every member except the Carbon Butte, which consists primarily of sandstone.

The age of the Chuar Group is constrained by a U-Pb zircon age of 742 ± 6 Ma from a 1 cm thick ash layer at the top of the Walcott Member on Nankoweap Butte (Karlstrom et al., 2000) and by a U-Pb detrital zircon age of ca. 782 Ma from the underlying Nankoweap Formation (Dehler et al., 2014). An age of 751 ± 17 Ma from $^{40}Ar/^{39}Ar$ analyses on marcasite nodules in the lower Awatubi Member is consistent with these constraints, as are estimates based on cyclostratigraphy that the Chuar Group represents ca. 30 Myr of time (Dehler et al., 2001b, 2014).

Chuar sediments were deposited in a shallow sea (10s to 100s meters deep; Dehler et al., 2001b) located between 2° and 18° of the equator (Weil et al., 2004) on the NW margin of Laurentia (Li et al., 2013). Similarities in fossil assemblages, C-isotopes, litho- and physical stratigraphy suggest that the Chuar basin was part of a restricted seaway that connected several other ca. 780–740 Ma basins along the Cordilleran margin, including the Uinta Mountain Group in Utah and the Pahrump Group in Death Valley, California (the "ChUMP" seaway hypothesis; Dehler et al., 2001a). Although some early workers favored a lacustrine setting (Elston, 1989), several lines of evidence suggest marine conditions predominated. These include mudcracked, mud-draped symmetric ripples and bipolar cross bedding, indicating a tidally influenced shoreline; locally high pyrite content (common in marine settings but rare in lakes); and the lack of unequivocal terrestrial deposits (Dehler et al., 2001b). The fact that several organic-walled and vase-shaped microfossil species in the Chuar assemblage are found elsewhere in marine successions (e.g., the Akademikerbreen Group, Svalbard, and the Eleonore Bay Group, Greenland; see Table 1 and Porter et al., 2003) also suggests a marine setting: protists have a limited range of salinity tolerances, and it is rare that a species occupies both marine and freshwater (or marine and hypersaline) environments, or that a species switches between the two (Hughes Martiny et al., 2006; Logares et al., 2009). Thus, unless Chuar sediments were deposited in a lake with salinity levels comparable to that of the global ocean, or the other marine successions in which Chuar species have been found were influenced by significant freshwater runoff, the Chuar basin had a marine connection.

Iron and sulfur chemistry indicate that subsurface waters in the Chuar basin were commonly anoxic and ferruginous with intermittent euxinic (anoxic + sulfide-rich) conditions during late Awatubi and Walcott time (Johnston et al., 2010). The appearance of sulfidic conditions has been linked to enhanced export of organic carbon (OC) to Chuar bottom waters (Johnston et al., 2010). In the absence of oxygen and nitrate, iron respiration would have been the favored metabolism in

https://doi.org/10.1017/jpa.2016.57 Published online by Cambridge University Press

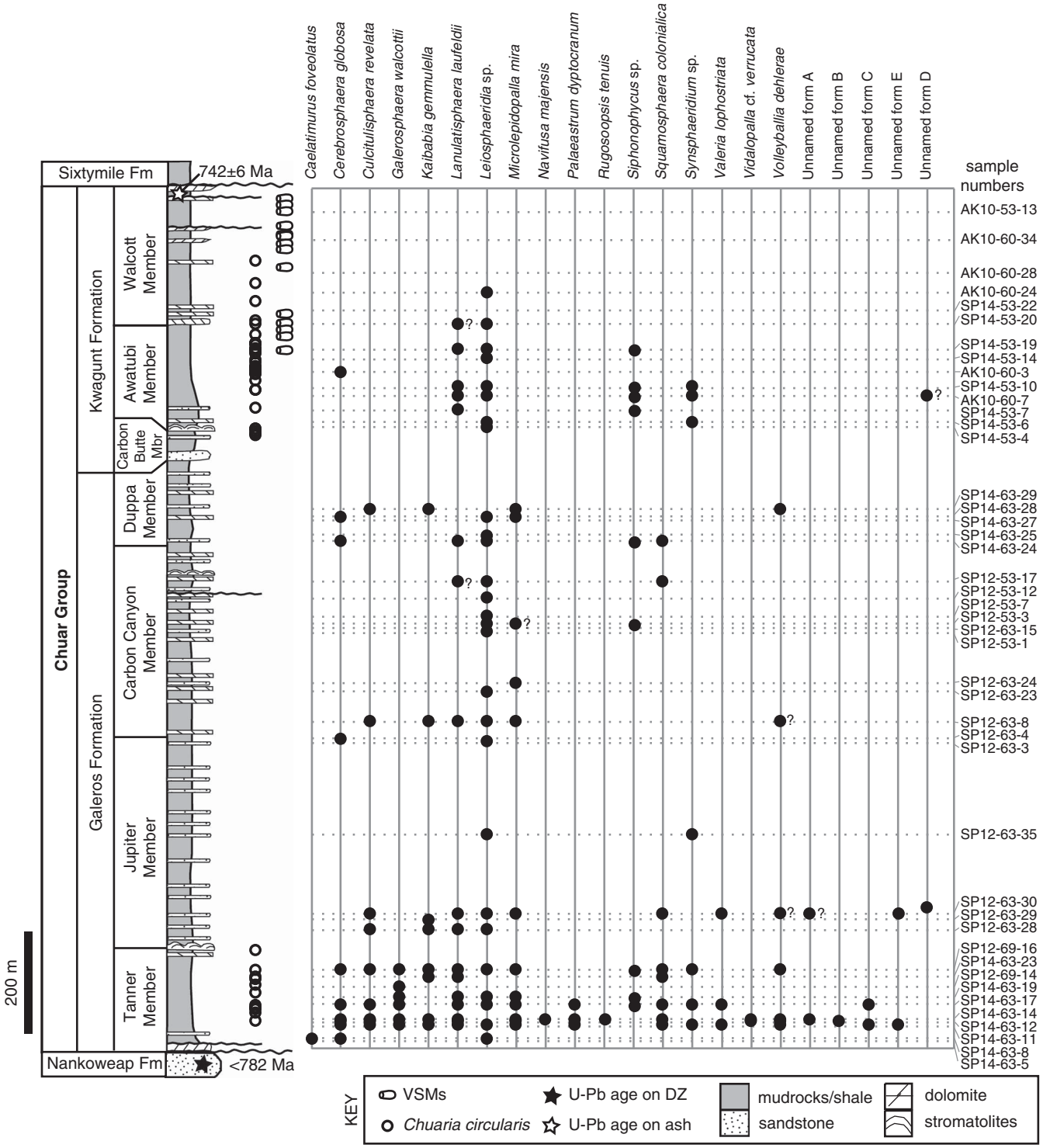

Figure 2. Observed occurrences of organic-walled microfossil taxa in the Chuar Group (filled circles; possible occurrences indicated with "?"). Dotted horizontal lines indicate levels sampled for organic-walled microfossils; some samples were barren. Chuar stratigraphy modified from Dehler et al. (2001b); radiometric dates from Karlstrom et al. (2000) and Dehler et al. (2014). See supplemental data table for more details.

subsurface waters during early Chuar time, but higher rates of OC export (up to 27.8 wt% TOC in Awatubi and Walcott shales; Dahl et al., 2011) would have exhausted the pool of reactive Fe^{3+}, leaving the remaining OC available for sulfate respiration (SO_4^{2-} is thermodynamically favored as an electron acceptor after Fe^{3+}; Johnston et al., 2010). Molybdenum (Mo) isotope analyses on Walcott shales (Dahl et al., 2011) suggest that euxinic conditions were widespread during this time, with sulfidic waters covering an estimated 1%–4% of the global seafloor (Dahl et al., 2011). Thus, although a restricted basin, patterns in Chuar seawater chemistry may broadly reflect global changes during this time, consistent with paleontological patterns in the unit (see the section 'Stratigraphic patterns in Chuar fossil assemblages' in the Discussion).

https://doi.org/10.1017/jpa.2016.57 Published online by Cambridge University Press

Table 1. Chuar Group organic-walled microfossils, their diagnostic characters, sizes, and distributions both within the Chuar Group and worldwide (only convincing occurrences listed here). T = Tanner Member; J = Jupiter Member; CC = Carbon Canyon Member; D = Duppa Member; A = Awatubi Member; unnamed forms and form taxa (leiosphaerids, *Navifusa majensis*, filaments, *Synsphaeridium* sp.) not included. See text for references.

Taxon	Diagnostic characters	Size range	Occurrence in Chuar Group	Other definite occurrences
Caelatimurus foveolatus	Round to elliptical depressions on vesicle surface	29 µm diameter [N = 1]	T	Alinya Fm and Roper Group, Australia; Muhos Fnm Finland
Cerebrosphaera globosa	Regularly, prominently wrinkled walls; wrinkles sinuous, anastomosing, never intersecting	160–375 µm diameter [N = 17]	T, CC, D, A	Svanbergfjellet, Draken, and Ryssö fms, Svalbard; Burra Group, 'Finke beds,' and Hussar, Kanpa, and Pirrilyungka fms, Australia; Chichkan Fm, Kazakhstan; Gouhou Fm, China
Culcitulisphaera revelata	Tightly packed 1- to 3-µm cushion-shaped outpockets	24–127 µm diameter [N = 15]	T, J, CC, D	Alinya Fm, Australia; Lakhanda Group, Siberia; Eleonore Bay Group, Greenland
Galerosphaera walcottii	Funnel-like processes that support an outer envelope	35–51 µm diameter [N = 7]	T, A[1]	None
Kaibabia gemmulella	Circular operculum covered in ~1-µm granulae	30–67 µm diameter [N = 14]	T, J, CC, D, A[1]	None
Lanulatisphaera laufeldii	<1-µm-thick solid processes that fuse distally forming cone-like structures, or that fuse and branch to form networks	24–84 µm diameter [N = 79]	T, J, CC, D, A, W?	Alinya Fm, Australia; Karuyarvinskaya Fm, Russia; Visingsö Group, Sweden, Uinta Mountain Group, USA
Microlepidopalla mira	Circular clusters composed of numerous ellipsoidal structures ~2–8 µm in length	9–31 µm diameter [N = 19]	T, J, CC, D, A	Uinta Mountain Group, USA
Palaeastrum dyptocranum	Monostromatic spheroidal to elliptical colonies composed of cells 10–25 µm in diameter, connected by thickened discs 3–5 µm in diameter	360–580 µm in length [N = 5]	T	Svanbergfjellet Fm, Svalbard; Kotuikan Fm, Siberia
Squamosphaera colonialica	Spherical to irregularly shaped envelopes bearing numerous rounded bulges	60–410 µm in length [N = 25]	T, J, CC, D, A[1]	Veteranen Group, Svalbard; Kildinskaya Group, Russia; Steptoe, Kanpa, and Hussar fms, Officer Basin, Australia; Narssârssuk, Dundas, and Baffin Bay gps, Thule Supergroup, Greenland; Gouhou Fm, North China
Valeria lophostriata	Concentric ridges ~1 µm apart on inner surface of vesicle	55–180 µm diameter [N = 6]	T, J	Widely distributed in Proterozoic rocks
Vidalopalla cf. *verrucata*	Rounded, closely spaced verrucae 0.3–0.6 µm in diameter	32 µm diameter [N = 1]	T, D	None
Volleyballia dehlerae	Sets of ~1 µm spaced ridges and valleys; each set <10 µm in length and oriented at angle to others	25–45 µm diameter [N = 12]	T, CC?, D	Alinya and Browne fms, Australia; Conselheiro Mata Group, Espinhaço Supergroup, Brazil

[1]Reported by Vidal and Ford (1985) but presence not confirmed in this study.

Materials and methods

The Chuar Group fossils were collected during two field trips to the Grand Canyon in September 1998 and September 1999 as part of a larger study that also included stratigraphic, sedimentologic, geochemical, paleomagnetic, and tectonic studies of the unit (e.g., Karlstrom et al., 2000; Dehler et al., 2001b, 2005; Timmons et al., 2001, Weil et al., 2004). Forty-four samples from the Tanner Member (N = 10), Jupiter Member (4), Carbon Canyon Member (11), Duppa Member (5), Awatubi Member (8), and Walcott Member (6) (Fig. 2) were macerated with hydrochloric and hydrofluoric acid in SMP's laboratory following techniques described in Grey (1999) or were processed either by Laola Pty Ltd (now Core Labs, Australia) using the Grey (1999) technique or by Waanders Palynology Consulting, Inc., using a technique that involves centrifugation and heavy liquid ($ZnBr_2$) separation of the acid insoluble residue. (Nitric acid, sometimes used to increase the translucence of organic material via oxidation, was not employed in any of the processing.) Centrifugation and heavy liquid separation has been implicated in the loss or destruction of acritarchs, but we noted no differences in acritarch assemblages when the same sample was processed using centrifugation and heavy liquid separation vs. the more gentle Grey (1999) method. SEM and FIB-SEM were conducted following the same protocols described in Schiffbauer and Xiao (2009) and Riedman and Porter (2016). Wall ultrastructure was examined via TEM using an FEI Tecnai G2 Sphera Microscope and an FEI Titan 300 kV FEG TEM/STEM system, both housed at UCSB's Materials Research Laboratory. TEM samples were prepared via lift-out technique in the FIB using the Omniprobe needle assembly and trimmed to a thickness of ~150 nm.

Systematic paleontology

Specimens are reposited in the microfossil collections of the University of California Museum of Paleontology (UCMP) under accession numbers 36072–36106 and locality numbers MF7688–MF7689. (A few illustrated specimens could not be relocated; they have not been assigned UCMP numbers.) Sample numbers are provided in the captions for all figured specimens; these correspond to sample numbers listed in Figure 2. For holotype specimens mounted on glass slides, England Finder coordinates are also provided (slide is oriented so that label is opposite fixed corner of the stage; England Finder graticule is oriented so that upper left corner [A1] is in the fixed corner such that the letters and numbers appear right-side-up when viewed under the microscope). The location of the holotype of *Microlepidopalla mira* n. sp. is indicated in a map of its SEM stub included in the supplementary information.

https://doi.org/10.1017/jpa.2016.57 Published online by Cambridge University Press

Because of the relatively small number of characters available for diagnosis, Precambrian microfossil genera have in many cases become wastebasket taxa, encompassing species that collectively may range from Proterozoic to Pleistocene in age (e.g., *Dictyotidium* Eisenack, 1955; Fensome et al., 1990) and almost certainly are not closely related. Here we have followed the principle that unless there is strong evidence that two species are closely related—for example, they have identical morphology and differ only in size distributions—we will not place them in the same genus. Thus, we tend toward being splitters with respect to the designation of genera. In delimiting species, however, we tend toward being lumpers: unless there is clear evidence for a break in morphological variation, we group specimens with similar morphologies together into a single species. As a result, we have erected several new genera herein, but each one is monotypic. In addition, we have made a particular effort to understand the range of taphonomic and biological variation exhibited by a species, and this has resulted in grouping together forms that previously had been separated into distinct species.

Taxa are listed below in alphabetical order under the broad designation 'Organic-walled microfossils.' Other higher groupings such as 'acritarchs' or 'colonial forms' have been avoided as these are regarded as artificial. Following convention for organic-walled microfossils of Precambrian age (e.g, Evitt, 1963), the fossils are treated under the International Code of Nomenclature for Algae, Fungi, and Plants (ICN, Melbourne Code, 2011).

This paper was written at a time when the Neoproterozoic community was transitioning to a GSSP-defined Cryogenian Period; in the interim, the start of the period has been defined as ca. 720 Ma (Shields-Zhou et al., 2016). The Tonian Period thus extends from 1000 to ca. 720 Ma. We use these definitions throughout.

Organic-walled microfossils

Genus *Caelatimurus* Riedman and Porter, 2016

Type species.—*Caelatimurus foveolatus* Riedman and Porter, 2016, by monotypy.

Caelatimurus foveolatus Riedman and Porter, 2016
Figure 3.1

1978 Sphere with type I reticulate surface; Peat et al., p. 5, fig. 3A.
1978 Sphere with type II reticulate surface; Peat et al., p. 5, fig. 3B, D–F.
1984 *Turuchanica maculata*; Tynni and Uutela, p. 24, ?fig. 175, fig. 176, non 177, nec 178–179, ?180–182, nec 183–186.
2016 *Caelatimurus foveolatus* Riedman and Porter, p. 859, fig. 3.6–3.8.

Holotype.—South Australian Museum Collection number P49508 (fig. 3.6–3.7), from sample 1265.57 m- slide19A, Giles 1 drill core, Neoproterozoic Alinya Formation, Officer Basin, Australia (Riedman and Porter, 2016).

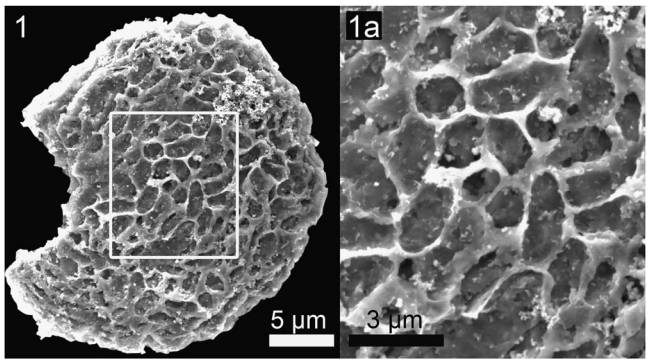

Figure 3. *Caelatimurus foveolatus* Riedman and Porter, 2016: (**1, 1a**) UCMP 36105a, SP14-63-8.

Description.—Organic-walled vesicle 29 µm in diameter with wall consisting of a raised network surrounding circular to elliptical depressions, 1.0 to 3.0 µm in maximum length and 1.0–1.5 µm in width. There are approximately 40 depressions per 100 μm^2 area of the vesicle surface.

Materials.—A single specimen (sample SP14-63-8).

Remarks.—The type and all other reported specimens of this species are known only from light microscopy, making direct comparisons with the Chuar material difficult. (See Riedman and Porter, 2016, for a discussion of the species concept.) Nonetheless, the size, shape, distribution, and arrangement of the depressions in the wall of the Chuar specimen are indistinguishable from the 'ellipsoidal depressions' exhibited by other *C. foveolatus* specimens (Riedman and Porter, 2016), and the size of the Chuar vesicle falls within error of the range reported for the other material (~30–60 µm; Riedman and Porter, 2016). We therefore assign this specimen to *C. foveolatus*.

Genus *Cerebrosphaera* Butterfield in Butterfield, Knoll, and Swett, 1994

Type species.—*Cerebrosphaera globosa* (Ogurtsova and Sergeev, 1989) Sergeev and Schopf, 2010.

Diagnosis.—As for type species by monotypy (emended from Butterfield et al., 1994).

Remarks.—Butterfield et al. (1994) provided separate diagnoses for the genus *Cerebrosphaera* and its single species, stating that the latter is characterized by vesicles 100-1,000 µm in diameter. We have produced a single diagnosis for the species and its monotypic genus, modifying the generic diagnosis given by Butterfield et al. (1994) to include the vesicle sizes. We have also changed the stated vesicle wall thickness, formerly ~1.5 µm, to accommodate the new specimens studied here.

Cerebrosphaera globosa (Ogurtsova and Sergeev, 1989) Sergeev and Schopf, 2010
Figure 4.1–4.9

1983 Unnamed Form B of Knoll (1983); Knoll and Calder, pl. 60, fig. 6.
1984 Unnamed Form B; Knoll, p. 160, fig. 9D–F.

https://doi.org/10.1017/jpa.2016.57 Published online by Cambridge University Press

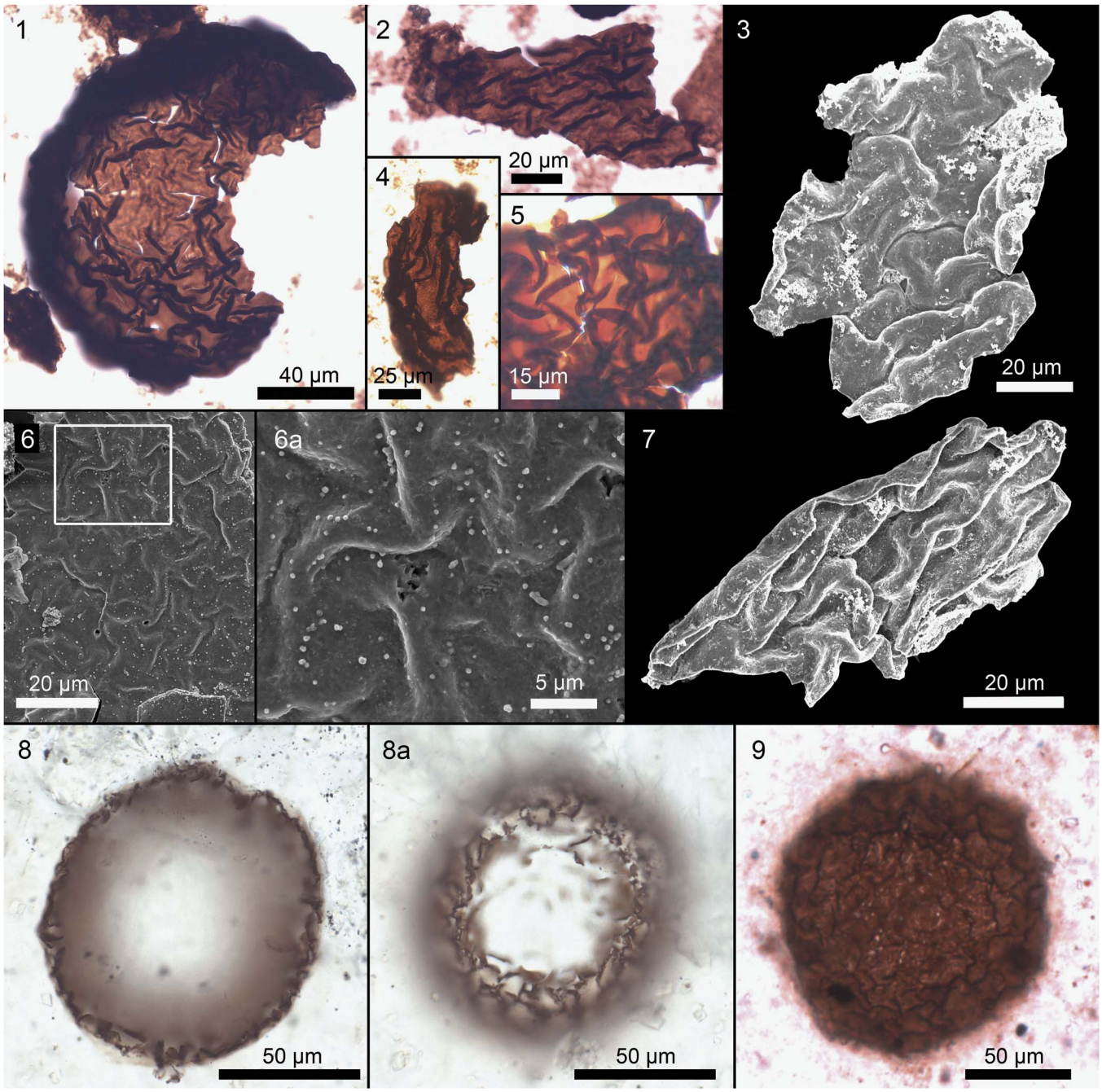

Figure 4. *Cerebrosphaera globosa* (Ogurtsova and Sergeev, 1989) Sergeev and Schopf, 2010. (**1**) Specimen showing marked variation in wrinkle widths, UCMP 36106a, SP14-63-08. (**2**) Fragment of vesicle with subparallel wrinkles, UCMP 36106b, SP14-63-08. (**3**) View of vesicle wall's inner surface, UCMP 36105b, SP14-63-8. (**4**) UCMP 36106c, SP14-63-08. (**5**) Fragment of vesicle showing semielliptical shape of wrinkles, SP14-63-14. (**6, 6a**) UCMP 36086a, SP14-63-12. (**6a**) Note subtle pocked texture of vesicle surface, as well as partly degraded area of wall; location of image is indicated by box in (**6**). (**7**) Folded fragment showing thickness of vesicle wall, UCMP 36105c, SP14-63-8. (**8, 9**) Three-dimensional vesicles preserved in chert from the Lower Dolomite Member, Svanbergfjellet Formation, Krystalfjellet Peninsula, eastern Murchisonfjord, Svalbard, appear closely similar to specimens of *C. globosa* described by Ogurtsova and Sergeev (1989) and Sergeev and Schopf (2010). (**8, 8a**) The same specimen at different focal planes, sample G155.100.6 TS5. (**9**) Sample G155.100.6 TS4.

1989 *Chuaria globosa* Ogurtsova and Sergeev, p. 121, fig. 1a, г, з.
1991 *Leiosphaeridia* sp. cf. *L. atava*; Knoll et al., p. 558, fig. 21.2, 21.3.
1992b *Stictosphaeridium sinapticuliferum*; Zang and Walter, p. 311, pl. 8K.
1994 *Cerebrosphaera buickii* Butterfield; Butterfield et al., p. 30, fig. 12.
1999 *Cerebrosphaera buickii*; Cotter, p. 70, fig. 6D, F–H.
1999 *Cerebrosphaera ananguae* Cotter, p. 69, fig. 6A, B, E.
2000 *Cerebrosphaera buickii*; Hill et al., fig. 7.
2006 ?*Cerebrosphaera globosa*; Sergeev, pl. 48, figs. 8–10, ?11–?13.
2009 *Cerebrosphaera buickii*; Nagy et al., fig. 1K.
2010 ?*Cerebrosphaera globosa*; Sergeev and Schopf, p. 394, fig. 13.5, 13.5A, 13.8.
2011 *Cerebrosphaera buickii*; Grey et al., fig. 8.6A–I.

https://doi.org/10.1017/jpa.2016.57 Published online by Cambridge University Press

Holotype.—ИГ АН Киргизской ССР, thin section ЧК 1-83, No. 1. Neoproterozoic Chichkan Formation, Shabakty, Maly Karatau Range, Kazakhstan (Ogurtsova and Sergeev, 1989, fig. 1a).

Diagnosis.—Spheroidal vesicles typically 100 to 1,000 μm in diameter with regularly and prominently wrinkled walls. Wrinkles sinuous: anastomosing, interfingering, or rarely, subparallel, but never intersecting. Vesicle walls ~1.0 to 1.5 μm thick, inelastic, and often opaque. Outer, thin-walled envelope sometimes present (emended from Sergeev and Schopf, 2010; adapted from Butterfield et al., 1994).

Occurrence.—Tanner, Carbon Canyon, and Duppa members, Chuar Group; widespread in other late Tonian units including the Chichkan Formation, southern Kazakhstan (Ogurtsova and Sergeev, 1989; Sergeev and Schopf, 2010); Svanbergfjellet and Draken formations, Akademikerbreen Group, Svalbard (Knoll et al., 1991; Butterfield et al., 1994); Ryssö Formation, Murchisonfjorden Supergroup, Svalbard (Knoll and Calder, 1983); Gouhou Formation, Huaibei Group, China (Zang and Walter, 1992b); Hussar and Kanpa formations (Empress 1A, Hussar 1, Lungkarta 1, and Lancer 1 drill cores), Pirrilyungka Formation (Vines 1 drill core), and Kanpa Formation (Yowalga 2 drill core), Officer Basin, Western Australia (Cotter, 1999; Hill et al., 2000; Grey et al., 2011); Skillogalee Dolomite (BLD 4 drill core), and Anama Siltstone Member, Rhynie Sandstone, Burra Group (PP12 drill core), Stuart Shelf, South Australia (Hill et al., 2000; Grey et al., 2011); 'Finke beds,' Amadeus Basin, Australia (Grey et al., 2011).

Description.—Spheroidal vesicles 160 to 375 μm in diameter (mean = 242 μm, SD = 70 μm, N = 17), with complexly wrinkled walls. Wrinkles sinuous and may occur singly or may anastomose. Wrinkles vary in width within individual specimens from >4 μm thick to barely visible, reflecting the degree to which the wall is folded on itself (Fig. 4.1, 4.4). Wrinkle widths also vary along the length of a single wrinkle, with some wrinkles forming semi-elliptical shapes, tapering off at both ends (Fig. 4.5). Wrinkles vary in width among specimens from 1.5 to 5.5 μm (N = 19; based on measurements of the narrowest wrinkles in each specimen). Wrinkle orientations may vary within and between vesicles, with neighboring wrinkles subperpendicular (Fig. 4.5, 4.6) to subparallel (Fig. 4.2, 4.4). On the outer surface of the vesicle, wrinkles take the form of ridges separated by U-shaped valleys. On the internal surface of the vesicle, wrinkles take the form of narrow, sinuous valleys separated by raised, smoothly rounded, sinuous hills (Fig. 4.3), giving the surface an appearance similar to cerebral convolutions of the human brain.

Vesicle wall is 1.0 to 1.2 μm thick (N = 2; Fig. 4.7) and exhibits a subtle pocked texture (Fig. 4.6, 4.6a; cf. the 'psilate to slightly granular' wall of Cotter, 1999), likely taphonomic in origin (Grey and Willman, 2009).

Materials.—Seventeen complete or nearly complete vesicles and 45 fragments (samples SP14-63-8, -12, -14, -17, and -24).

Remarks.—Following the suggestion of Sergeev (2006), Sergeev and Schopf (2010) transferred *Chuaria globosa* Ogurtsova and Sergeev, 1989 with question to *Cerebrosphaera*. Although the description and images of ?*C. globosa* specimens suggest they are closely comparable to the type material of *C. buickii* (also see the discussion of Butterfield et al., 1994), Sergeev and Schopf (2010) left them in a separate species because their different mode of preservation made it difficult to compare them in detail (three-dimensional vesicles in chert vs. the flattened carbonaceous disks illustrated in Butterfield et al., 1994). Newly discovered specimens from the Svanbergfjellet Formation preserved three dimensionally in chert (Fig. 4.8, 4.9) are closely similar to those illustrated from the Chichkan Formation; indeed, we see no obvious basis for distinguishing these two populations. We therefore formally synonymize these two species. Because *C. globosa* was erected first (by Ogurtsova and Sergeev, 1989), that specific epithet has priority. We agree with Sergeev (2006) and Sergeev and Schopf (2010) that this species is sufficiently different from the type species of *Chuaria, C. circularis*, both in terms of its size and its characteristic wrinkling, that it should be removed from that genus. We place it here, without question, in *Cerebrosphaera* Butterfield in Butterfield et al., 1994.

Cotter (1999) erected a new species of *Cerebrosphaera*, *C. ananguae*, that she distinguished from *C. buickii* on the basis of its looser pattern of wrinkles and its greater wall thickness (>2 μm), the latter inferred by measuring the average width of the narrowest wrinkles and dividing by two. Wrinkle thicknesses in the Chuar specimens spanned the thicknesses cited for *C. buickii* and *C. ananguae* in Cotter (1999) and we found no clear breaks in this distribution, nor did we find obvious clustering related to the wrinkle spacing (i.e., loosely vs. tightly spaced wrinkles). Furthermore, in the Chuar specimens, there does not appear to be a correlation between wall thickness and the width of the narrowest wrinkles, at least for the two specimens in which wall thickness could be ascertained (e.g., Fig. 4.7). Indeed, the fact that wrinkles vary rather widely in thickness, spacing, and relative orientation both within and among specimens suggests that the variation in these characteristics is likely related to differences in postmortem shrinkage and/or compaction. (The distinctive pattern of the wrinkling itself, however, a pattern that is visible even in strongly flattened specimens [Fig. 4.1, 4.6] and in three-dimensionally preserved specimens [Fig. 4.8, 4.9], suggests that the wrinkles reflect the biological character of wall composition.) Because of the continuous variation in wrinkle thickness and spacing, and because this variation likely reflects taphonomic differences, we regard *C. ananguae* as a junior synonym of *C. globosa*. We also revise the diagnosis for *C. globosa,* replacing it with a diagnosis modified from that given by Butterfield et al. (1994) for the genus *Cerebrosphaera*.

One of three specimens described as *Stictosphaeridium sinapticuliferum* Timofeev by Zang and Walter (1992b: pl. 8, fig. K) is interpreted here to be *C. globosa*. This specimen comes from the Gouhou Formation, Huaibei Group, at the Gouhou section, Suxian County, Huaibei Province, China. Other fossils reported from the Gouhou Formation (e.g., *Chuaria*, *Tawuia*, *Trachyhystrichosphaera aimika* Hermann in Timofeev et al. 1976, emend. Butterfield et al., 1994, and *Valeria lophostriata* [Jankauskas, 1979b] Jankauskas, 1982) indicate a late Tonian age (Tang et al., 2015).

https://doi.org/10.1017/jpa.2016.57 Published online by Cambridge University Press

Genus *Culcitulisphaera* Riedman and Porter, 2016

Type species.—*Culcitulisphaera revelata* Riedman and Porter, 2016, by monotypy.

Culcitulisphaera revelata Riedman and Porter, 2016
Figure 5.1–5.7

1979 *Kildinella* sp.; Vidal, pl. 4, figs. C–D.
?1985 *Trachysphaeridium* sp. A; Vidal and Ford, p. 377, fig. 8B, D.
1992 *Trachysphaeridium laminaritum*; Schopf, pl. 14, fig. A
2009 *Trachysphaeridium laminaritum*; Nagy et al., fig. 1H.
2016 *Culcitulisphaera revelata* Riedman and Porter, p. 861, figs. 5, 6.4–6.6, 7, 8.

Holotype.—South Australian Museum Collection number P49519, sample 1265.56 m- slide 19A, Giles 1 drill core, Neoproterozoic Alinya Formation, Officer Basin, Australia (Riedman and Porter, 2016, fig. 5.1).

Diagnosis.—Optically dense sphaeromorphic organic-walled microfossil distinguished by a surface ornament of tightly packed 1- to 3-µm cushion-shaped outpockets of the vesicle that may appear only as ~1-µm diameter light spots or alveolae under light microscopy (from Riedman and Porter, 2016).

Occurrence.—Tanner, Jupiter, Carbon Canyon, and Duppa members, Chuar Group; also occurs in the Neoproterozoic Alinya Formation in the Giles 1 drill core, Officer Basin, Australia (Riedman and Porter, 2016); in bed 19, of the late Tonian Limestone-Dolomite Series, Eleonore Bay Group, Greenland (Vidal, 1979); and in the latest Mesoproterozoic–earliest Neoproterozoic Lakhanda Group, Khabarovsk region, Siberia (Schopf, 1992). Possible occurrence in the late Tonian Uinta Mountain Group, Utah (Vidal and Ford, 1985).

Description.—Organic-walled vesicles 24 to 127 µm in diameter (mean = 48 µm, SD = 26, N = 15) with an outer layer that formed pillow-like outpocketings 1 to 2 µm in diameter (mean = 1.5 µm, SD = 0.2 µm, N = 27). These may appear deflated (Fig. 5.1, 5.2) or sunken into the surface of the vesicle (Fig. 5.3). In the latter, the vesicle surface has a honeycomb-like appearance, which we interpret as reflecting a mechanically resistant structure that subtended the outer layer and supported the pillows. In some specimens, the outer layer is missing, revealing a complex, spongy material that forms the honeycomb-like structure that supports the pillows (Fig. 5.4, 5.5; see reconstruction of the wall in Fig. 25). Under transmitted light microscopy, the pillows appear as spots that are less optically dense than their surroundings (Fig. 5.5a, 5.6). This likely reflects the fact that the spongy material is thinner in these areas.

A few specimens are covered by a thin, smooth wall that is cracked in places to reveal a smooth, honeycomb-like surface underneath—not the spongy material of the inner vesicle layer (Fig. 5.7). This is interpreted to represent an envelope that covered the outer, pillow-forming layer of the vesicle wall (Fig. 25). No specimens exhibit evidence for excystment structures.

Materials.—Twenty-one specimens (samples SP12-63-8, -28, -30, and SP14-63-11, -12, -14, -17, and -29).

Remarks.—Riedman and Porter (2016) provide a thorough discussion of *C. revelata* and its species concept. The Chuar assemblage closely resembles that described by Riedman and Porter (2016) in the Alinya Formation, Giles 1 drill core, Australia. Particularly noteworthy is the frequent presence of 30- to 600-nm nanopores in the walls of specimens from the Alinya Formation, revealed during serial sectioning via FIB-SEM (Riedman and Porter, 2016). Their size, position, and distribution make it likely that these are spaces in the spongy network visible in some Chuar specimens (e.g., Fig. 5.5).

Genus *Galerosphaera* new genus

Type species.—*Galerosphaera walcottii* Vidal and Ford, 1985 n. comb., by monotypy.

Diagnosis.—As for type species by monotypy.

Etymology.—From the Galeros Formation, the lower, acritarch-rich unit of the Chuar Group, and the Latin *sphaera*, meaning sphere.

Remarks.—Vidal and Ford (1985) were the first to describe specimens of *G. walcottii* and placed the species in the genus *Vandalosphaeridium* Vidal (1981). Although the diagnosis of *Vandalosphaeridium* is broad enough to permit the inclusion of *G. walcottii*, this species is quite distinct from the type species of *Vandalosphaeridium*, *V. reticulatum* (= *Peteinosphaeridium reticulatum* Vidal [1976b], misspelled as *Pteinosphaeridium reticulatum* in that same paper). In *V. reticulatum* the processes furcate distally to form polygonal ("net-like": Vidal, 1976b, p. 27 and fig. 14A–K) compartments, whereas in *G. walcottii* the processes expand distally but do not connect with one another. Given the differences in the shape and topology of their processes, we see no convincing reason to think that *G. walcottii* and *V. reticulatum* have a close biological relationship, and thus we remove *G. walcottii* from *Vandalosphaeridium*. By contrast, the other species in *Vandalosphaeridium*, *V. koksuicum* Sergeev and Schopf, 2010 and *V. varangeri* Vidal, 1981, appear to exhibit the same polygonal compartments observed in *V. reticulatum*, supporting their inclusion in *Vandalosphaeridium*.

Among extant protists, cysts with funnel-like processes are known in dinoflagellates, green algae, and ciliates (Foissner et al., 2007; Moczydłowska, 2010). Thus this character has apparently evolved several times independently and is not likely to be useful by itself in establishing taxonomic relationships.

Galerosphaera walcottii (Vidal and Ford, 1985) new combination
Figure 6.1–6.8

1985 *Vandalosphaeridium walcottii* Vidal and Ford, p. 376, fig. 8E, F.
2009 *Vandalosphaeridium walcottii*; Nagy et al., fig. 1G.

https://doi.org/10.1017/jpa.2016.57 Published online by Cambridge University Press

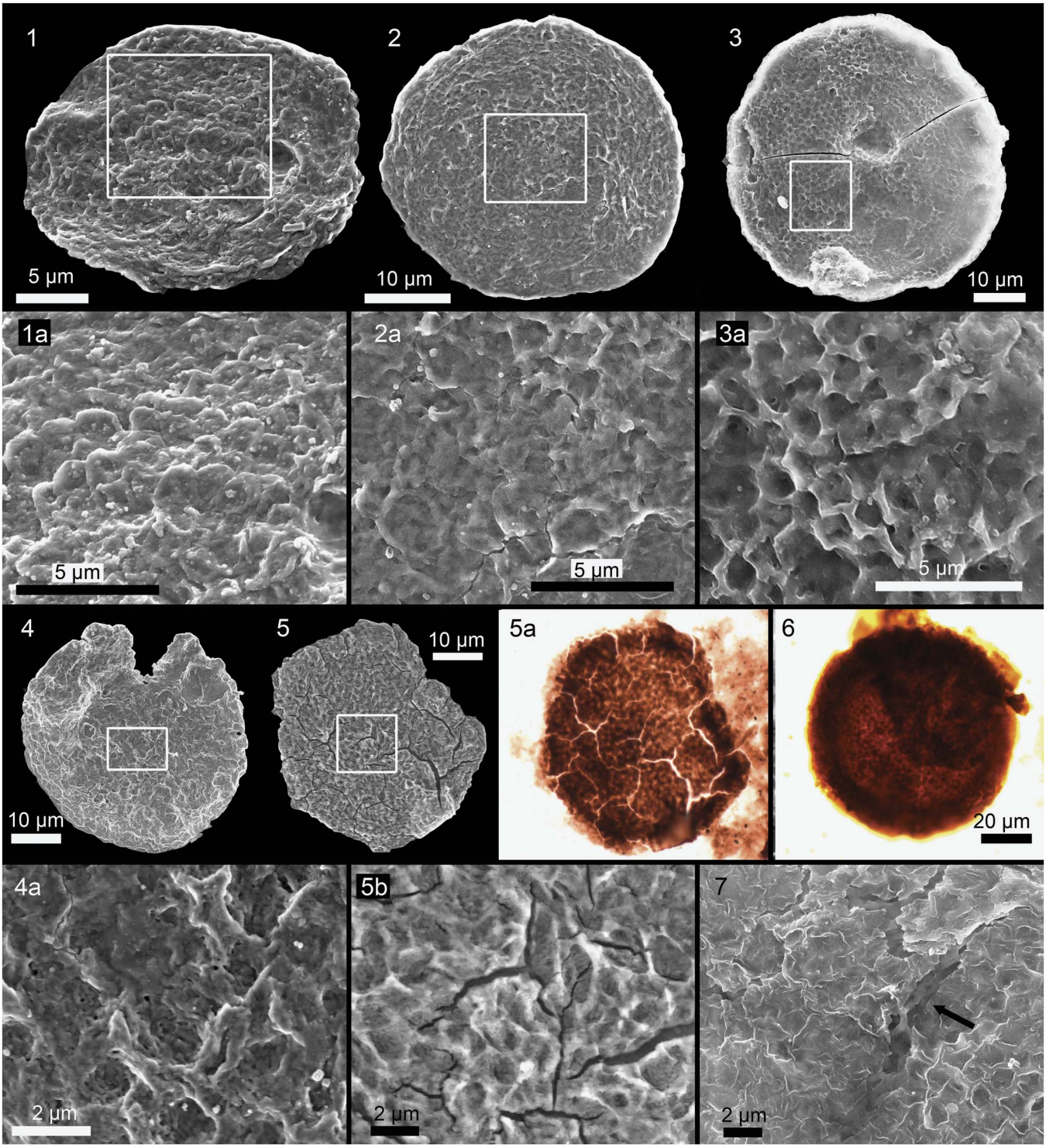

Figure 5. *Culcitulisphaera revelata* Riedman and Porter, 2016. (**1–3**) Three specimens showing variation in preservation of pillows, with increasing deflation from left to right. (**1, 1a**) UCMP 36104a, SP14-63-29; (**2, 2a**) UCMP 36091a, SP14-63-14; (**3, 3a**) UCMP 36073a, SP12-63-30. (**4–5**) Two specimens, each with outer layer missing, revealing spongy structure beneath. (**4, 4a**) UCMP 36093a, SP14-63-14; (**5, 5a, 5b**) UCMP 36080a, SP14-63-11. (**6**) TLM image of vesicle showing lighter spots where pillows occur (also see **5a**), UCMP 36088a, SP14-63-14. (**7**) Vesicle with envelope preserved; crack in the envelope (indicated by arrow) reveals the smooth outer layer of the vesicle wall underneath; UCMP 36092a, SP14-63-14. Scale bar in (**5**) also for (**5a**).

Holotype.—LO 5661, slide GC-80-13:2-A, Collections of the Department of Historical Geology and Palaeontology, University of Lund; late Tonian Awatubi Member, Kwagunt Formation, Chuar Group (Vidal and Ford, 1985: fig. 8E). (The holotype entry states Walcott Member, but elsewhere in the text the sample is referred to the Awatubi Member.) Eastern Grand Canyon, Arizona. Specific locality information not provided.

Diagnosis.—Spheroidal vesicle covered by evenly scattered, widely spaced, short, sturdy processes with funnel-like distal

https://doi.org/10.1017/jpa.2016.57 Published online by Cambridge University Press

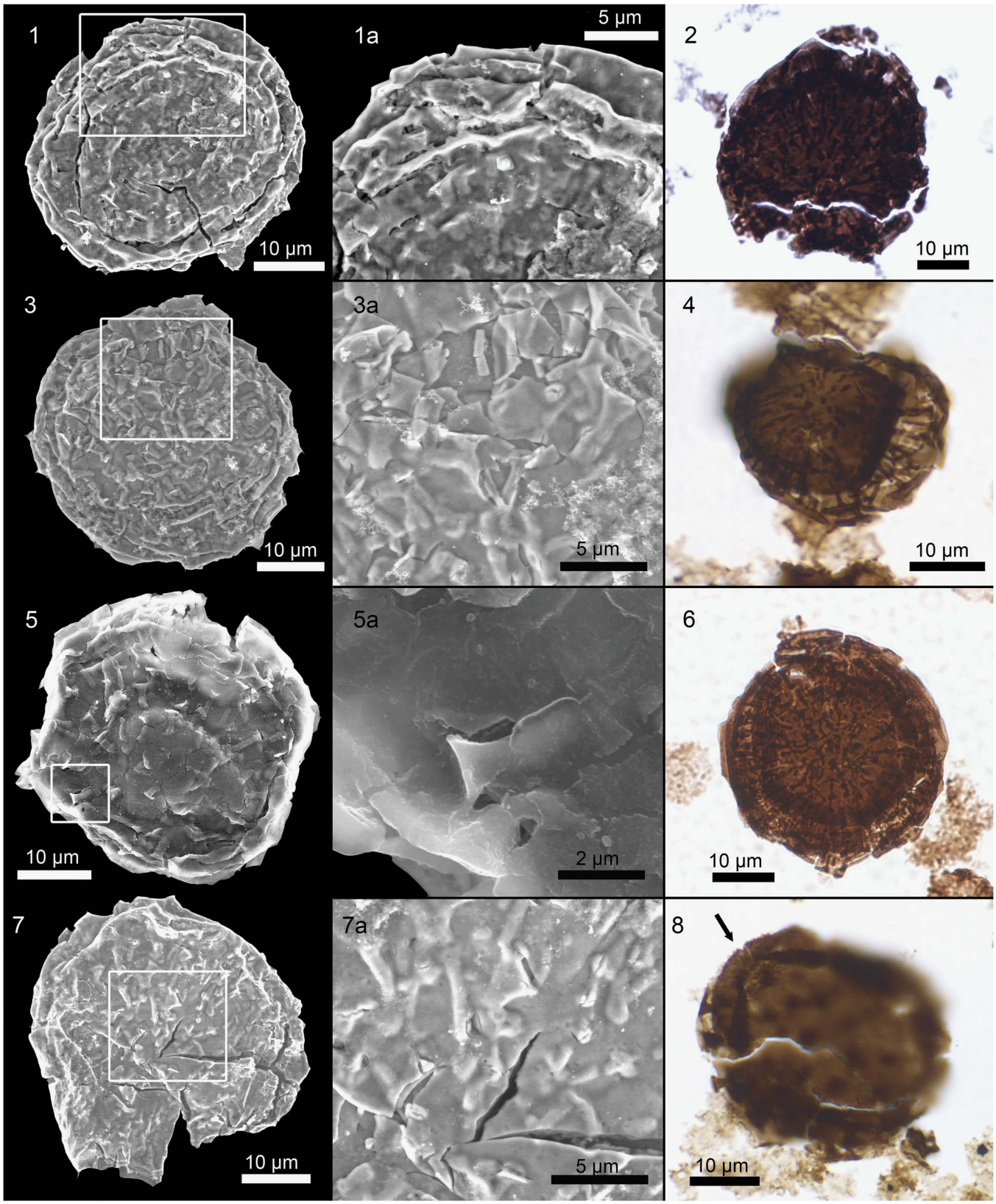

Figure 6. *Galerosphaera walcottii* (Vidal and Ford, 1985) n. comb. (**1, 1a**) UCMP 36080b, SP14-63-11. (**2**) UCMP 36083a, SP14-63-11. (**3, 3a**) UCMP 36088b, SP14-63-14. (**4**) SP14-63-11. (**5, 5a**) Note flaring of process tip to form funnel-like structure, UCMP 36092b, SP14-63-14. (**6**) SP14-63-11. (**7, 7a**) UCMP 36080c, SP14-63-11. (**8**) Arrow points to hair-like structures on vesicle surface; SP12-69-14.

https://doi.org/10.1017/jpa.2016.57 Published online by Cambridge University Press

portions that support an external translucent and smooth envelope completely enclosing the vesicle (emended from Vidal and Ford, 1985).

Occurrence.—Tanner Member; Vidal and Ford (1985) also report *G. walcottii* from the Awatubi Member (their reported occurrence in the Walcott Member is apparently erroneous; see the preceding).

Description.—Organic-walled microfossils 35 to 51 µm in maximum diameter (mean = 40 µm, SD = 5 µm, N = 7), with processes 2 to 5 µm in length that connect to an outer envelope (= 'membrane; of Vidal and Ford, 1985). Processes are ~1 µm in width proximally but flare at their distal end to form funnel-like structures ~2 µm in maximum width (Fig. 6.5a). Funnel-like distal portions appear to be wider in one dimension than the other (i.e., they appear flattened; Figs. 6.5, 6.6, 25), but it is possible this reflects compaction. Processes are more or less evenly and widely spaced, with ~10 per 100 µm^2 area. The outer envelope is translucent under light microscopy and exhibits both ductile deformation (folding over the underlying processes) and brittle deformation. One specimen exhibits short (<<1 µm) fine hair-like structures arising from the surface of the vesicle between the processes (Fig. 6.8, black arrow).

Materials.—Ten specimens (samples SP14-63-11, -14, and SP12-69-14).

Basionym.—*Vandalosphaeridium walcottii* Vidal and Ford, 1985 (p. 376–377.)

Remarks.—Vidal and Ford's (1985) diagnosis is emended here so that reference to a rigid (as opposed to flexible) outer envelope has been removed as specimens studied here do not show evidence for rigidity. We have been unable to determine whether the processes are hollow.

Genus *Kaibabia* new genus

Type species.—*Kaibabia gemmulella* n. gen. n. sp., by monotypy

Diagnosis.—As for type species by monotypy.

Etymology.—Named for the Kaibab Tribe of the southern Paiute, whose traditional lands include the north rim of the Grand Canyon.

Remarks.—Vidal and Ford (1985) assigned similar specimens from the Chuar Group to *Leiosphaeridia* Eisenack, 1958b, comparing them to *L. asperata* (Naumova, 1950) Lindgren, 1982 but leaving them in open nomenclature. However, *Leiosphaeridia* is a form genus comprising species that themselves are form taxa and that are characterized by a lack of ornament or sculpture (Jankauskas et al., 1989). By contrast, the distinctive granulate operculum that is diagnostic of *K. gemmulella* contradicts its placement in the smooth-walled *Leiosphaeridia* and suggests it is a real biological taxon. Because of this distinctive and unique feature, we here erect the new genus *Kaibabia* for this new species.

Kaibabia gemmulella new species
Figure 7.1–7.9

?1980 *Leiosphaeridia kulgunica* Jankauskas, p. 192, fig. 1.1–1.4.
1985 *Leiosphaeridia* sp. A; Vidal and Ford, p. 364, figs. 4B, 4D, 7C.
?1989 *Leiosphaeridia kulgunica*; Jankauskas et al., p. 78, pl. 11, 8–10.
?1992 *Leiosphaeridia kulgunica*; Schopf, pl. 19G.
2009 *Leiosphaeridia* sp. A; Nagy et al., fig. 1C.

Holotype.—UCMP 36082a, SP14-63-11, SEM slide ker-5, EF = A39, Lava Chuar Canyon locality, Tanner Member, Galeros Formation, Chuar Group, Grand Canyon (Fig. 7.1).

Diagnosis.—Originally spheroidal, smooth, organic-walled microfossils with elliptical to circular operculum; outer surface of operculum covered in numerous ~1-µm-diameter granulae. Operculum may be absent, leaving a well-defined circular hole. Outer envelope may be present.

Occurrence.—Tanner, Jupiter, Carbon Canyon, and Duppa members. Vidal and Ford (1985) also reported the species from the Awatubi Member.

Description.—Smooth-walled vesicles 30 to 67 µm in diameter (mean = 42 µm, SD = 11 µm, N = 14), with circular to elliptical operculum; outer surface of operculum covered in ~1-µm-diameter hemispherical granulae. Opercula are 6 to 13 µm in diameter (long axis; mean = 9 µm, SD = 2 µm, N = 14), and bear on their surface between 10 and 40 granulae. Operculum diameter positively correlated with both the number of granulae (Pearson's correlation coefficient, r = 0.7, R^2 = 0.5) and the diameter of the vesicle (r = 0.8, R^2 = 0.7) (Fig. 8). Granulae vary more widely in diameter within a single operculum in specimens with higher numbers of granulae. In some specimens, the operculum is partly detached (Fig. 7.2) or missing (Fig. 7.4) revealing a circular hole with a smooth margin. Outer envelope, when present, exhibits impressions of granulae underneath (Fig. 7.5). One specimen exhibits several structures that may be short (~1 µm) processes (Fig. 7.7).

Etymology.—Double diminutive form of the Latin *gemma*, meaning jewel.

Materials.—Twenty-one specimens (samples SP12-63-8, SP14-63-11, -14, and -23).

Remarks.—The consistent sizes of the granulae (~1 µm) together with continuous variation in vesicle and operculum size (Fig. 8) suggests that the specimens examined here are part of the same species. The presence of an outer envelope—likely representing the vegetative cell wall—suggests the vesicle itself was a cyst, consistent with the presence of an operculum. (Note that, by itself, the presence of an operculum does not imply the vesicle is a cyst as some vegetative cells also possess opercula [Moczydłowska, 2010]).

Vidal and Ford (1985) noted similarities between *Kaibabia gemmulella* (= *Leiosphaerida* sp. A) and *Leiosphaeridia*

https://doi.org/10.1017/jpa.2016.57 Published online by Cambridge University Press

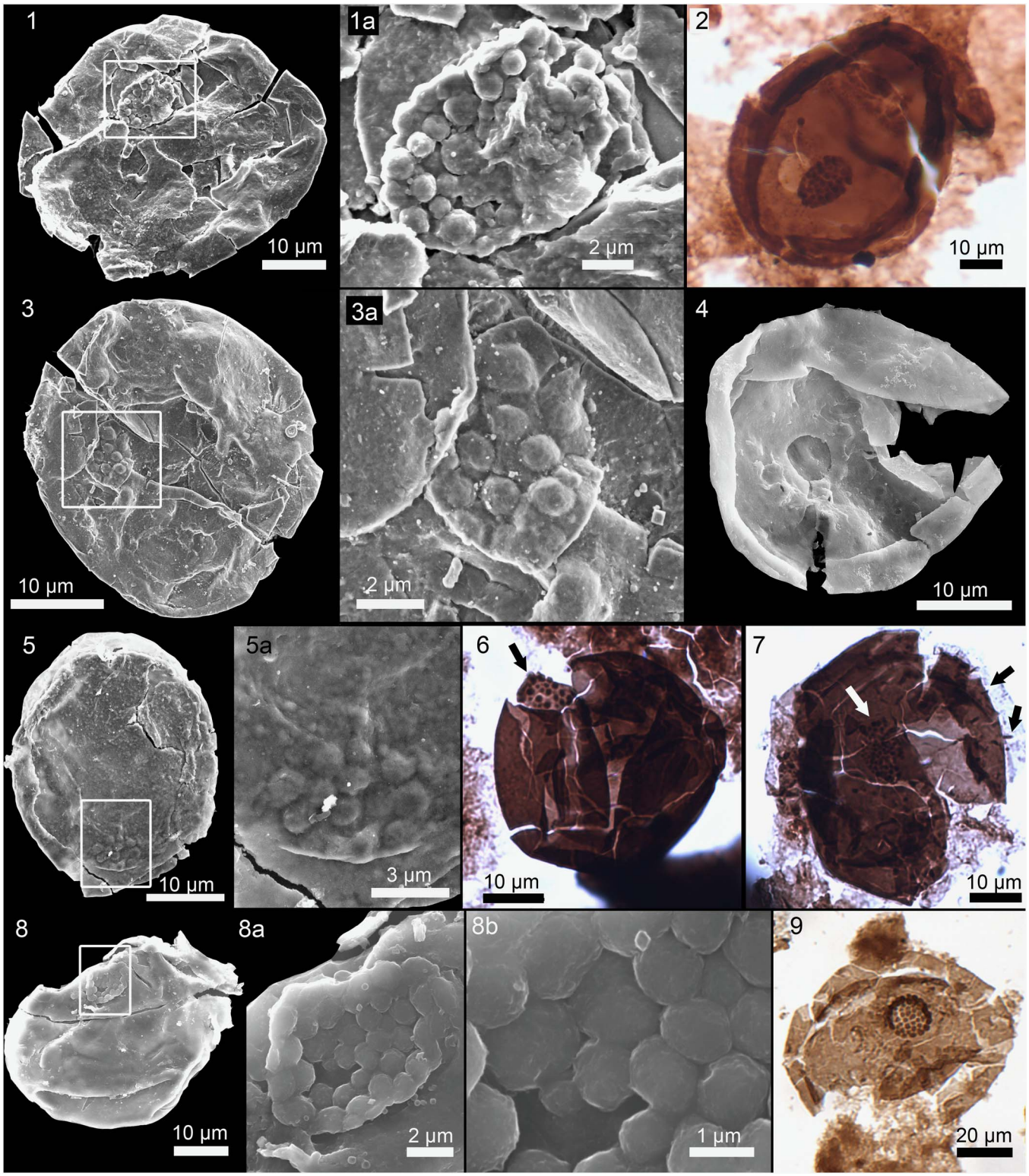

Figure 7. *Kaibabia gemmulella*. n. gen. n. sp. (**1, 1a**) Holotype, UCMP 36082a, SP14-63-11. (**2**) Specimen in which operculum is partially detached, revealing a hole in the wall, SP14-63-11. (**3, 3a**) Specimen with relatively small operculum and few granulae, UCMP 36093b, SP14-63-14. (**4**) Specimen with circular hole in the wall, similar to that in (**2**), likely where operculum once was, UCMP 36099a, SP14-63-23. (**5, 5a**) Specimen with outer envelope preserved, showing impressions of opercular granulae beneath, UCMP 36091b, SP14-63-14. (**6**) TLM image showing partly detached operculum (arrow), UCMP 36083b, SP14-63-11. (**7**) Specimen with possible processes (black arrows) and thin outer envelope (visible on left side). Operculum indicated by white arrow, UCMP 36083c, SP14-63-11. (**8, 8a, 8b**) UCMP 36098, SP14-63-23. (**8a, 8b**) Closeup images of operculum showing numerous ~1 µm diameter granulae. (**9**) UCMP 36076, SP12-63-8.

https://doi.org/10.1017/jpa.2016.57 Published online by Cambridge University Press

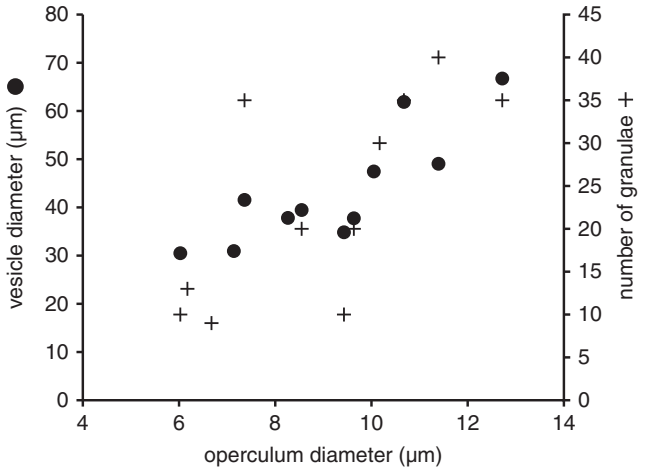

Figure 8. Relationship of the diameter of the operculum in *Kaibabia gemmulella* to the diameter of the vesicle (filled circles) and to number of granulae on the operculum (crosses). Both pairs of variables are positively correlated, indicating that larger opercula are associated both with larger vesicles and with higher numbers of granulae.

asperata (Naumova, 1950) Lindgren, 1982, but regarded *K. gemmulella* as most likely representing a different species on the basis of its distinctive operculum. They suggested the operculum was similar to the protuberances exhibited by some specimens of *Lanulatisphaera laufeldii* (Vidal, 1976b) n. comb. (= *Trachysphaeridium laufeldi*, see illustrations under the species), but the similarity is superficial. We agree that the operculum of *K. gemmulella* can be used as a diagnostic character and herein formalize the assignment of *K. gemmulella* to a distinct taxon.

Vidal and Ford (1985) compared *K. gemmulella* (= *Leiosphaeridia* sp. A) to *Leiosphaeridia kulgunica* Jankauskas, 1980, described from the upper Riphean (Tonian) Shisheniak microbiota of the South Urals (see also Jankauskas et al., 1989; Schopf, 1992, in which the same specimens are illustrated). The holotype of *L. kulgunica* also has a circular hole in the vesicle wall, presumably where an operculum once was. Both the diameter of its vesicle (~30 μm) and that of the hole (~9 μm) fall within the range of sizes exhibited by *K. gemmulella*, and it appears similar to specimens of *K. gemmulella* in which the operculum is missing (e.g., Fig. 7.4). Other specimens in the Shisheniak assemblage, however, fall significantly outside the size range for *K. gemmulella* (Jankauskas, 1980, fig. 1.4). It is possible that *K. gemmulella* is conspecific with *L. kulgunica*, but the absence of an operculum in the latter makes this difficult to assess.

Genus *Lanulatisphaera* new genus

Type species.—*Lanulatisphaera laufeldii* (Vidal, 1976b) n. comb., by monotypy.

Diagnosis.—As for type species.

Etymology.—From the Latin *lanulata*, a diminutive for 'woolly,' referring to the dense, matted appearance of the filaments between the vesicles; and *sphaera* in reference to the shape of the whole of the fossil.

Remarks.—New morphological data require the placement of '*Trachysphaeridium*' *laufeldii* into a new genus. The original description of *Trachysphaeridium* (Timofeev, 1959) lacked a diagnosis but was described as "thick, dense vesicle with shagreen surface" (translated from Timofeev, 1959, p. 28) and as "single-layered sphaerical vesicles 60 to 250 μm in diameter of varying thickness and density with shagreen surface that is usually compressed into folds" (translated from Timofeev, 1966, p. 36). The genus *Trachysphaeridium* was synonymized with *Leiosphaeridia* by Jankauskas et al., (1989) because features Timofeev used to distinguish these two genera, such as folding and a rough-textured vesicle, were considered to be taphonomically induced. This is likely to be the correct placement for some species of *Trachysphaeridium*, including the type species, *T. attenuatum*. However, forms attributed to *T. laufeldii* possess morphological features inconsistent with a placement in *Leiosphaeridia*, a form genus of smooth-walled sphaeroids. Samuelsson (1997) interpreted the processes of this species to be tubercles upon the vesicle and transferred it to *Lophosphaeridium* Timofeev, 1959 ex Downie, 1963, a genus diagnosed by a thick vesicle with a knobby, tuberculate surface sculpture. That transfer is rejected here as a tuberculate sculpture has not been borne out by SEM study. Because no existing genus is known that can accommodate the features diagnostic of this species, a new genus and combination is established here.

Lanulatisphaera laufeldii (Vidal, 1976b) new combination
Figures 9.1–9.6, 10.1–10.7, 11.1–11.4, 12.1–12.7, ?12.8

?1976a *Trachysphaeridium laufeldi*; Vidal, fig. 2A.
1976b *Trachysphaeridium laminaritum*; Vidal, p. 35, fig. 20A–B, F–H.
1976b *Trachysphaeridium laufeldi* Vidal, p. 36, fig. 21A–N.
?1985 cf. *Cymatiosphaeroides kullingii*; Vidal and Ford, p. 359, fig. 3B.
1985 *Trachysphaeridium laufeldi*; Vidal and Ford, p. 375, fig. 7A, B.
?1985 *Trachysphaeridium laufeldi*; Vidal and Ford, p. 375, fig. 7D, F.
1985 *Trachysphaeridium laminaritum*; Vidal and Ford, p. 373, fig. 8A, C.
1996 *Trachysphaeridium laminaritum*; Knoll, pl. 4, fig. 6.
1997 *Lophosphaeridium laufeldii*; Samuelsson, p. 174, fig. 7 F, H, I.
2009 *Lophosphaeridium laufeldi*; Nagy et al., fig. 1J.
?2009 ?*Kildinosphaera verrucata*; Nagy et al., fig. 1F.
2016 *Lanulatisphaera laufeldii*; Riedman and Porter, p. 866, figs. 6.1–6.3, 9.9–9.12, 10.

Holotype.—BV/83.60—1:X/53.3, middle member of the Neoproterozoic Visingsö Group, 83.6 m depth in the Kumlaby borehole, Visingsö Island, Sweden (Vidal, 1976b: fig. 21A-E).

Diagnosis.—Double-walled, originally spheroidal, organic-walled microfossil bearing abundant submicron-diameter solid filamentous processes that arise from the exterior of the inner vesicle and fuse distally forming cone-like structures ~1 to 3 μm long or fuse and branch forming complex networks. Outer envelope bearing ~50 to 100 nm diameter mammillae; filamentous

https://doi.org/10.1017/jpa.2016.57 Published online by Cambridge University Press

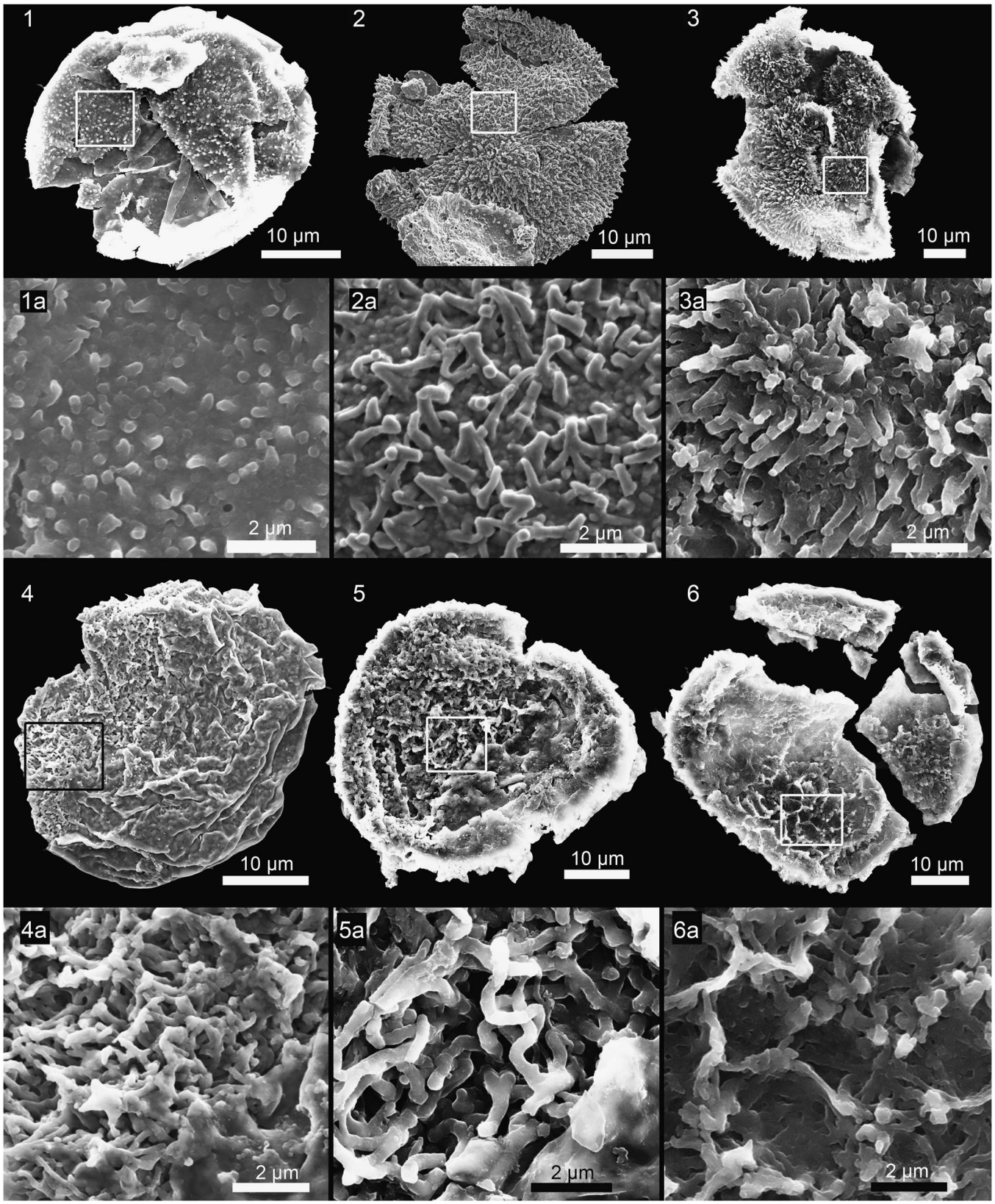

Figure 9. *Lanulatisphaera laufeldii* (Vidal and Ford, 1985) n. comb., showing possible ontogenetic or ecophenotypic series, from (**1, 1a**) individual fibers to (**2, 2a**) cones formed from coalesced fibers, to (**3, 3a, 4, 4a**) a mix of cones and anastomosing network, to (**5, 5a**) network only, to (**6, 6a**) a higher order arrangement of the network. (**1, 1a**) UCMP 36090a, SP14-63-14. (**2, 2a**) UCMP 36085a, SP14-63-12_010. (**3, 3a**) UCMP 36073b, SP12-63-30. (**4, 4a**) Specimen also shown using TLM in Fig. 12.5; UCMP 36072a, SP12-63-30. (**5, 5a**) UCMP 36073c, SP12-63-30. (**6, 6a**) UCMP 36073d, SP12-63-30.

https://doi.org/10.1017/jpa.2016.57 Published online by Cambridge University Press

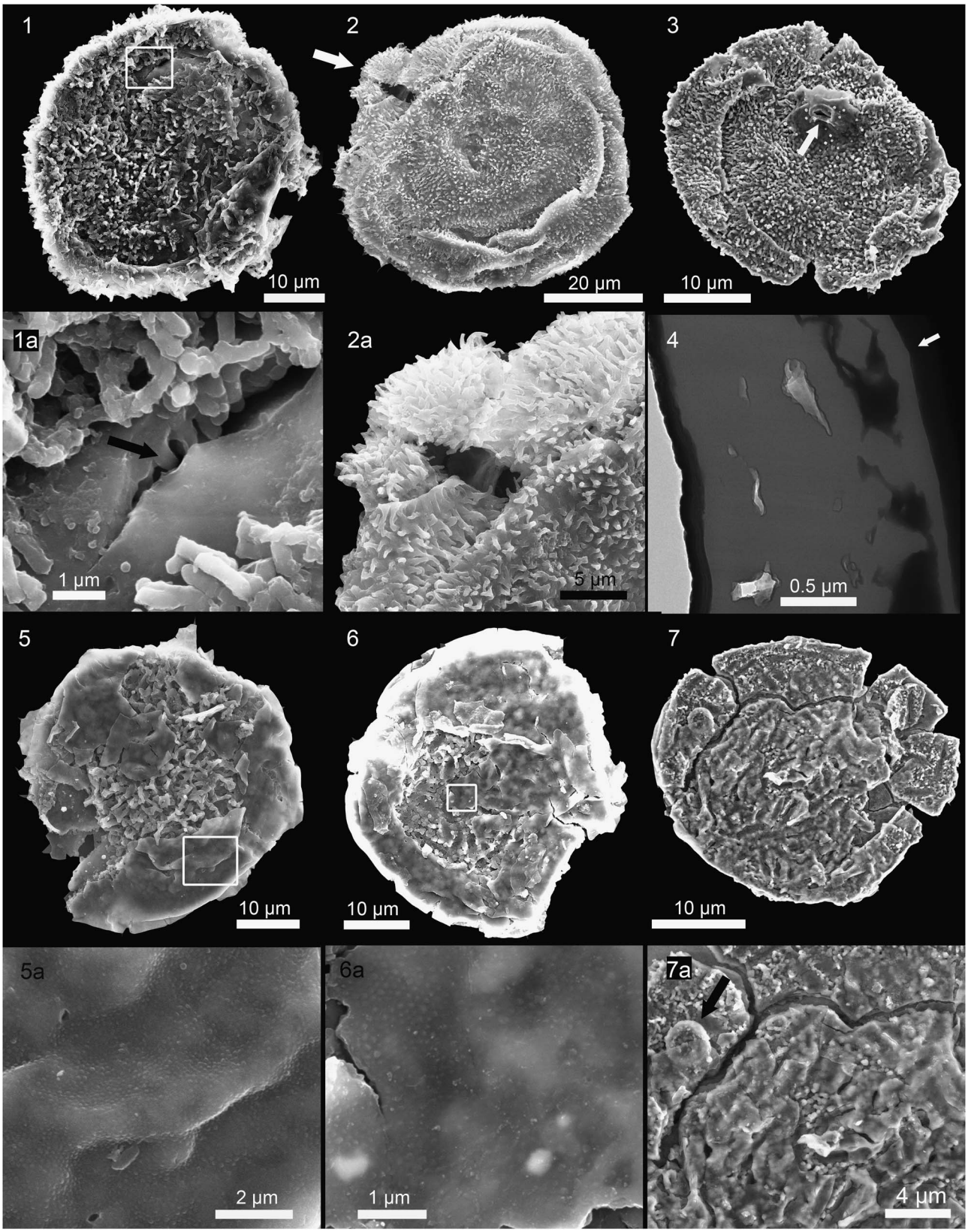

Figure 10. *Lanulatisphaera laufeldii* (Vidal and Ford, 1985) n. comb. (**1, 1a**) Torn specimen showing that the vesicle's interior surface is smooth and that the fibers are outgrowths of the vesicle wall (black arrow in **1a**), UCMP 36073f, SP12-63-30. (**2, 2a**) Specimen with rounded protuberance (white arrow in **2**) UCMP 36099b, SP14-63-23. (**3**) Specimen with circular opening (white arrow) in its outer envelope (only a fragment of the envelope is preserved), UCMP 36086b, SP14-63-12. (**4**) Bright field TEM image of vesicle wall and envelope in cross section. Envelope clearly visible on right; white arrow points to possible mamilla in cross section; UCMP 36087b, SP14-63-14. (**5, 5a**) Specimen showing nano-scale mammillae on the outer surface of the envelope, UCMP 36090b, SP14-63-14. (**6, 6a**) Specimen showing (**6**) furrows as well as (**6a**) mammillae, UCMP 36087a, SP14-63-14. (**7, 7a**) specimen showing (**7**) furrows and (**7a**) ~2-µm-diameter disc (black arrow), UCMP 36079a, SP14-63-11.

https://doi.org/10.1017/jpa.2016.57 Published online by Cambridge University Press

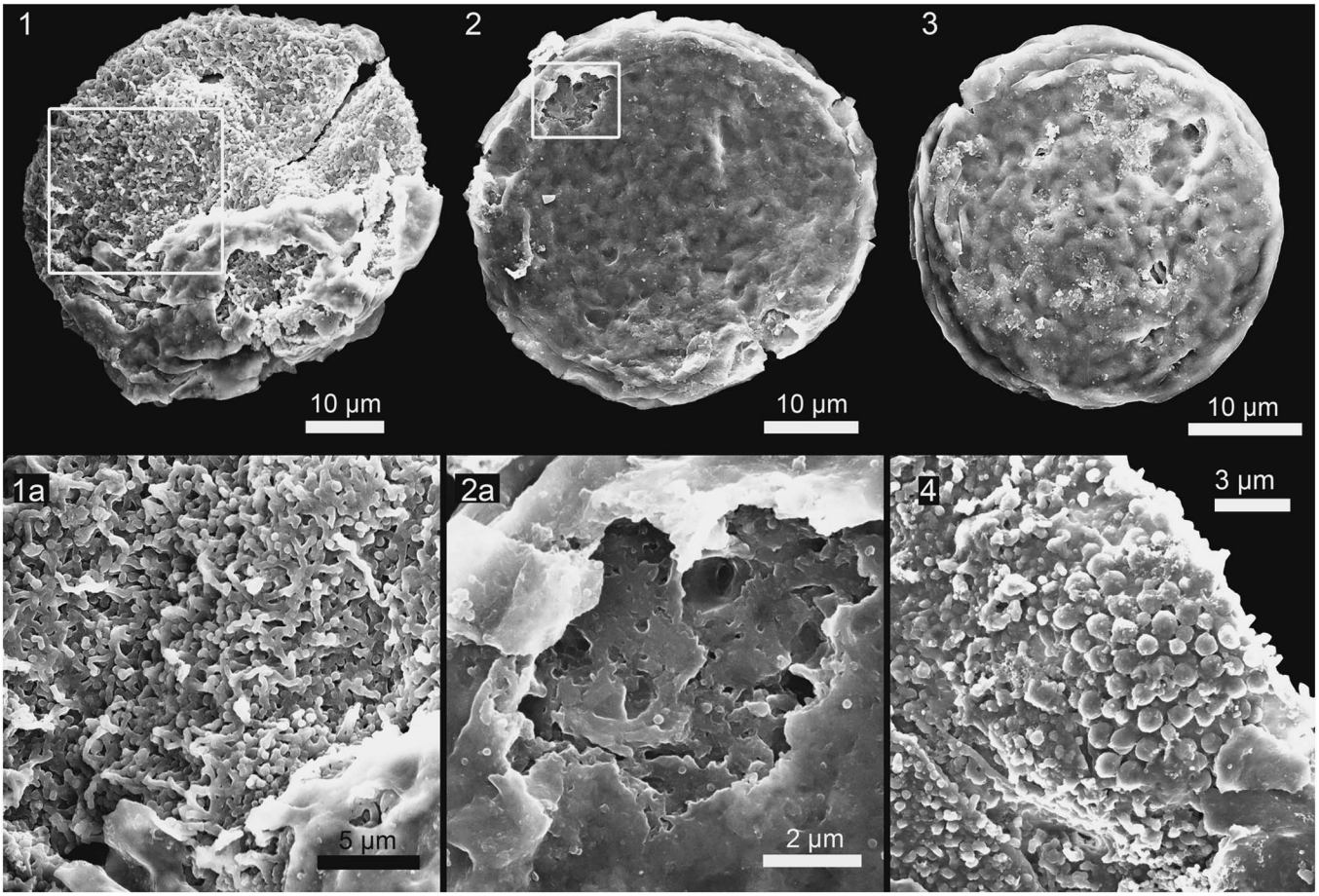

Figure 11. *Lanulatisphaera laufeldii* (Vidal and Ford, 1985) n. comb. (**1, 1a**) Specimen with compressed network of fibers, UCMP 36073g, SP12-63-30. (**2, 2a**) Specimen with outer envelope preserved, showing network with fused fibers, likely reflecting taphonomic processes, UCMP 36073h, SP12-63-30. (**3**) Specimen with complete outer envelope (closeup images of holes in the outer envelope, not shown, reveal the presence of fibers beneath, confirming its assignment to *L. laufeldii*); UCMP 36073e, SP12-63-30. (**4**) Specimen showing possible opercula consisting of multiple rounded granulae, similar to the opercula of *Kaibabia gemmulella*, UCMP 36096a, SP14-63-17.

processes appear to make no contact with outer envelope (emended from Vidal, 1976b.)

Occurrence.—Tanner, Jupiter, Carbon Canyon, Duppa, and Awatubi members of the Chuar Group and a possible occurrence in the Walcott Member; also occurs in other Tonian units including the Alinya Formation, Giles 1 drill core, Officer Basin, Australia (Riedman and Porter, 2016); Visingsö Group, Sweden (Vidal, 1976b); the Karuyarvinskaya Formation, Kildinskaya Group, Kola Peninsula, Russia (Samuelsson, 1997); and the Mount Watson and Red Pine Shale, Uinta Mountain Group (Vidal and Ford, 1985; unpublished data, Porter, 2014). Reported but not illustrated from the late Tonian Vadsø and Tanafjorden groups, East Finnmark, Norway (Vidal, 1981); and the Ryssö Formation, Nordaustlandet, Svalbard (Knoll and Calder, 1983). Possible occurrence in the Neoproterozoic Eleonore Bay Group (Vidal, 1976a).

Description.—Organic-walled vesicles 24 to 84 µm in diameter (mean = 42 µm, SD = 10 µm, N = 79), with walls ~0.5 µm thick. Electron density of walls homogeneous in cross section (Fig. 10.4). Inner surface of wall smooth (Fig. 10.1). Continuous with, and arising from (Fig. 10.1), the outer surface of the vesicle are moderately to densely packed solid fibers, ~0.2 to 0.4 µm in diameter. In some specimens, the fibers coalesce to form cone-like structures 0.5 to 2.9 µm high (mean = 1.4 µm, SD = 0.6 µm, N = 20) and up to 2 µm wide at their base, with a tapered tip comparable in diameter to a single fiber (Fig. 9.2). In other specimens, the fibers both coalesce and branch, forming a network (Fig. 9.5) in which the fibers may appear to be more or less densely woven or even fused (Fig. 11.1, 11.2), the latter state likely reflecting taphonomic alteration. Some specimens exhibit an intermediate state, with both the network and cone-like structures visible (Fig. 9.3, 9.4). The network may form higher-order structures consisting of hollow spaces ~2 to 4 µm wide, separated by thin walls formed of the fiber network (Fig. 9.6), although whether this is original or reflects taphonomic processes is not clear (see the following). One specimen exhibits a rounded protuberance ~15 µm in diameter, also covered in fibers, and extending ~7 µm out from the wall (Fig. 10.2; cf. the "bulbous spiny protuberance" of Vidal and Ford, 1985, p. 375, fig. 7D–H; see also Vidal, 1976b, fig. 21A–N).

Several specimens exhibit a system of furrows in the network or the cones (Fig. 10.6, 10.7). Furrows are ~1 µm wide, straight or slightly sinuous, and often occur in parallel sets, with different sets at angles to each other. The furrows appear to be

https://doi.org/10.1017/jpa.2016.57 Published online by Cambridge University Press

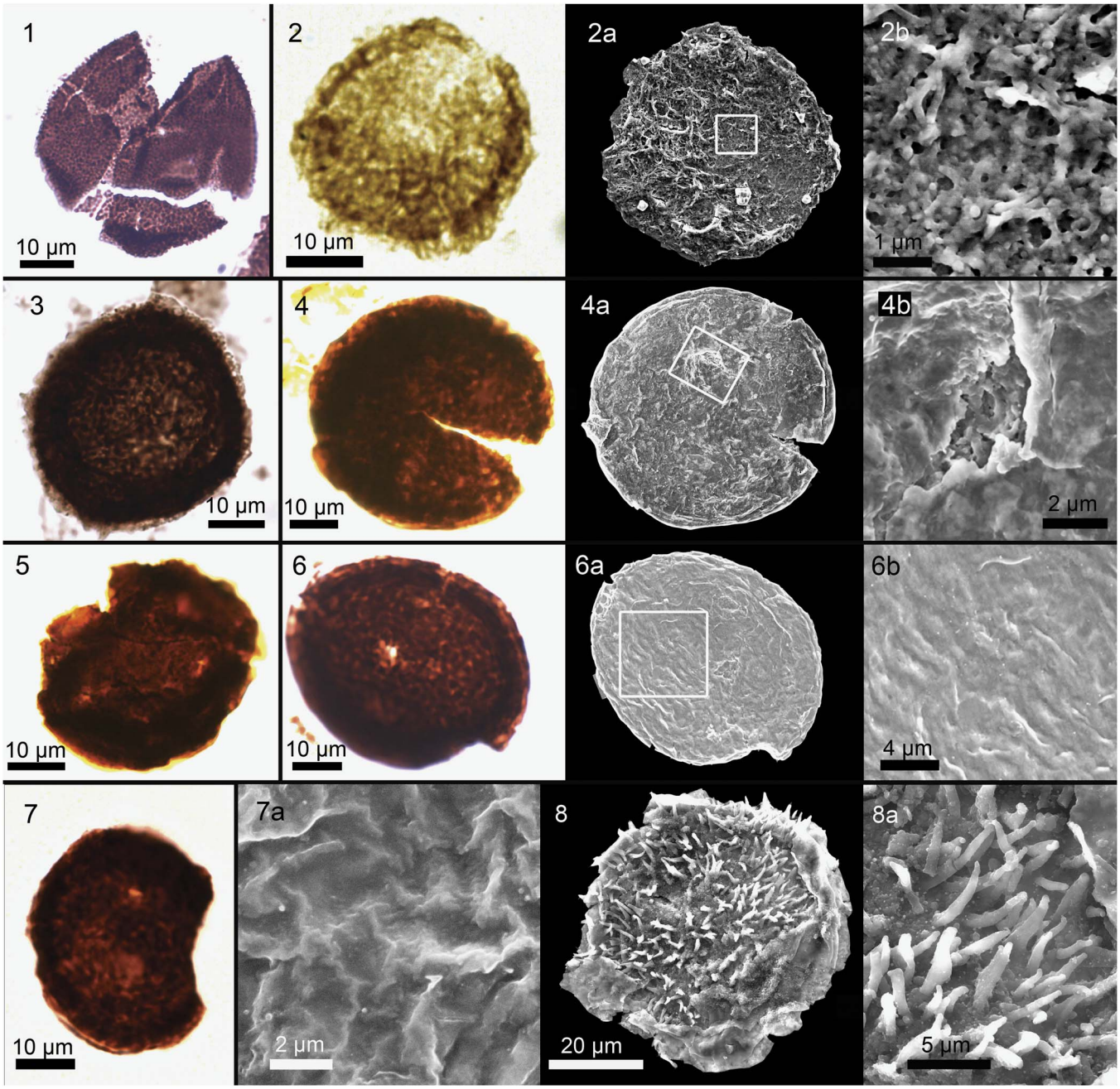

Figure 12. (**1–7**) *Lanulatisphaera laufeldii* (Vidal and Ford, 1985) n. comb. and (**8**) ?*L. laufeldii*. (**1**) Specimen with cones, UCMP 36083d, SP14-63-11. (**2, 2a, 2b, 4, 4a, 4b**) Specimens with mottled alveolar appearance similar to *Trachysphaeridium laminaritum* sensu Vidal (1976b) and Vidal and Ford (1985) that exhibit anastomosing filamentous processes (**2a, 2b, 4a, 4b**; note fused network visible beneath the envelope). (**2, 2a, 2b**) UCMP 36102, SP14-63-11. (**4, 4a, 4b**) UCMP 36082b, SP14-63-11. (**3**) Specimen with fibrous network visible on vesicle perimeter, UCMP 36083j, SP14-63-11. (**5**) Specimen with irregular textured appearance; SEM image of the same specimen illustrated in Figure 9.4, UCMP 36072b, SP12-63-30. (**6, 6a, 6b, 7, 7a**) Specimens with alveolar appearance similar to *T. laminaritum* sensu Vidal (1976b) and Vidal and Ford (1985), with outer envelopes similar to those of confirmed specimens of *L. laufeldii* (**6a, 7a**). (**6, 6a, 6b**) UCMP 36080e, SP14-63-11. (**7, 7a**) UCMP 36089b, SP14-63-14. (**8, 8a**) ?*L. laufeldii* specimens similar to those described as cf. *Cymatiosphaeroides kullingii* by Vidal and Ford (1985), UCMP 36074a, SP12-63-30.

carved into the vesicle ornamentation and occur both in specimens with a network of filaments (Fig. 10.6) and in those with cone-like structures (Fig. 10.7). These furrows appear similar to the higher-order structures mentioned previously (Fig. 9.6) but differ in that the hollow spaces are rounded or polygonal rather than sets of straight parallel channels. Nonetheless, these features may be related, although it is not clear whether they represent taphonomic or biological variants of *Lanulatisphaera laufeldii*. The furrows also appear similar to sets of parallel crests and troughs that characterize the ornament of *Volleyballia dehlerae* n. gen. n. sp. They are distinguished, however, by the fact that *V. dehlerae* lacks filamentous processes.

Some specimens retain an outer envelope, ~0.1 μm thick, translucent in transmitted light, and covered in 50- to 100-nm-diameter mammillae, regularly spaced and somewhat regularly arranged on the outer surface (Fig. 10.5a, 10.6a). TEM images

https://doi.org/10.1017/jpa.2016.57 Published online by Cambridge University Press

show that mammillae are continuous with the wall of the envelope; they are not compositionally or structurally distinct from it (Fig. 10.4). In one specimen a partly preserved outer envelope exhibits a ~2-µm-diameter circular opening surrounded by a rim (Fig. 10.3; cf. "circular opening" of Vidal and Ford, 1985, p. 375). The outer envelope may be irregularly wrinkled or unwrinkled or may be dimpled (Figs. 9.4, 10.6, 11.2, 11.3). We suspect that the dimpling reflects the higher-order structures and, possibly, furrows in the underlying network (discussed previously; Figs. 9.6, 10.6, 10.7).

Possible opercula have been observed in a handful of specimens (Fig. 11.4). They consist of a number of closely packed rounded granulae, similar in size and shape to those found on the opercula of *Kaibabia gemmulella*. It is not clear whether they are related to the circular openings described in the preceding.

Specimens appear highly variable under transmitted light microscopy. In some, cones are visible (Fig. 12.1). In others, the fibrous network may be visible around the edges of the fossil (Fig 12.3) but otherwise appears as a mottled pattern on the fossil surface. This mottled pattern appears similar to the alveolar structures reported by Vidal and Ford (1985) and Vidal (1976b) in their description of specimens they assigned to *Trachysphaeridium laminaritum* and which we place in *L. laufeldii* (see 'Remarks'). Many specimens appear distinct from both of these, exhibiting, for example, irregularly spotted walls (Fig. 12.5).

Materials.—Hundreds of specimens (samples SP14-63-11, -12, -14, -17, -23, and SP12-63-30).

Basionym.—*Trachysphaeridium laufeldi* Vidal, 1976b (p. 36–38).

Remarks.—Here we assign to a single species specimens that Vidal ascribed to two species, *Trachysphaeridium laufeldi* and *T. laminaritum* Timofeev, 1966 (see Vidal, 1976b; Vidal and Ford, 1985). Although these specimens appear distinct under light microscopy, we believe they are part of a single species showing continuous variation in form from '*T. laufeldi*' type (vesicles covered in ~1-µm-long cones) to '*T. laminaritum*' type (a network of fibers covered by an outer envelope). Definitive confirmation of this is difficult because specimens that under light microscopy have the characteristic 'alveolar' appearance of *T. laminaritum* sensu Vidal (Vidal, 1976b; Vidal and Ford, 1985) have an intact outer envelope; the filamentous processes that are diagnostic of *L. laufeldii* are not visible. Nonetheless, several lines of evidence support this assignment. First, a few specimens that do demonstrably have filamentous processes (Fig. 12.3, 12.4) appear similar under transmitted light to specimens of *T. laminaritum* sensu Vidal—athough their preservation is not good enough to confirm conspecificity. Second, the outer envelopes of those specimens that are confidently interpreted under TLM to be conspecific with *T. laminaritum* sensu Vidal (Fig. 12.6, 12.7) are similar to the outer envelopes of specimens known to be *L. laufeldii* (e.g., Fig. 11.2, 11.3) and different from the outer envelopes of other taxa in the assemblage, most notably *Culcitulisphaera revelata* Riedman and Porter, 2016, the species most likely to be mistaken for *T. laminaritum* sensu Vidal (see synonymy and remarks for *C. revelata* in the preceding). Third, light microscopy observations suggest that *T. laminaritum* sensu Vidal is among the most common constituents of the Chuar assemblage, whereas SEM observations indicate that *L. laufeldii*—as represented by the full range of forms from cone-bearing vesicles to those with anastomosing networks—is the most common constituent of Chuar assemblages. If *T. laminaritum* sensu Vidal is not part of the *L. laufeldii* species, it's not clear which of the species observed under SEM it might otherwise be. Finally, in every unit that *T. laminaritum* sensu Vidal has been reported, *T. laufeldii* sensu Vidal has also been observed (Vidal, 1976b; Vidal, 1981; Vidal and Ford, 1985; Riedman and Porter, 2016; L. Riedman, personal observation), consistent with what would be expected if these two forms are morphological variants of the same species.

The name *T. laminaritum* has priority over *Lanulatisphaera laufeldii*—it was erected in 1966 by Timofeev—but it appears to have been erroneously applied to the Chuar specimens. Timofeev's (1966) illustration (hand drawing; pl. 7, fig. 3) shows a specimen that is much larger than the Chuar specimens (vesicles have a diameter of "70 to 250 microns, usually 120–200 microns"; Timofeev, 1966, p. 36) and is covered by numerous very fine dots (~1 µm scale). (The specimen illustrated by Schopf, 1992, as the holotype of *T. laminaritum* is apparently in error and is instead a specimen of *Culcitulisphaera revelata*; see Riedman and Porter, 2016). The name *L. laufeldii* is therefore used for this species, with the suffix corrected according to Article 60.12 and 60.C1 of the International Code of Nomenclature for Algae, Fungi, and Plants (Samuelsson, 1997).

It is likely that forms described by Vidal and Ford (1985) under the designation cf. *Cymatiosphaeroides kullingii* Knoll, 1984 also belong in *L. laufeldii* because similar specimens observed under SEM appear to exhibit processes formed via the coalescence of fibers (Fig. 12.8). These are, in any case, distinct from *Cymatiosphaeroides* Knoll, 1984 emend. Knoll, Swett, and Mark, 1991 in that the processes do not connect to an outer wall or thicken at their distal end. In addition, the specimens illustrated here and in Vidal and Ford (1985) exhibit only a thin outer envelope, whereas in *Cymatiosphaeroides*, the outer wall comprises a relatively thick inner layer and as many as six thin outer layers (Knoll, 1984; Knoll et al., 1991).

As documented here, *L. laufeldii* exhibits extensive, continuous variation in morphology (Fig. 25) ranging from specimens with short fibrous processes not yet coalesced (Fig. 9.1) to specimens with fibrous processes coalesced into cones (= *T. laufeldi* sensu Vidal and Ford, 1985; Fig. 9.2), specimens with both cones and networks (Fig. 9.3, 9.4,), specimens with extensive networks (Fig. 9.5), and specimens in which the network is organized into a higher-order structure (Fig. 9.6). Similarly wide-ranging variation occurs in other fossil and modern cysts (e.g., Lewis and Hallet, 1997; Agić et al., 2015) and can reflect either ontogenetic or ecophenotypic variation. For example, in the dinoflagellate *Lingulodinium polyedrum* (Stein, 1883) Dodge, 1989, premature rupture of the outermost membrane surrounding the cyst truncates its morphological development, resulting in cysts with fewer, more irregularly distributed processes and/or processes of very different sizes and shapes (Kokinos and Anderson, 1995). Ecophenotypic variation in cyst morphology has also been documented in dinoflagellates, where differences in the salinity

https://doi.org/10.1017/jpa.2016.57 Published online by Cambridge University Press

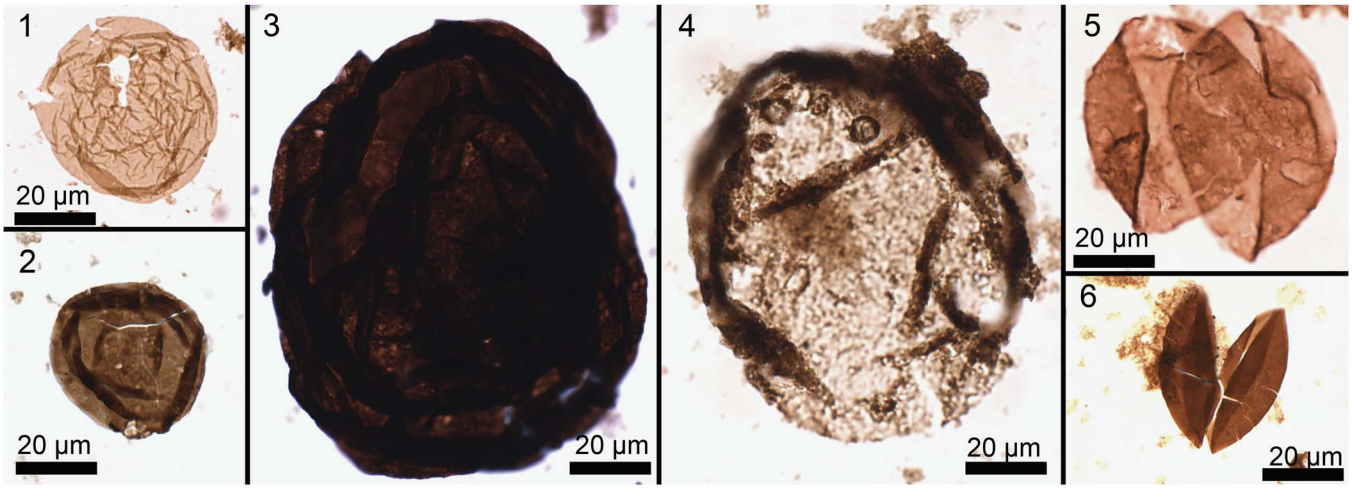

Figure 13. *Leiosphaeridia* Eisenack, 1958b. (**1, 5**) *Leiosphaeridia minutissima* (Naumova, 1949) Jankauskas in Jankauskas et al., 1989. (**1**) UCMP 36094a, SP14-63-14; (**5**) UCMP 36097a, SP14-63-17. (**2, 6**) *Leiosphaeridia crassa* (Naumova, 1949) Jankauskas in Jankauskas et al., 1989. (**2**) UCMP 36078, SP14-53-6; (**6**) UCMP 36094b, SP14-63-14. (**3**) *Leiosphaeridia jacutica* (Timofeev, 1966) Mikhailova and Jankauskas in Jankauskas et al., 1989, UCMP 36083e, SP14-63-11. (**4**) *Leiosphaeridia tenuissima* Eisenack, 1958a, note degraded wall, UCMP 36077, SP14-53-20.

and temperature of seawater in which the cysts formed can influence the length and density of their processes (e.g., Ellegaard, 2000; Mertens et al., 2009). Whatever the source of variation in *L. laufeldii*, this study underscores the importance of examining numerous specimens of varying preservational quality so that a species' full range of biological and taphonomic variability can be documented (cf. Riedman and Porter, 2016).

Genus *Leiosphaeridia* Eisenack, 1958b

Type species.—*Leiosphaeridia baltica* Eisenack, 1958b.

Occurrence.—Occurs throughout the Chuar Group; widespread in Proterozoic and Phanerozoic assemblages.

Remarks.—*Leiosphaeridia* is a form genus containing smooth-walled spherical to ellipsoidal microfossils. Here we follow Butterfield et al. (1994) and divide *Leiosphaeridia* specimens into one of four species based on to wall thickness (thin walled vs. thicker walled, as determined by degree of opacity) and diameter (<70 μm vs. >70 μm). That this is an artificial classification is evidenced by the difficulty we had in assigning specimens to one of the four species. Wall opacity, which may or may not be an accurate indicator of wall thickness, varies widely and continuously among Chuar specimens. Many specimens exhibit what we considered medium opacity and thus are neither thick walled (*L. crassa* [Naumova, 1949] and *L. jacutica* [Timofeev, 1966]) nor thin walled (*L. minutissima* [Naumova, 1949] and *L. tenuissima* [Eisenack, 1958a]). Similarly, vesicle diameters exhibited unimodal distribution centered at 48 μm; there was no natural break at or around 70 μm (in contrast to that reported by Butterfield et al., 1994, fig. 4, p. 40). Nonetheless, this classification is broadly useful in that it revealed a possible stratigraphic pattern in the distribution of leiosphaerid sizes: upper Awatubi and Walcott samples showed a preponderance of larger specimens (mostly *L. tenuissima)* compared to those in the lower Chuar, in which almost all leiosphaerids are small (57% of vesicles are greater than 70 μm in the upper part of the Chuar vs. 12% in the lower part). It is possible that a more biologically realistic taxonomy could be developed for the Chuar leiosphaerids, but that is beyond the scope of this paper.

Leiosphaeridia crassa (Naumova, 1949)
Jankauskas in Jankauskas, Mikhailova, and Hermann, 1989
Figure 13.2, 13.6

1949 *Leiotriletes crassus* Naumova, p. 54, pl. 1, figs. 5, 6, pl. 2, figs. 5, 6.
1989 *Leiosphaeridia crassa*; Jankauskas et al., p. 75, pl. 9, figs. 5–10.

Holotype.—No holotype was designated by Naumova (1949). Jankauskas (in Jankauskas et al., 1989, p. 75) designated a specimen (plate 1, fig. 3) from Naumova (1949) as lectotype. However, this specimen was not of a species they synonymized with *Leiosphaeridia crassa,* but was instead part of *Leiotriletes simplicissimus*, a species Jankauskas et al., (1989) synonymized with a different species of *Leiosphaeridia*, *L. minutissima*.

Description.—Solitary, spheroidal, smooth, single-walled vesicles 21 to 70 μm in diameter (mean = 44 μm, SD = 12 μm, N = 28). Wall medium to dark but translucent. Some specimens with medial split.

Materials.—Twenty-eight specimens (samples AK10-60-7, SP12-63-23, SP14-53-6, -7, -10, -14, SP14-63-8, -14, -17, and -19).

Leiosphaeridia jacutica (Timofeev, 1966)
Mikhailova and Jankauskas in Jankauskas, Mikhailova, and Hermann, 1989
Figure 13.3

1966 *Kildinella jacutica* Timofeev, p. 30, pl. 7, fig. 2.
1989 *Leiosphaeridia jacutica*; Jankauskas et al. p. 77, pl. 12, figs. 3, 7, 9.

https://doi.org/10.1017/jpa.2016.57 Published online by Cambridge University Press

Holotype.—Preparation number 452/1, Biostratigraphy Laboratory, ЛИГЕД АН СССР Maya River Collection, late Mesoproterozoic/early Neoproterozoic Lakhanda Group, Russia (Timofeev, 1966: pl. 7, fig. 2).

Description.—Solitary, spheroidal, smooth, single-walled vesicles 72 to 102 µm in diameter (mean = 92 µm, SD = 21 µm, N = 6). Vesicle dark but translucent.

Materials.—Six specimens (samples SP12-63-30, SP14-53-14, SP14-63-11, -17, and -19).

Leiosphaeridia minutissima (Naumova, 1949) Jankauskas in Jankauskas, Mikhailova, and Hermann, 1989
Figure 13.1, 13.5

1949 *Leiotriletes minutissimus* Naumova, p. 52, pl. 1, figs. 1, 2, pl. 2, figs. 1, 2.
1989 *Leiosphaeridia minutissima*; Jankauskas et al., p. 79, pl. 9, figs. 1–4, 11.

Lectotype.—No holotype was designated by Naumova (1949). Jankauskas (in Jankauskas et al., 1989, p. 80) designated a specimen of *Leiotriletes minutissimus* (pl. 1, fig. 1) from Naumova (1949) as lectotype.

Description.—Solitary, spheroidal, smooth, single-walled vesicles 14 to 60 µm in diameter (mean = 42 µm, SD = 12 µm, N = 60). Vesicle medium-thin to very thin walled. Some specimens with medial split (Fig. 13.5, 13.6).

Materials.—Sixty specimens (samples AK10-60-7, SP14-53-7, -10, -20, SP14-63-8, -11, -14, -17, and -19).

Remarks.—The thinnest-walled specimens of *L. minutissima* (e.g., Fig. 13.1) may be outer envelopes of co-occuring ornamented acritarch species (e.g., Moczydłowska, 2010; see section on 'Biological affinities of Chuar microfossils' later in this paper).

Leiosphaeridia tenuissima Eisenack, 1958a
Figure 13.4

1958a *Leiosphaeridia tenuissima* Eisenack, p. 391, pl. 1, figs. 2, 3.
1989 *Leiosphaeridia tenuissima*; Jankauskas et al., p. 81, pl. 9, figs. 12, 13.

Holotype.—Preparation A_3, 3 number 4 from the *Dictyonema*-shales of the Ordovician Baltic (Eisenack, 1958a: pl. 1, fig. 2).

Description.—Solitary, spheroidal, smooth, single-walled vesicles 72 to 132 µm in diameter (mean = 91 µm, SD = 16 µm, N = 22). Vesicle medium-thin to very thin walled. Some specimens with medial split.

Materials.—Twenty-two specimens (samples AK10-60-7, SP14-53-14, -20, SP14-63-8, -11, and -17).

Microlepidopalla new genus

Type species.—*Microlepidopalla mira* n. sp., by monotypy.

Diagnosis.—As for type species by monotypy.

Etymology.—A combination of the Greek *mikros*, meaning little, *lepidos*, meaning scale, and *palla*, meaning ball, thus 'little scaly ball,' in reference to its appearance and similarities to scale-bearing protists.

Remarks.—Although the shape and size of *Microlepidopalla mira* ellipsoids are broadly comparable to those of *Eosynechococcus moorei* Hofmann, 1976, their occurrence in tightly formed circular clusters is distinct from the irregularly shaped, loose aggregates of *E. moorei*. (Other aggregates of cell-like structures, e.g., *Sphaerophycus parvum* Schopf, 1968 and *Gloeotheceopsis aggregata* Zhang, 1988, are even less like *M. mira*, in terms of both the shapes and sizes of their cells and their arrangement in the aggregates.) Furthermore, none of the hundreds of ellipsoids of *M. mira* that have been observed show any evidence of transverse fission, in constrast to *E. moorei* (Golubic and Campbell, 1979) and other bacterial fossils. Indeed, as will be detailed further in another paper (see Porter et al., 2013), these fossils bear strong similarities with scale-bearing protists, including centrohelids, haptophytes, and pompholyxophryids. Given their distinctive appearance, new genus and species names are erected herein for these specimens.

Microlepidopalla mira new species
Figure 14.1–14.7

?1984 *Sphaerophycus* aff. *parvum*; Tynni and Uutela, p. 16, figs. 65, 66.

Holotype.—UCMP 36104b, sample SP14-63-29, SEM stub 6, Duppa Member, Galeros Formation, Lava Chuar Canyon locality (Fig. 14.6; for location of specimen on stub see Fig. S1).

Diagnosis.—Circular clusters, ~10 to 30 µm in diameter, composed of numerous overlapping organic-walled ellipsoidal structures, 2 to 8 µm in length and 1 to 4 µm in width.

Occurrence.—Tanner, Jupiter, Carbon Canyon, Duppa, and Awatubi members, Chuar Group; late Tonian Moosehorn Lake Formation, Uinta Mountain Group, Utah (SMP personal observation). Possible occurrences in the poorly constrained ?Mesoproterozoic Muhos Formation, western Finland (Tynni and Uutela, 1984).

Description.—Circular or subcircular clusters of flattened ellipsoids; ellipsoids 2.2 to 7.4 µm in length (mean = 4.0 µm, SD = 1.0 µm, N = 164), 1.3 to 3.3 µm in width (mean = 2.1 µm, SD = 0.4 µm, N = 156), and with aspect ratios 1.1 to 3.4 (mean = 1.9, SD = 0.4, N = 153). Circular clusters 9 to 31 µm in diameter (mean = 19 µm, SD = 8 µm, N = 19). Ellipsoids may also occur singly, sometimes lying atop other microfossils. Within a cluster, ellipsoids may overlap but are not

https://doi.org/10.1017/jpa.2016.57 Published online by Cambridge University Press

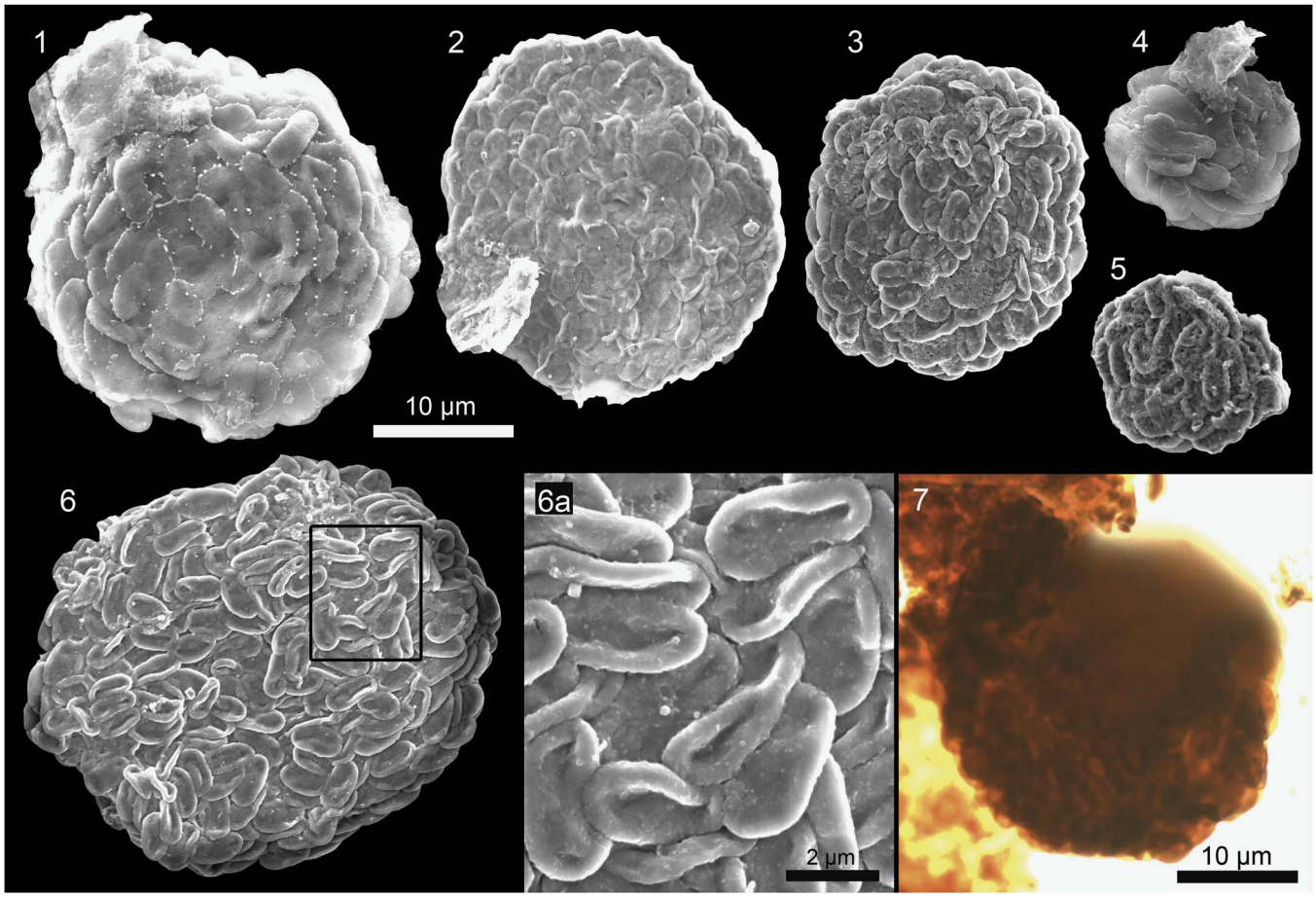

Figure 14. *Microlepidopalla mira* n. gen. n. sp. (**1**) UCMP 36074b, SP12-63-30. (**2**) UCMP 36091c, SP14-63-14. (**3**) UCMP 36103, SP14-63-29. (**4**) UCMP 36074c, SP12-63-30. (**5**) UCMP 36101, SP14-63-29. (**6, 6a**) Holotype, UCMP 36104b, SP14-63-29. (**7**) Transmitted light image of *M. mira*, UCMP 36094e, SP14-63-14. Same scale bar for (**1–6**).

imbricated; some lie fully on top of others such that their entire outline is visible.

Etymology.—From the Latin *mira*, meaning strange and wonderful, with reference to the fossil's aesthetic beauty and to the wonder one feels discovering beautiful fossils in rocks so old.

Materials.—Forty-eight clusters and more than a dozen isolated ellipsoids (samples SP12-63-30, SP14-63-11, -12, -14, -17, -24, -29, and -30.)

Remarks.—The wide variation in cluster diameter (cf. Fig. 14.4, 14.5 vs. Fig. 14.6) may point to the presence of more than one species in the Chuar assemblage, but we were unable to reject the null hypothesis that the distribution of cluster diameters is unimodal, and therefore place these specimens in a single species.

Genus *Navifusa* Combaz, Lange, and Pansart, 1967 ex Eisenack, 1976

Type species.—*Navifusa navis* (Eisenack, 1938) Eisenack, 1976

Navifusa majensis Pyatiletov, 1980
Figure 23.1

1980 *Navifusa majensis* Pyatiletov, p. 144, fig. 1.
1994 *Navifusa majensis*; Hofmann and Jackson, p. 20, fig. 15.1–15.4.

Holotype.—ИГиГ СО АН СССР Preparation number 685 from Khabarovsk Krai, left bank of Maya River, late Mesoproterozoic–early Neoproterozoic Lakhanda Group, third subsuite, Russia (Pyatiletov, 1980, fig. 1a).

Materials.—A single specimen, 60 µm long and 30 µm wide (sample SP14-63-14).

Genus *Palaeastrum* Butterfield in Butterfield, Knoll, and Swett, 1994

Type species.—*Palaeastrum dyptocranum* Butterfield *in* Butterfield et al., 1994, by monotypy.

Diagnosis.—As for type species (emended from Butterfield et al., 1994).

Remarks.—Butterfield et al. (1994) provided a separate diagnosis for the genus *Palaeastrum* and for its single species, *P. dyptocranum*, differentiating the latter from the former by stating that the latter is "[a] species of *Palaeastrum* with

https://doi.org/10.1017/jpa.2016.57 Published online by Cambridge University Press

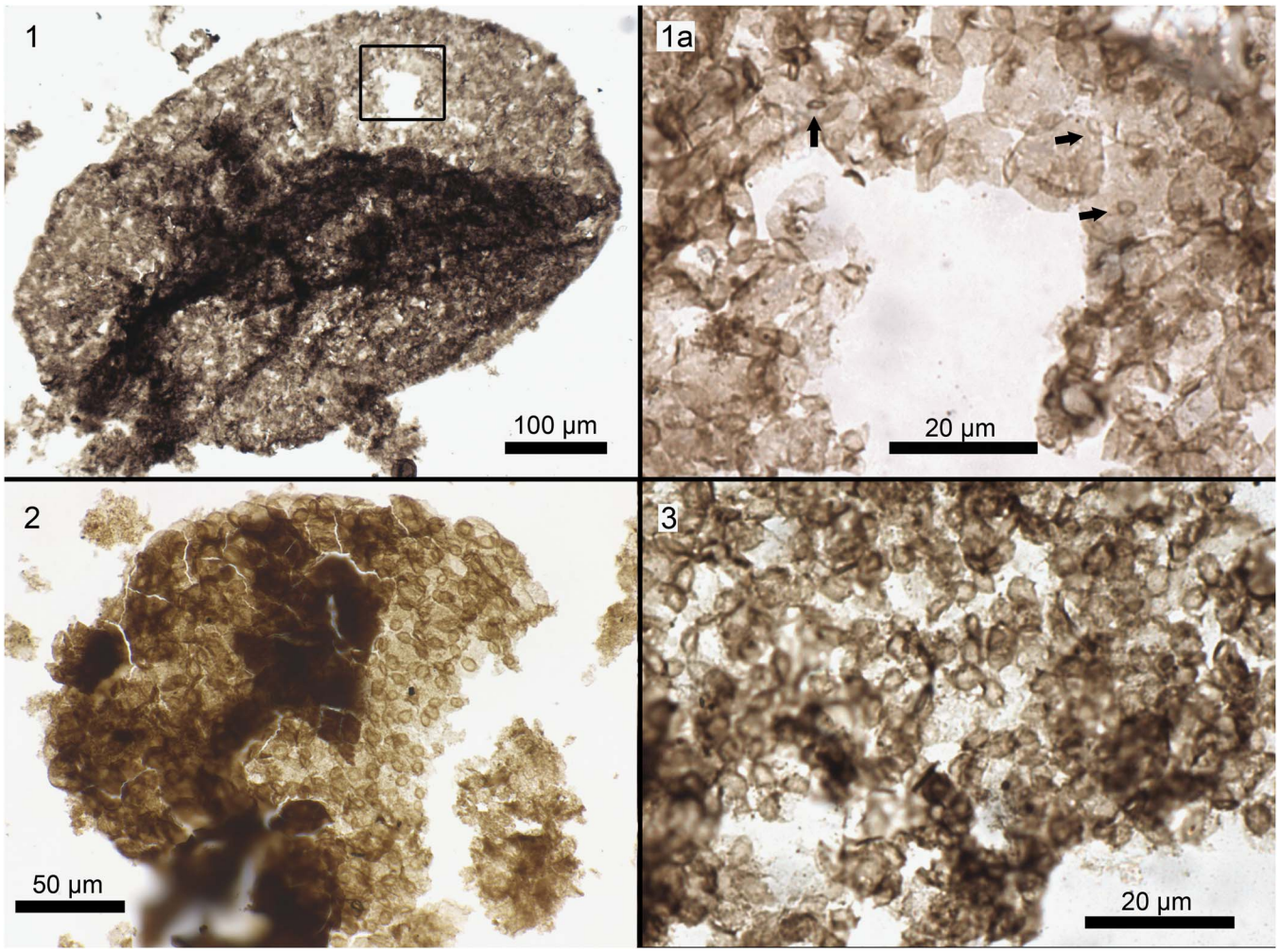

Figure 15. *Palaeastrum dyptocranum* Butterfield in Butterfield et al., 1994. (**1, 2**) Nearly complete colonies showing ellipsoidal shape. (**1, 1a**) UCMP 36096g, SP14-63-17. Black arrows indicate several of the attachment discs; others are also visible in the image. (**2**) SP14-63-11. (**3**) Constituent cells are partly degraded and difficult to see; the dark circular and elliptical structures, most easily seen in the center of the image, are attachment discs, UCMP 36096f, SP14-63-17.

cells 10–25 µm in diameter" (p. 20). However, given that there are no other species within the genus with which to compare *P. dyptocranum*, it is not possible to know the range of cell diameters that delimit this species. Indeed, a specimen in the collection described here falls slightly outside these boundaries, and rather than emend the range of cell diameters listed in the species diagnosis so as to include this specimen (and leave open the necessity for future taxonomists to emend it again if specimens with slightly smaller or larger cell sizes are discovered), we have removed reference to cell diameters altogether and have produced a single diagnosis for both the species and the genus. This diagnosis is similar to the original diagnosis provided for the genus but is modified to include the characteristic of an enclosed three-dimensional (spheroidal or ellipsoidal) colony.

Palaeastrum dyptocranum Butterfield in Butterfield, Knoll, and Swett, 1994
Figure 15.1–15.3

1994 *Palaeastrum dyptocranum* Butterfield, in Butterfield et al., p. 18, fig. 5A–C.

2009 *Palaeastrum*; Butterfield, fig. 1E–G.

2015 *Palaeastrum dyptocranum*; Vorob'eva et al., p. 217, fig. 8.1, 8.3, 8.4.

Holotype.—HUPC 62708, slide 86-G-62-46, England Finder coordinates M-48-1, late Tonian Algal Dolomite Member, Svanbergfjellet Formation, Geerabukta, Svalbard (Butterfield et al., 1994, fig. 5A, p. 18).

Diagnosis.—Colonial, spheroidal to ellipsoidal cells with prominent intercellular attachment discs; discs circular with a reinforced rim. Colonies monostromatic, forming enclosed spheroidal or ellipsoidal structures hundreds of micrometers in diameter (emended from Butterfield et al., 1994).

Occurrence.—Tanner Member, Chuar Group; Neoproterozoic Svanbergfjellet Formation, Akademikerbreen Group, Svalbard (Butterfield et al., 1994; Butterfield, 2009); and Mesoproterozoic Kotuikan Formation, northern Siberia (Vorob'eva et al., 2015).

https://doi.org/10.1017/jpa.2016.57 Published online by Cambridge University Press

Figure 16. (**1**) *Rugosoopsis tenuis* Timofeev and Hermann, 1979, UCMP 36094c SP14-63-14. (**2**) *Siphonophycus septatum* (Schopf, 1968) Knoll, Swett, and Mark, 1991, note longitudinal splits in some (e.g., black arrows), UCMP 36083g, SP14-63-11. (**3**) *Siphonophycus typicum* (Hermann, 1974) Buttterfield in Butterfield et al., 1994, note longitudinal split, UCMP 36083h, SP14-63-11. (**4**) *Siphonophycus robustum* (Schopf, 1968) Knoll, Swett, and Mark, 1991, UCMP 36100, SP14-63-24.

Description.—Ellipsoidal to spheroidal colonies, 210 to 360 µm in width (mean = 270 µm; N = 5) and 360 to 580 µm in length (mean = 360 µm, N = 5), consisting of a single layer of ellipsoidal to spheroidal cells 9 to 17 µm in diameter (mean = 14 µm, N = 25) attached to each other via thickened discs 3 to 5 µm in diameter (mean = 4 µm; N = 27). In some specimens the cell walls are degraded and only the attachment discs are clearly visible, suggesting that the latter have greater preservation potential (Fig. 15.2, 15.3; cf. Butterfield et al., 1994). Typically four attachment discs per cell; hundreds of cells per colony.

Materials.—Twelve specimens (samples SP14-63-11, -14, -17).

Remarks.—Butterfield et al. (1994) placed *Palaeastrum* in the Order Chlorococcales, Division Chlorophyta, noting that the extant chlorococcalean algae *Pediastrum* and *Coelastrum* also form multicellular coenobia in which the cells are attached to each other via differentiated 'plaques' (e.g., Marchant, 1977). Because of the subsequent discovery of complete specimens illustrating that *Palaeastrum* coenobia formed hollow ellipsoids similar to those formed in the extant alga *Hydrodictyon*, Butterfield (2009, p. 204) stated that *Palaeastrum* could be "reliably assigned to the Hydrodictyaceae (Sphaeropleales, Chlorophyceae, Chlorophyta)." (Note that many members of the Chlorococcales including *Pediastrum* and *Coelastrum* are now considered part of the order Sphaeropleales; Deason et al., 1991; Lewis and McCourt, 2004.)

Unfortunately, data on the phylogenetic distribution of *Palaeastrum's* diagnostic characters among extant taxa are either not known or not easily accessible. The data that are available suggest that these characters are not restricted to the Hydrodictyaceae; *Coelastrum* (Scenedesmidaceae; Tippery et al., 2012), for example, also possesses attachment plaques and three-dimensional coenobia (Marchant, 1977). Furthermore, molecular phylogenetic analyses indicate that three-dimensional coenobia evolved at least twice within the Hydrodictyaceae (Buchheim et al., 2005), raising the possibility that similarities with *Palaeastrum* reflect convergent evolution. More generally, there is accumulating evidence that within the green algae, morphology can be phylogenetically misleading (Lewis and McCourt, 2004; McManus and Lewis, 2011). Therefore, while it is reasonable to suggest that *Palaeastrum* may be part of the Sphaeropleales, a monophyletic group that includes taxa that do have a good fossil record (Colbath and Grenfell, 1995), we are not at all confident in that assignment, nor are we strongly confident in the assignment to the Chloroplastida (= Viridiplantae).

Genus *Rugosoopsis* Timofeev and Hermann, 1979

Type species.—*Rugosoopsis tenuis* Timofeev and Hermann, 1979.

Rugosoopsis tenuis Timofeev and Hermann, 1979
Figure 16.1

1979 *Rugosoopsis tenuis* Timofeev and Hermann, p. 139, pl. 29, figs. 5, 7.

1994 *Rugosoopsis tenuis*; Butterfield et al., p. 62, figs. 25A-D, 27B.

Holotype.—Preparation number 1-22/1-77/1, late Mesoproterozoic–early Neoproterozoic Lakhanda Group, Maya River, Khabarovsk Krai, Siberia (Timofeev and Hermann, 1979, pl. 29, fig. 7).

Occurrence.—Tanner Member, Chuar Group; the Neoproterozoic Svanbergfjellet Formation, Svalbard (Butterfield et al., 1994), Lone Land Formation, Franklin Mountains, Canada (Samuelsson and Butterfield, 2001), Alinya Formation, Officer Basin (Riedman and Porter, 2016), and the late Mesoproterozoic–early Neoproterozoic Lakhanda Group, Siberia (Timofeev and Hermann, 1979).

Description.—Rugose filaments 32 to 41 µm in width (N = 3); wrinkles are ~1 to 3 µm in width and are roughly perpendicular to filament axis. All three specimens are broken and reach only

https://doi.org/10.1017/jpa.2016.57 Published online by Cambridge University Press

65 to 88 µm in length. One specimen exhibits an unwrinkled portion at one end.

Materials.—Three specimens (sample SP14-63-14).

Genus *Siphonophycus* Schopf, 1968

Type species.—*Siphonophycus kestron* Schopf, 1968.

Occurrence.—Occurs throughout the Chuar Group; widespread in Proterozoic and Phanerozoic assemblages.

Remarks.—*Siphonophycus* is a form genus that encompasses smooth-walled, nonbranching, nonseptate tubular filaments with open or closed hemispherical terminations (Knoll et al., 1991). Species are distinguished on the basis of filament width.

Siphonophycus robustum (Schopf, 1968) Knoll, Swett, and Mark, 1991
Figure 16.4

1968 *Eomycetopsis robusta* Schopf, p. 685, pl. 82, figs. 2, 3 and pl. 83, figs. 1–4.
1991 *Siphonophycus robustum*; Knoll et al., p. 565, fig. 10.3, 10.5.
1994 *Siphonophycus robustum*; Butterfield et al., p. 64, fig. 26A, G.

Holotype.—Thin section Bit. Spr. 10-1, Paleobotanical collections, Harvard University number 58491 from Neoproterozoic Bitter Springs Formation, Amadeus Basin, Australia (Schopf, 1968, pl. 83, fig. 1).

Description.—Filaments 2 to 4 µm in diameter (N = 7). May occur singly or as aggregates.

Materials.—Dozens of specimens (samples SP14-53-10, SP14-63-14, -17, -19, -24, and -29).

Siphonophycus septatum (Schopf, 1968) Knoll, Swett, and Mark, 1991
Figure 16.2

1968 *Tenuofilum septatum* Schopf, p. 679, pl. 86, figs. 10–12.
1991 *Siphonophycus septatum*; Knoll et al., p. 565, fig. 10.2.

Holotype.—Thin section Bit/Spr 6–3, Paleobotanical collections, Harvard University, number 58527 from the Neoproterozoic Bitter Springs Formation, Amadeus Basin, Australia (Schopf, 1968, pl. 86, fig. 11).

Description.—Filaments 1 to 2 µm in diameter (N = 8). Several specimens exhibit longitudinal splits (Fig. 16.2). May occur singly or as aggregates.

Materials.—Dozens of specimens (samples SP14-53-10, SP14-63-11, and -24).

Siphonophycus typicum (Hermann, 1974) Butterfield in Butterfield, Knoll, and Swett, 1994
Figure 16.3

1974 *Leiothrichoides tipicus* Hermann; p. 7, pl. 6, figs. 1, 2.
1994 *Siphonophycus typicum*; Butterfield et al., p. 66, figs. 23 B–D, 26B, H, I.

Holotype.—Preparation number 49/2T, Neoproterozoic Miroyedikha Formation, Krasnoyarsk Krai in Turukhansk region, near Maya River, Siberia (Hermann, 1974, p. 7, pl. 6, figs. 1, 2).

Description.—Filaments 4 to 8 µm in diameter (N = 10). One specimen exhibits a longitudinal split (Fig. 16.3).

Materials.—Dozens of specimens (samples SP14-53-10, -14, SP14-63-11, and -19).

Genus *Squamosphaera* Tang, Pang, Yuan, Wan, and Xiao, 2015

Type species.—*Squamosphaera colonialica* (Jankauskas, 1979b) Tang et al., 2015, by monotypy.

Diagnosis.—As for type species by monotypy (emended from Tang et al., 2015).

Remarks.—Vidal and Ford (1985) described specimens of *Squamosphaera colonialica* from the Chuar Group under the name *Satka colonialica* Jankauskas, 1979b. The type species of *Satka*, *S. favosa* Jankauskas, 1979a, is characterized by a wall composed of numerous polygonal plates; studies of other populations attributed to *S. favosa* show that these plates are sutured together and can break apart along these sutures (Hofmann and Jackson, 1994, fig. 18.26; Javaux et al., 2004, fig. 3a–f). By contrast, the holotype of *Squamosphaera colonialica*—as well as better-known collections from the Chuar and elsewhere—consists of a single continuous wall with numerous rounded bulges, not the plates diagnostic of *Satka*. The similarities between *Satka favosa* and *Squamosphaera colonialica* therefore appear to be superficial. Recognizing these differences, Tang et al. (2015) removed *S. colonialica* from the genus *Satka* and placed it in a new genus, *Squamosphaera*. We follow that here, although we emend the diagnosis of this monotypic genus so that it is the same as that for the species and modify the species diagnosis to accommodate the Chuar material (see the following).

Squamosphaera colonialica (Jankauskas, 1979b) Tang, Pang, Yuan, Wan, and Xiao, 2015
Figure 17.1–17.7

?1966 *Gloeocapsomorpha hebeica* Timofeev, p. 43, pl. 4, fig. 1.
?1976 "Sphaeromorphs in the process of division"; Timofeev et al., pl. 8, figs. 6, 8, 9.
1979b *Satka colonialica* Jankauskas, p. 192, pl. 1, figs. 4, 6.
?1980 *Synsphaeridium* sp.; Tynni and Donner, pl. I.7.
1985 *Satka colonialica*; Knoll and Swett, p. 468, pl. 53, figs. 4–6, 8.
1985 *Satka colonialica*; Vidal and Ford, p. 369, fig. 6.

https://doi.org/10.1017/jpa.2016.57 Published online by Cambridge University Press

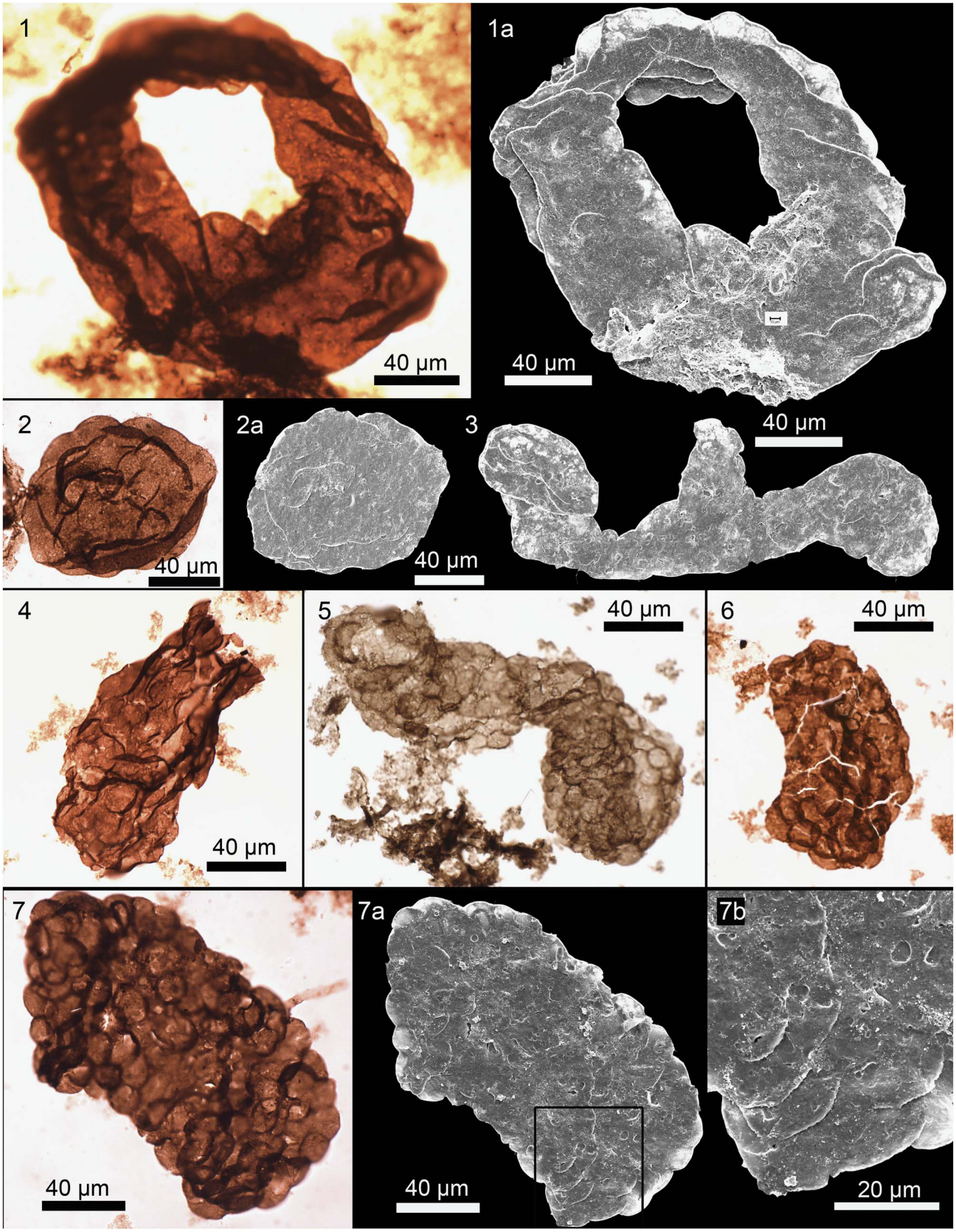

Figure 17. *Squamosphaera colonialica* (Jankauskas, 1979b) Tang et al., 2015. (**1, 1a**) Toroidal specimen, UCMP 36096c, SP14-63-17. (**2, 2a**) Specimen with subcircular outline, UCMP 36096d, SP14-63-17. (**3**) Irregularly shaped specimen, UCMP 36096b, SP14-63-17. (**4**) UCMP 36084c, SP14-63-11. (**5**) UCMP 36097b, sample SP14-63-17. (**6**) UCMP 36075a, SP12-63-30. (**7, 7a, 7b**) UCMP 36096e, SP14-63-17. (**7b**) Note pocked texture of wall, reflecting taphonomic degradation.

https://doi.org/10.1017/jpa.2016.57 Published online by Cambridge University Press

1989 *Satka colonialica*; Jankauskas et al., p. 51, pl. 4, figs. 4, 7.
1992 *Satka colonialica*; Schopf, pl. 42B.
non 1992a *Satka compacta*; Zang and Walter, p. 93 fig. 69F, H.
?1994 *Satka colonialica*; Yin and Sun, p. 107, fig. 5G.
non 1994 *Satka colonialica*; Yin and Sun, p. 107, fig. 7K, L.
1997 *Satka colonialica*; Samuelsson, p. 175, fig. 9A, B.
1999 *Satka colonialica*; Cotter, p. 77, fig. 7C.
1999 *Satka colonialica*; Samuelsson et al., fig. 4G.
non 1999 *Satka colonialica*; Yin and Guan, p. 134, fig. 7.1, 7.3, 7.8, 7,9.
2009 *Satka colonialica*; Nagy et al., fig. 1L.
non 2011 *Satka* sp. cf. *S. colonialica*; Couëffé and Vecoli, fig. 7.2.
2015 *Squamosphaera colonialica*; Tang et al., p. 312, figs. 12, 13.

Holotype.—ЛитНИГРИ, number 16-62-4762/22, slide 1. Well Kabakovo-62, 4762–4765 m. Neoproterozoic Zigazino-Komarovo Formation, Ufa, Bashkirian Urals (Jankauskas, 1979b, fig. 4).

Diagnosis.—Single-walled, spheroidal, tomaculate, toroidal, or irregularly shaped vesicles with an irregular outline characterized by numerous broadly domical bulges. Vesicles typically 80–500 µm in maximum dimension; bulges typically 5–30 µm in basal width (emended from Jankauskas, 1979b; Tang et al., 2015).

Occurrence.—Tanner, Jupiter, Carbon Canyon, and Duppa members, Chuar Group; depths of 4,762–4,765 m in Kobakovo 62 drill hole, Ufa, Bashkirian Urals (Jankauskas, 1979b); Glasgowbreen and Oxfordbreen formations, Veteranen Group, Svalbard (Knoll and Swett, 1985); Iernovskaya, Chernorechenskaya, Poropelonskaya, and Karuyarvinskaya formations, Kildinskaya Group, Kola Peninsula, Russia (Samuelsson, 1997); Steptoe Formation, Kanpa 1A drill core, and Kanpa and Hussar formations, Hussar 1 drill core, Officer Basin, Australia (Cotter, 1999); Imilik Formation, Narssârssuk Group; Steensby Land and Kap Powell formations, Dundas Group, and Qaanaaq and Robertson Fjord formations, Baffin Bay Group, Thule Supergroup, northwest Greenland (Samuelsson et al., 1999); Gouhou Formation, Huaibei region, North China (Tang et al., 2015). *Squamosphaera colonialica* has also been noted (as *Satka colonialica*) but not described or illustrated from the lower part of the upper Visingsö Group (Vidal and Ford, 1985) and the Red Pine Shale, Uinta Mountain Group, Utah (Nagy and Porter, 2005; Dehler et al., 2007). Late Mesoproterozoic to Tonian in age.

Description.—Spherical (Fig. 17.2), tomaculate (Fig. 17.4, 17.5, 17.7), toroidal (Fig. 17.1), or irregularly shaped (Fig. 17.3) vesicles ~100 to 410 µm in maximum dimension (mean = 160 µm, SD = 74 µm, N = 22), bearing numerous rounded bulges. Bulges may be clearly distinct, occurring as hemispherical outpocketings (e.g., Fig. 17.4–17.7), or they may be most clearly visible as a slight scalloped pattern along the periphery of the vesicle (Fig. 17.1–17.3). The vesicles are empty, but folding and compaction can make it appear as though internal bodies are present (e.g., Fig. 17.6, 17.7).

The size of the bulges ranges from 10 to 35 µm (mean = 17 µm, SD = 5 µm, N = 84; size of bulges measured at widest span). Within a single vesicle, the range of sizes is much narrower, with diameters of individual bulges typically within 4 µm of each other (e.g., 16 to 20 µm diameter). There is little correlation (r = −0.09, N = 22) between the diameter of the bulges and the maximum dimension of the vesicle. In some specimens viewed under TLM, the wall appears to have a subtle texture, but evidence from specimens observed using SEM suggests that the wall is in fact smooth and that the subtle texture likely arises from the impressions of minerals that grew into the wall after deposition (Fig. 17.7b).

Materials.—Thirty specimens (samples SP12-63-30, SP14-63-11, -14, -17, and -24).

Remarks.—In the Chuar assemblage, the size and shape of the vesicles and the number, size, and expression of the bulges is highly variable. It is possible this reflects lumping of several distinct species, but we were unable to identify convincing gaps in the variation that would indicate this is the case. Instead we interpret this to represent intraspecific—possibly ecophenotypic—variation, and group all of the Chuar specimens into a single highly variable species.

Vidal and Ford (1985) suggested that the undulating outline of the vesicle (= 'envelope' of Vidal and Ford, 1985) reflects compression around colonial clusters of spherical cells, a view that was followed by Knoll and Swett (1985). They illustrate one specimen (Vidal and Ford, 1985, fig. 6D–F) that appears to retain one of these cells. However, the cell appears to be outside the vesicle, and although it is similar in size to the bulges on the vesicle, it is possible that it is a small leiosphaerid, unrelated to the vesicle, that became fortuitously attached after death. While there are fossils in the Chuar Group that consist of numerous tightly packed spherical bodies (e.g., Fig. 18.3), these are distinct from *S. colonialica* in that they are not surrounded by an outer envelope. (These have been placed in open nomenclature in the form genus *Synsphaeridium*.) Many of the *S. colonialica* specimens in the Chuar Group—as well as the holotype specimen from the Urals and specimens from elsewhere (e.g., Tang et al., 2015)—show no evidence of rupture, indicating that the absence of internal bodies does not simply reflect their departure from the vesicle.

Noting the lack of evidence for internal bodies, Tang et al. (2015) described the bulges on the vesicle wall as "domical processes" that "freely communicate with the vesicle cavity" rather than as "circular impressions on the wall" (p. 310). However, the absence of preserved internal bodies does not imply that they were not once there; taphonomic studies of modern filamentous cyanobacteria, for example, show that extracellular sheaths are more likely to be preserved than trichomes (Bartley, 1996). Given the uncertainty in the interpretation of these features, we have emended the diagnosis of Tang et al. (2015) so that it refers to bulges rather than processes. We believe that this change leaves open the question of how they arose—either as processes ornamenting a vesicle

https://doi.org/10.1017/jpa.2016.57 Published online by Cambridge University Press

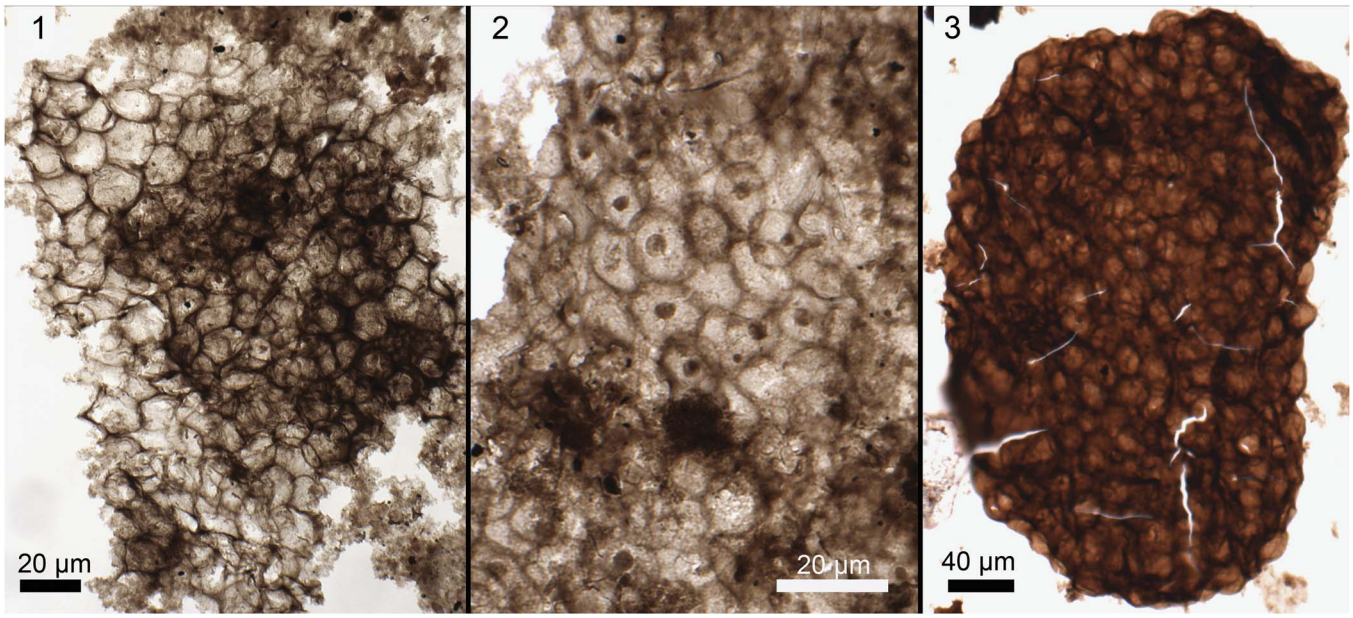

Figure 18. *Synsphaeridium* Eisenack, 1965. (**1**) UCMP 36084a, SP14-63-11. (**2**) Note dark circular bodies on some cells, UCMP 36084b, SP14-63-11. (**3**) Specimen with rounded margins suggesting preservation of the original outline of the colony, UCMP 36083f, SP14-63-11.

wall (cf. Tang et al., 2015) or, as favored here, impressions of internal cells no longer preserved (cf. Knoll and Swett, 1985; Vidal and Ford, 1985). We have also emended the diagnosis to accommodate the range of vesicle shapes exhibited by the Chuar material (including toroidal and irregular).

Possible occurrences of *Squamosphaera colonialica* include a single specimen (and the presumed holotype) of *Gloeocapsomorpha hebeica* Timofeev, 1966. Although the hand-drawn sketch suggests a single vesicle with multiple bulges, the accompanying text describes the species as "[a]n accumulation of large, thin, smooth subspherical coalesced vesicles," i.e., an aggregate of leiosphaerids similar to *Synsphaeridium* sp. (Timofeev, 1966, p. 43). The Chuar specimens are therefore not assigned to *G. hebeica*, which otherwise would have priority.

Other possible occurrences of *S. colonialica* are three of nine specimens illustrated by Timofeev et al. (1976) as "[s]phaeromorphs in the process of division" (pl. 8, figs. 6, 8, 9). Although they appear similar to smaller specimens of *S. colonialica* described here, their more pronounced bulges and co-occurrence with two- and three-celled dividing sphaeromorphs suggest they may indeed be dividing sphaeromorphs as well. Definite occurrences of *S. colonicalica* include those reported by Knoll and Swett (1985), Samuelsson (1997), Cotter (1999), and Samuelsson et al. (1999).

The organic-walled vesicles of *Timanisphaera apophysa* Vorob'eva, Sergeev, and Knoll, 2009 bear numerous hemispherical processes similar to the bulges of *S. colonialica*. However, the processes are much greater in size (50 to 90 µm wide vs. 10 to 35 µm), and the vesicles of *T. apophysa* (N = 18) do not show the range of unusual shapes observed in the *S. colonialica* specimens studied here (N = 30).

Several specimens of aggregated cells assigned in the literature to *Satka colonialica* or *Satka* cf. *Satka colonialica* are here excluded from *Squamosphaera colonialica* because they do not show evidence of an outer envelope (cf. Fig. 18.3): specimens described as *Satka compacta* Zang and Walter, 1992a, ascribed to *Satka colonialica* by Samuelsson (1997); specimens described as *Satka colonialica* by Yin and Sun (1994) and Yin and Guan (1999); and specimens described as *Satka* cf. *Satka colonialica* by Couëffé and Vecoli (2011).

Genus *Synsphaeridium* Eisenack, 1965

Type species.—*Synsphaeridium gotlandicum* Eisenack, 1965.

Synsphaeridium spp.
Figure 18.1–18.3

Occurrence.—Tanner, Jupiter, and Awatubi members, Chuar Group. Widespread in Proterozoic and Phanerozoic rocks.

Description.—Aggregates of organic-walled spheroidal vesicles 8 to 29 µm in diameter (mean = 16 µm, SD = 5 µm, N = 64 vesicles in 16 colonies). Tight packing of vesicles may result in a polygonal outline of each vesicle. Areas of vesicle contact are typically more resistant to degradation (e.g., Fig. 18.1). Aggregates vary with respect to the tightness of vesicle packing and the arrangement of vesicles (from monostromatic to three-dimensional, ellipsoidal colonies). Within four of the aggregates, vesicles exhibit dark circular spots (Fig. 18.2). These appear to be part of or fused to the vesicle wall (cf. Pang et al., 2013) because they are in the same focal plane. The spots range from 2.4 to 3.7 µm in diameter (mean = 2.9 µm, SD = 0.4 µm, N = 13 spots in 4 colonies) and occur in vesicles 8 to 13 µm in diameter. Spots are not uniformly present throughout an aggregate; a vesicle without a spot may lie adjacent to a vesicle with one.

Materials.—Nineteen specimens (samples SP12-63-30, SP14-63-11, -12, -14, -17, and -23).

https://doi.org/10.1017/jpa.2016.57 Published online by Cambridge University Press

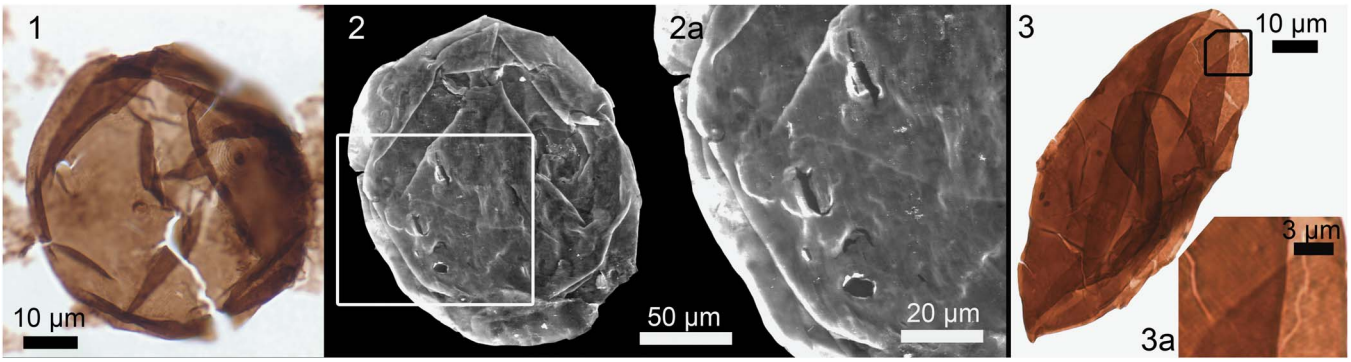

Figure 19. *Valeria lophostriata* (Jankauskas, 1979b) Jankauskas, 1982. (**1**) SP14-63-11. (**2, 2a**) Specimen with striae visible on outer surface, UCMP 36095, SP14-63-17. (**3, 3a**) Specimen partly split with the two halves enrolled to form a fusiform shape. (**3a**) Closeup of specimen showing the striations characteristic of this species, UCMP 36075b, SP12-63-30.

Remarks.—Simple characters unite this group, which is almost certainly polyphyletic. A number of generic names have been applied to aggregates of smooth-walled vesicles, but these overlap to varying degrees in their diagnoses (see Riedman and Porter, 2016), and it is not clear that parsing out the Chuar specimens into different taxa would be either meaningful or possible. We therefore follow Riedman and Porter (2016) and place these specimens in open nomenclature in the earliest erected genus of smooth-walled aggregates, *Synsphaeridium* Eisenack (1965).

Genus *Valeria* Jankauskas, 1982

Type Species.—*Valeria lophostriata* (Jankauskas, 1979b) Jankauskas, 1982.

Valeria lophostriata (Jankauskas, 1979b) Jankauskas, 1982
Figure 19.1–19.3

1979b *Kildinella lophostriata* Jankauskas, p. 53, fig. 1.13–1.15.
1982 *Valeria lophostriata*; Jankauskas, p.109, pl. 39, fig. 2.
1989 *Valeria lophostriata*; Jankauskas et al., p. 86, pl. 16, figs. 1–5.
1995 *Valeria lophostriata*; Zang, p. 170, fig. 28I.
1999 *Valeria lophostriata*; Samuelsson et al., fig. 8E.
2001 *Valeria lophostriata*; Javaux et al., fig. 1D.
2004 *Valeria lophostriata*; Javaux et al., fig. 2F–I.
2009 *Valeria lophostriata*; Nagy et al., fig. 1A, B
2009 *Valeria lophostriata*; Nagovitsin, p. 144, fig. 4E.
?2011 *Valeria lophostriata*; Couëffé and Vecoli, fig. 6.4.
?2012 dark-walled megasphaeric coccoid; Battison and Brasier, fig. 8B.
2015 *Valeria lophostriata*; Tang et al., p. 315, fig. 11.
2016 *Valeria lophostriata*; Riedman and Porter, p. 862, fig. 4.1.

(For additional synonymy, see Jankauskas et al., 1989; Hofmann, 1999, table 1)

Holotype.—ЛитНИГРИ, number 16-62-4762/16, sp. 1, DH Kabakovo 62 drill core, depth 4,762 to 4,765 meters, Neoproterozoic Zigazino-Komarovo Formation, southern Urals (Jankauskas, 1979b, fig. 1.14).

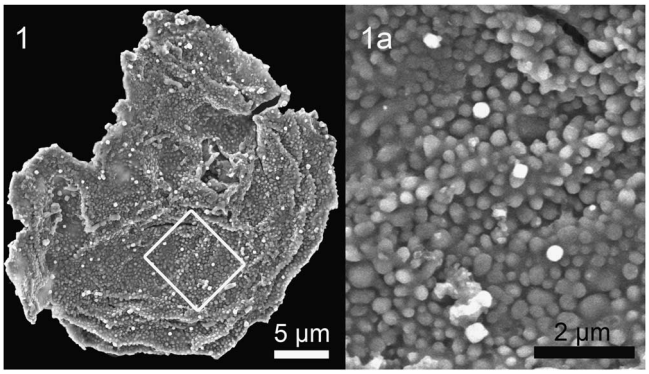

Figure 20. *Vidalopalla* cf. *verrucata* (Vidal in Vidal and Siedlecka, 1983) Riedman and Porter, 2016. (**1, 1a**) UCMP 36085b, SP14-63-12.

Occurrence.—Tanner and Jupiter members, Chuar Group; widely distributed in late Paleoproterozoic through Tonian rocks.

Description.—Spherical vesicles 55 to 180 µm in diameter (mean = 85 µm, SD = 46 µm, N = 6) with concentric ridges spaced 0.5 to 1.0 µm apart; circular structures ~3 µm in diameter are located at each pole (Fig. 19.1). Javaux et al. (2004) showed that these ridges are on the inner surface of the vesicle; their presence is also visible under SEM on the outer surface of the wall (Fig. 19.2), although this may reflect penetration of the wall by the electron beam, compression of the vesicle, or thinning of the outer wall associated with degradation, rather than biological form. Some specimens split along striae; one specimen partly split with the two halves enrolled to form a fusiform shape (Fig. 19.3; cf. Javaux et al., 2004; Peng et al., 2009).

Materials.—Seven specimens (samples SP14-63-11, -17, and SP12-63-30).

Genus *Vidalopalla* Riedman and Porter, 2016

Type species.—*Vidalopalla verrucata* (Vidal in Vidal and Siedlecka, 1983) Riedman and Porter, 2016, by monotypy.

Remarks.—The Chuar specimen differs sufficiently from the type material that placement in the type and only species of

https://doi.org/10.1017/jpa.2016.57 Published online by Cambridge University Press

Vidalopalla, *V. verrucata*, is in question. Nonetheless, those differences are of a quantitative rather than qualitative nature (size and spacing of verrucae; size of vesicles), justifying their placement in the genus *Vidalopalla* Riedman and Porter, 2016.

Vidalopalla cf. *verrucata* (Vidal in Vidal and Siedlecka, 1983) Riedman and Porter, 2016
Figure 20.1

cf. 1981 *Kildinella* sp. B; Vidal p. 26, fig. 13A–D.
cf. 1983 *Kildinosphaera verrucata* Vidal; Vidal and Siedlecka, 1983, p. 62, fig. 5C.
cf. 1985 *Kildinosphaera verrucata*; Vidal and Ford, p. 363, fig. 4A.
cf. 2016 *Vidalopalla verrucata*; Riedman and Porter, p. 870, fig. 11.3, 11.4, 11.8.

Holotype.—Specimen E74–02: V/47 from the Neoproterozoic Ekkerøy Formation, Store Ekkerøy (locality 14), Varanger Peninsula, East Finnmark, Norway (Vidal, 1981, fig. 13A–D); in keeping with the original designation by Vidal and Siedlecka (1983).

Description.—Organic-walled spheroidal vesicle 32 µm in diameter covered in rounded verrucae 0.2 to 0.4 µm in diameter. Verrucae are closely spaced, nearly touching.

Materials.—A single specimen from the Tanner Member (sample SP14-63-12).

Remarks.—The Chuar specimen differs from the type material of *V. verrucata* in several ways, most notably the spacing of the verrucae (>1 µm apart in the type material vs. 0.1 µm in the Chuar specimens). The verrucae are also smaller in the Chuar material (0.2–0.4 µm in diameter vs. 1–1.5 µm in the type material; Vidal, 1981), as is the vesicle (32 µm in diameter vs. 40 to 135 µm; Vidal, 1981; Vidal and Siedlecka, 1983). Nonetheless, there are enough similarities between the specimen described here and other collections of *V. verrucata* (e.g., Riedman and Porter, 2016) that we cannot rule out the possibility that additional material will support inclusion of this specimen in *V. verrucata*. Vidal and Ford (1985) reported *V. verrucata* from the Chuar Group, and both their description and accompanying image (fig. 4A) are consistent with that taxonomic assignment. Thus, *V. verrucata* does occur in the Chuar Group—in the Awatubi Member, at least (Vidal and Ford, 1985)—and it is possible the specimen described here represents an end member of a species that varied widely in both vesicle size and verrucae size and spacing.

Genus *Volleyballia* new genus

Type species.—*Volleyballia dehlerae* n. sp., by monotypy.

Diagnosis.—As for type species.

Etymology.—Named for pattern of the vesicle wall, which is similar in appearance to that of a volleyball.

Remarks.—Although other acritarch species exhibit striations (see 'Remarks' in the following), none are sufficiently similar to suggest a close relationship with *V. dehlerae*. Thus we have chosen to erect a new genus for this species.

Volleyballia dehlerae new species
Figure 21.1–21.7

?1995 *Striasphaera radiata* Liu in Gao, Xing, and Liu, pp. 14, 20, pl. 2, figs. 10, 11.
?1995 *Striasphaera irregularia* Liu in Gao, Xing, and Liu, pp. 14, 20, pl. 2, fig. 12.
?1996 Unnamed form; Knoll, pl. 5, fig. 11.
1999 ?*Leiosphaeridia* sp.; Cotter, fig. 8H.
2000 Form 1; Simonetti and Fairchild, p. 25, fig. 8S.
2009 Unnamed form A; Nagy et al., fig. 1D.
2016 *Volleyballia dehlerae*; Riedman and Porter, p. 876, fig. 3.9–3.14.

Holotype.—UCMP 36080d, sample SP14-63-11, SEM slide=ker-2, EF=Q49. Lava Chuar Canyon locality, Tanner Member, Galeros Formation, Chuar Group, Grand Canyon (Fig. 21.1).

Diagnosis.—Organic-walled vesicle with sets of parallel, rounded ridges and valleys approximately equal in width and spaced ~1 µm apart from the crest of one ridge to the next. Ridges darker in transmitted light than are valleys. Surface may have several sets of ridges, with sets oriented at angles to each other; each set typically consists of two to seven ridges.

Occurrence.—Neoproterozoic Alinya Formation, Giles 1 drill core, and Browne Formation, Kanpa 1A drill hole, Officer Basin, Australia (Cotter, 1999; Riedman and Porter, 2016); Mesoproterozoic Conselheiro Mata Group (well 1-PSB-13-MG), Espinhaço Supergroup, Brazil (Simonetti and Fairchild, 2000).

Description.—Organic-walled vesicles 25 to 45 µm in diameter (mean = 32 µm, SD = 5, N = 12), with sets of two to seven parallel ridges. Ridges are spaced ~1 µm apart. Ridges may be up to 4 to 9 µm in length and are bounded—though not sharply—by other sets of ridges that are oriented at an angle to them (measured angles range from ~40° to 90°.) Ridges in contiguous ridge sets may be joined to form a 'V' (Fig. 21.1b, 21.2a). Under transmitted light, ridges and valleys can be distinguished by their different opacity: valleys are lighter in color (Fig. 21.1, 21.4a, 21.6). The ridges and valleys are sinusoidal in cross section and reflect variations in wall thickness; they do not merely reflect wrinkling of a uniformly thick wall (Fig. 21.7a). An outer envelope is present in some specimens. No excystment structures have been observed.

Etymology.—Named in honor of Carol Dehler, a geologist who has made significant contributions to Precambrian geology through her studies of the Chuar Group and its correlatives, and who was a cheerful, generous, and loyal field companion and colleague to SMP during the collection and study of these fossils.

https://doi.org/10.1017/jpa.2016.57 Published online by Cambridge University Press

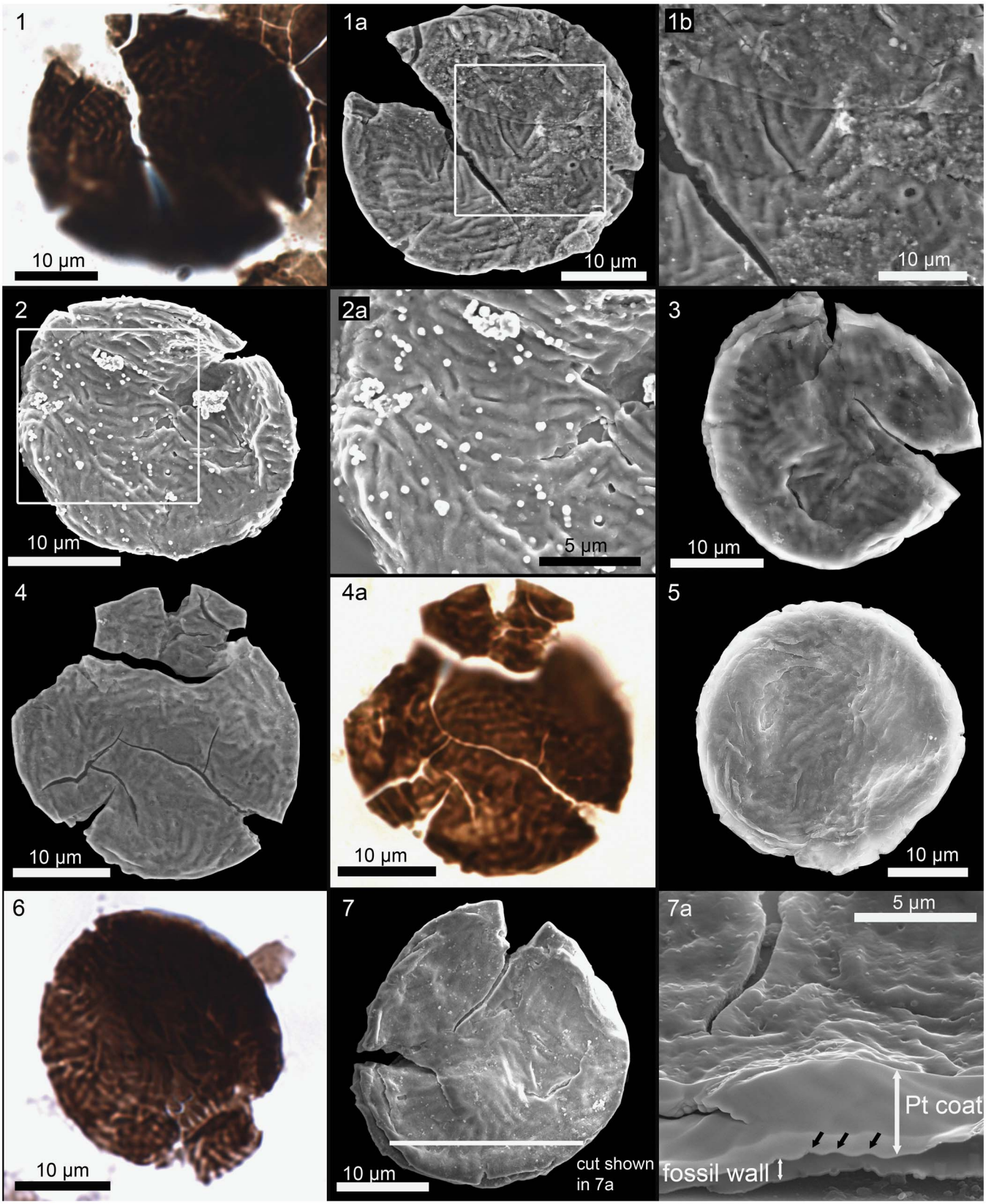

Figure 21. *Volleyballia dehlerae* n. gen. n. sp. (**1, 1a, 1b**) Holotype; UCMP 36080d, SP14-63-11, England Finder coordinate Q49. (**2, 2a**) UCMP 36086c, SP14-63-12. (**3**) UCMP 36081a, SP14-63-11. (**4, 4a**) UCMP 36079b, SP14-63-11. (**5**) UCMP 36089a, SP14-63-14. (**6**) UCMP 36083i, SP14-63-11. (**7, 7a**) 36081b, SP14-63-11. (**7a**) View of tilted (52°) specimen that has been cut using a focused ion beam. Specimen is partially coated with platinum (Pt); black arrows point to ridges on upper surface of vesicle wall.

https://doi.org/10.1017/jpa.2016.57 Published online by Cambridge University Press

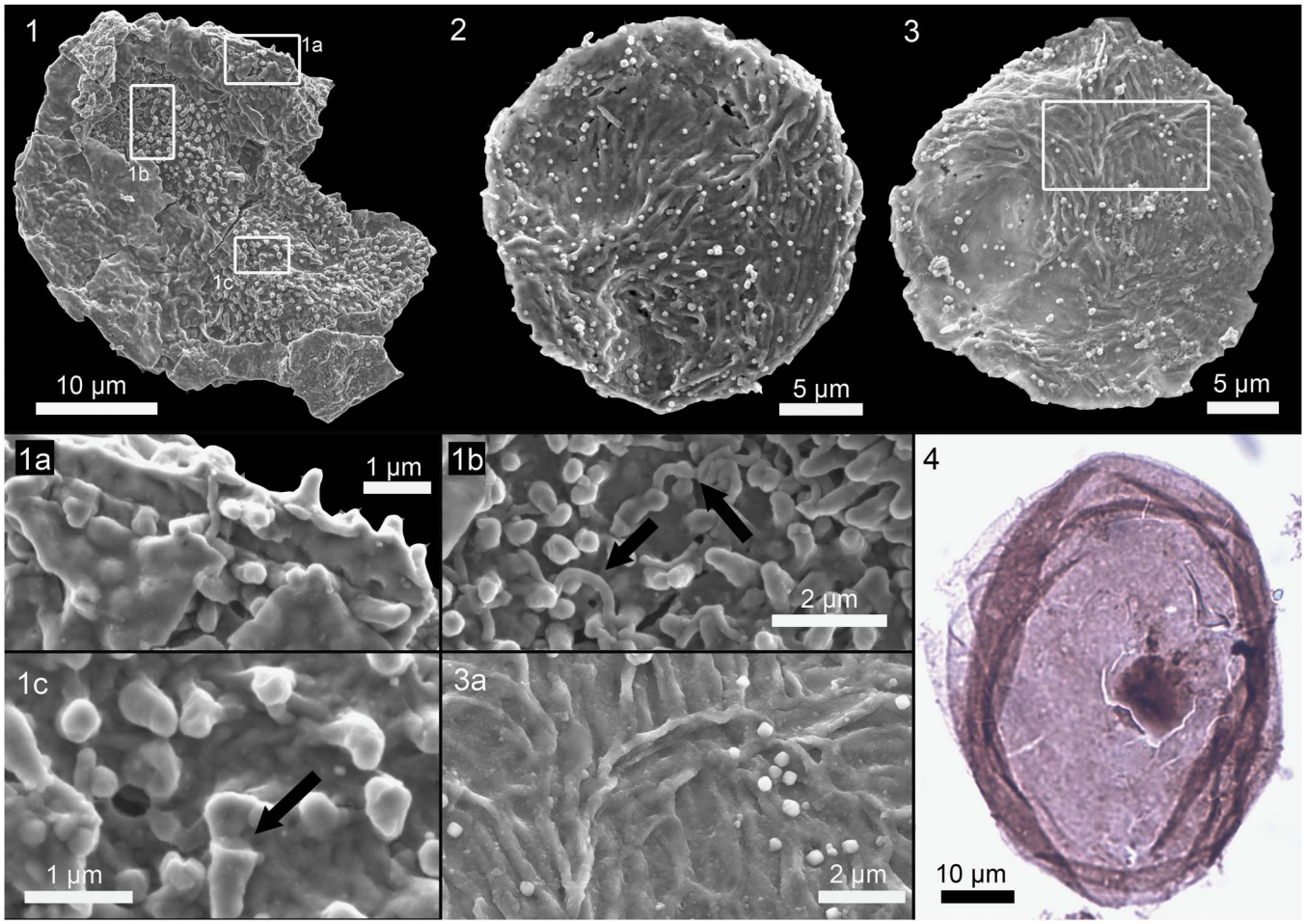

Figure 22. Unnamed forms A–C. (**1, 1a, 1b, 1c**) Unnamed form A, UCMP 36093c, SP14-63-14. (**1a**) Note dimpling on vesicle's inner surface where processes arise; (**1b**) closeup showing sinuous fibers (black arrows) extending horizontally along vesicle surface; (**1c**) closeup showing ropy texture on vesicle surface between processes; black arrow points to broken process showing solid construction. (**2, 3, 3a**) Unnamed form B. (**2**) UCMP 36086d, SP14-63-12; (**3, 3a**) UCMP 36085c, SP14-63-12. (**4**) Unnamed form C, UCMP 36083k, SP14-63-11.

Materials.—Twenty-five specimens (samples SP12-63-30, SP14-63-11, -12, -14, -29).

Remarks.—*Volleyballia dehlerae* differs from *Valeria lophostriata* in that the ridges in the latter form concentric circles and are expressed on the inner surface of the vesicle wall (Javaux et al., 2004). It differs from *Karenagare alinyaensis* Riedman and Porter, 2016 in having more closely spaced ridges (~1 µm from crest to crest in *V. dehlerae* vs. ~3 µm in *K. alinyaensis*) and having short (4 to 9 µm) 'ridge sets.' In addition, the ridges in *K. alinyaensis* do not appear to reflect variations in vesicle wall thickness but rather ripples in a wall of constant thickness (Riedman and Porter, 2016).

Striasphera radiata Liu in Gao et al., 1995 and *Striasphaera irregulari* Liu in Gao et al., 1995 from the Neoproterozoic Qinggouzi Formation, Hunjiang area, Jilin Province, China, also exhibit ridge-like ornaments on the vesicle (Gao et al., 1995). However, while it is difficult to confirm this with the images provided (Gao et al., 1995, pl. 2, figs. 10, 11), *S. radiata* appears to have a more complex topography than *V. dehlerae*, as suggested by the presence of rounded processes visible on the outer edges. *S. irregulari* differs from *V. dehlerae* in having wider valleys (2 to 3 µm), sets of parallel ridges that are greater in number, and a flange-like structure consisting of eleven ridges radiating away from the edge of the fossil (on the upper left of the fossil, pl. 2, fig. 12).

Unnamed form A
Figure 22.1

Description.—A single vesicle with numerous (2 to 3 per µm^2) blunt-tipped conical processes 0.7 to 1.1 µm in length and 0.3 to 0.5 µm in width at their base. The surface of the vesicle between the processes has a ropy texture, as if it is composed of thin fibers that have been fused together and are now barely distinguishable (Fig. 22.1c). The inner surface of the vesicle is dimpled where the processes arise (Fig. 22.1a); the processes are thus partly hollow, but occasional broken processes (Fig. 22.1c) reveal solid construction distally. Vesicle is 33 µm in diameter and covered by a thin, smooth outer envelope that closely replicates the underlying vesicle surface resulting in a verrucate appearance. A few thin sinuous fibers, 0.2 µm in width and up to 2.5 µm in length, extend horizontally along the vesicle surface (Fig. 22.1b). Fibers appear to arise from the vesicle surface and are perhaps related to the subtle ropy texture observed on the interprocess vesicle surface.

https://doi.org/10.1017/jpa.2016.57 Published online by Cambridge University Press

Materials.—One specimen from sample SP14-63-14, and a possible specimen from SP12-63-30.

Remarks.—Unlike *Lanulatisphaera laufeldii*, the cone-like processes observed in this specimen are not formed from distal fusion of several fibers that arise separately from the vesicle surface. There is also no evidence for dimpling on the inner vesicle surface of *L. laufeldii* (Fig. 10.1). However, the presence of fibers similar in width to those observed in *L. laufeldii* may indicate a relationship between these two, perhaps phylogenetic or ontogenetic.

A specimen from the Jupiter Member (sample SP12-63-30) may be related to the specimen described in the preceding. Unfortunately, it is poorly preserved, and the outer envelope obscures most of the details of the inner vesicle. The specimen is much larger in size (63 µm diameter) with longer (4 µm) and wider processes (1 µm at their base), but like the specimen described, the processes appear to be hollow, at least in their basal part.

Unnamed form B
Figure 22.2, 22.3

Description.—Organic-walled vesicles 23 to 26 µm in diameter (N = 2), with an outer surface that exhibits numerous grooves, ~3 µm long and 0.6 to 0.9 µm wide. Grooves appear to be formed by flattening of elongate pillow-like elements, judging from the wrinkled and folded appearance of the layer that forms the outer surface of the wall.

Materials.—Two specimens (sample SP14-63-12).

Remarks.—These specimens bear some similarities with *Volleyballia dehlerae* and with furrowed specimens of *Lanulatisphaera laufeldii* (Fig. 10.6, 10.7). However, the similarities appear to be superficial: the specimens lack the sets of wave-like ridges and valleys characteristic of *V. dehlerae* and the filamentous processes characteristic of *L. laufeldii*. Instead it seems likely these specimens represent a new species, but because of the limited material available, they are kept here in open nomenclature.

Unnamed form C
Figure 22.4

Description.—Smooth, organic-walled spheroidal vesicles 48 to 58 µm in diameter (N = 2) with a darkened circular spot ~10 µm in diameter on the vesicle wall. One specimen exhibits a very thin outer envelope (Fig. 22.4).

Material examined.—Two specimens (samples SP14-63-11 and -17).

Remarks.—These specimens differ from *Leiosphaeridia* Eisenack, 1958b in having an outer envelope around the vesicle. In addition, they exhibit darkened spots on the vesicle wall, which may be original biological features of the vesicle or which may represent contracted protoplast that was fused to the wall during late diagenesis (Pang et al., 2013). (That these spots are now part of the wall is suggested by the fact that cracks in the vesicle wall also run through the spot and that both are in the same focal plane; Fig. 22.4.) Given the uncertainty in the origin of the dark spot, we have refrained from placing these specimens in either the double-walled form *Pterospermopsimorpha* (Timofeev, 1966) emend. Mikhailova and Jankauskas in Jankauskas et al., 1989.

Unnamed form D
Figure 23.2

Description.—Vesicles 28 to 30 µm in diameter, with walls bearing polygonal pillows, now compressed, typically square in shape, though with rounded edges. The pillows are 3 to 4 µm in width and are bordered by thin furrows. Structure of the vesicle not discernible under transmitted light microscopy (Fig. 23.2b).

Materials.—Two overlapping specimens (sample SP12-63-30) and a possible single specimen (AK10-60-7)

Remarks.—It is not clear whether the overlapping contact of the two specimens reflects biological or accidental circumstances; it is assumed here to be accidental and that these are two distinct specimens.

Unnamed form E
Figure 24.1–24.3

Description.—Organic-walled vesicles 48 to 134 µm in diameter (mean = 85 µm, SD = 35 µm, N = 5) that exhibit a ropy

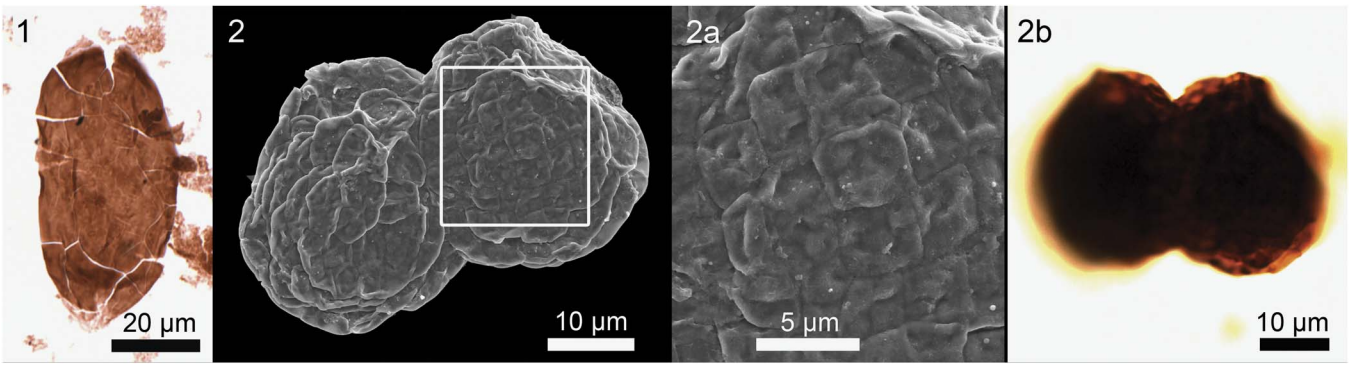

Figure 23. (**1**) *Navifusa majensis* Pyatiletov, 1980, UCMP 36094d, SP14-63-14. (**2, 2a, 2b**) Unnamed form D, UCMP 36072c, SP12-63-30.

https://doi.org/10.1017/jpa.2016.57 Published online by Cambridge University Press

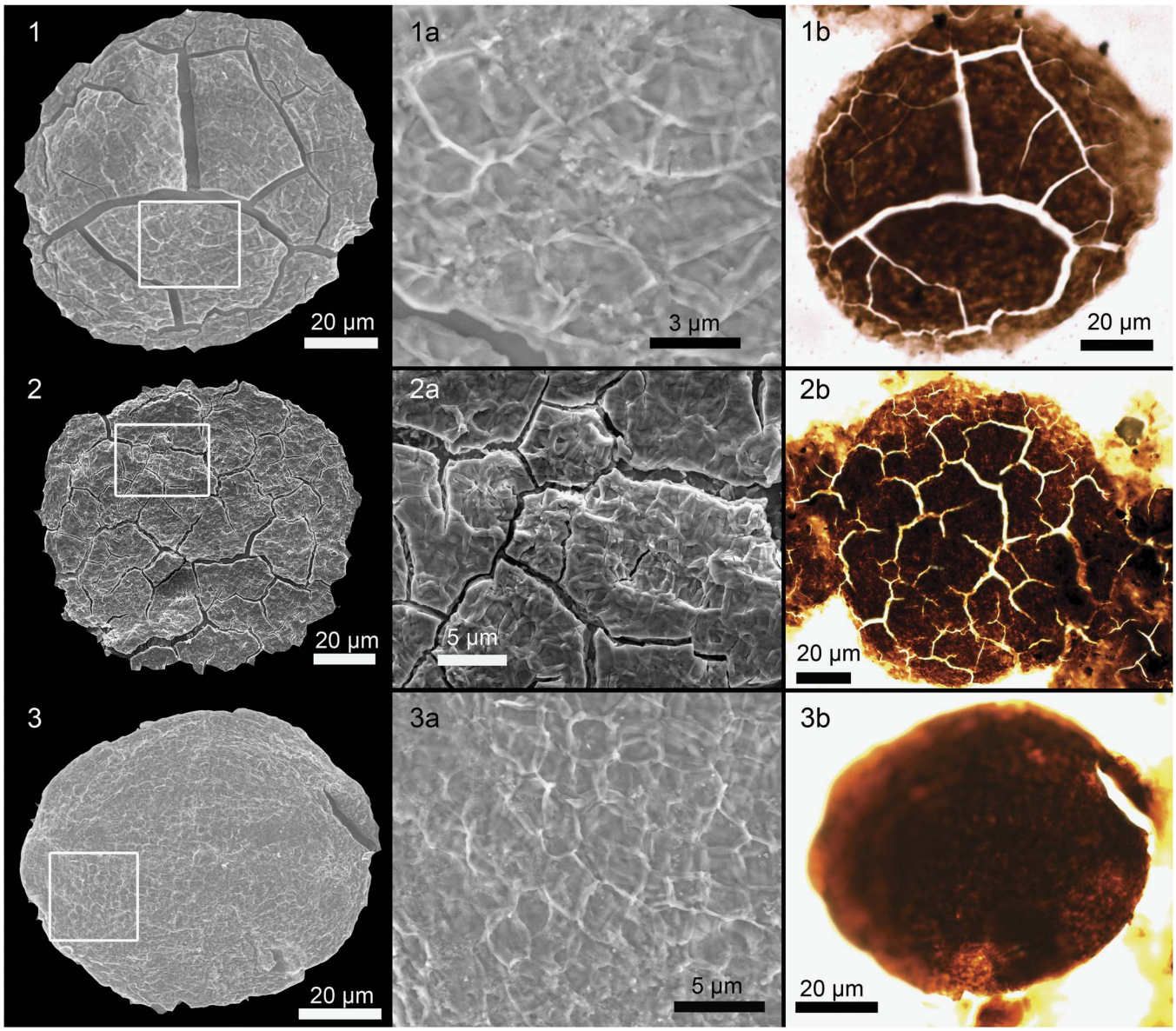

Figure 24. Unnamed form E. (**1, 1a, 1b**) UCMP 36079c, SP14-63-11. (**2, 2a, 2b**) UCMP 36082c, SP14-63-11. (**3, 3a, 3b**) UCMP 36079d, SP14-63-11. Specimen in (**3**) may, alternatively, be a form of *C. revelata.*

texture on their surface that appears to result from the flattening of originally convex elements roughly ~3 to 6 µm in diameter. These flattened elements appear to overlie additional ropy structures, which may reflect flattening of one or several underlying layers. Wall appears mottled in transmitted light (Fig. 24.1b, 24.2b, 24.3b).

Materials.—Five specimens (samples SP14-63-11 and SP12-63-30).

Remarks.—Although these five specimens are highly variable in size, they do share the same ropy appearance under SEM and mottled appearance under TLM. Whether some of these might represent degraded end member forms of *Culcitulisphaera revelata* (with unusually large pillow elements; Fig. 24.3a), much larger specimens of Unnamed form D, or a new species cannot be determined from present material.

Discussion

Biostratigraphic implications.—The Phanerozoic timescale is defined primarily on the basis of biostratigraphic events. By contrast, Proterozoic rocks are primarily correlated using carbon isotope anomalies and lithostratigraphic marker units (Dehler, 2014). This difference is attributable to the fact that, while fossils are reasonably common in Proterozoic rocks, most taxa have very long ranges, are geographically restricted, or are too poorly understood taxonomically to be of biostratigraphic use. The few species that are short ranging (by Precambrian standards), globally widespread, biologically meaningful, and easy to identify include

https://doi.org/10.1017/jpa.2016.57 Published online by Cambridge University Press

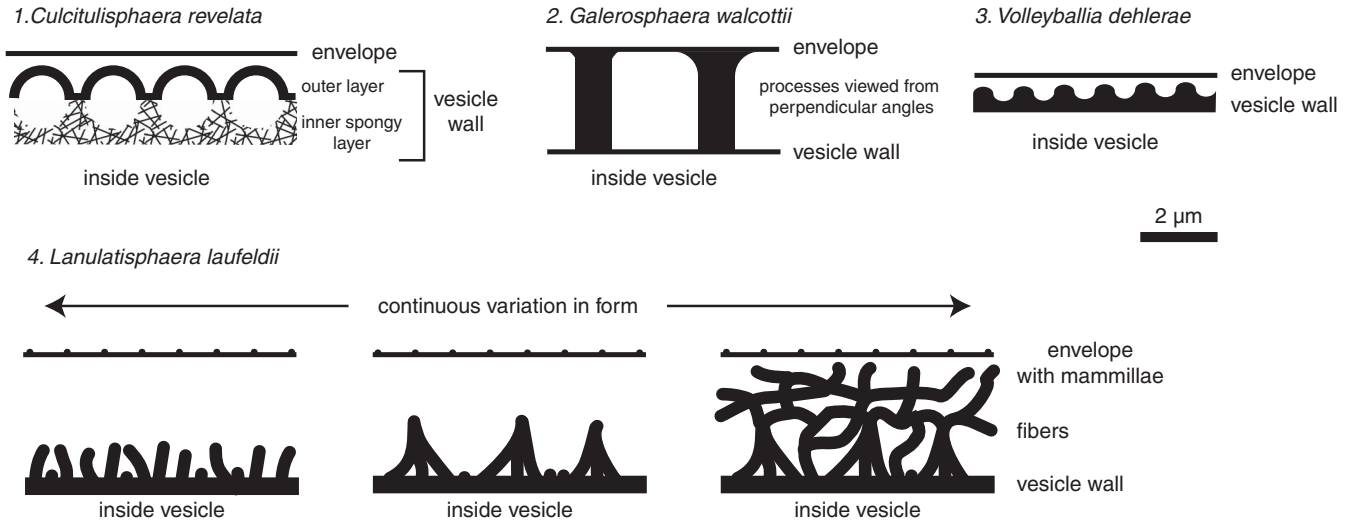

Figure 25. Reconstructions of selected species described in the text. (**1–3**) Reconstructions of vesicle wall structure for *Culcitulisphaera revelata*, *Galerosphaera walcottii*, *Volleyballia dehlerae*. (**4**) The range of continuous morphological variation exhibited by *Lanulatisphaera laufeldii*.

Cerebrosphaera globosa (= *C. buickii*), diagnostic of ca. 740–800 Ma rocks (Hill et al., 2000; Grey et al., 2011; this paper); *Trachyhystrichosphaera aimika*, diagnostic of ca. 720–1000 Ma rocks (Tang et al., 2013); and several species of vase-shaped microfossils (VSMs), diagnostic of rocks ca. 740 Ma (Porter et al., 2003; Strauss et al., 2014).

This study identifies two additional species that might be added to that list. The first is *Culcitulisphaera revelata*, which is known from the 1025 ±40 Ma Lakhanda Group, Siberia (Schopf, 1992; Semikhatov et al., 2000); the Tonian Limestone-Dolomite Series, Eleonore Bay Group, Greenland (Vidal, 1979); and the Tonian Alinya Formation, Giles 1 drill core, Officer Basin, Australia (Riedman and Porter, 2016) and thus appears to be a marker of latest Mesoproterozoic and Tonian time. The second, *Lanulatisphaera laufeldii*, is known from the Visingsö Group, Sweden (Vidal, 1976b); the Alinya Formation, Giles 1 drill core, Australia (Riedman and Porter, 2016); the Karuyarvinskaya Formation, Kildinskaya Group, Kola Peninsula, Russia (Samuelsson, 1997); the Uinta Mountain Group, Utah (Vidal and Ford, 1985; S. Porter, personal observation), and, possibly, the Limestone-Dolomite Series, Eleonore Bay Group, Greenland (Vidal, 1976a). It has also been reported (but not illustrated) from the Tanafjord and Vadsø groups, East Finnmark, Norway (Vidal, 1981), and the Ryssö Formation, Nordaustlandet, Svalbard (Knoll and Calder, 1983). All seven of these units are late Tonian in age, and in five of them (the Visingsö Group, the Ryssö Formation, the Uinta Mountain Group, the Eleonore Bay Group, and the Tanafjord and Vadsø groups), VSMs—thought to be a marker of ca. 740 Ma time (Strauss et al., 2014)—also occur. In all five cases, *L. laufeldii* always appears in rocks underlying those that preserve VSMs (although its range may extend into VSM-bearing rocks as well; Fig. 2). *L. laufeldii* thus may have particular promise as an index fossil: in addition to being robust, often abundant (e.g., in the Chuar and Visingsö groups), and globally widespread, it appears to be diagnostic of the time inverval just before ca. 740 Ma.

Biological affinities of Chuar microfossils.—An enduring challenge of Precambrian paleontology has been determining the biological affinities of Precambrian fossils. A handful of fossils have been convincingly assigned to clades within crown group Eukarya (Porter, 2004; Knoll et al., 2006; Javaux, 2011; Knoll, 2014; Butterfield, 2015), but most are problematic, some even at the level of domain. Part of this must be because many of these fossils are stem group representatives of major eukaryotic clades and thus may lack characters that might be helpful in diagnosing their affinities with living groups (cf. Budd and Jensen, 2000). In addition, many fossils are morphologically simple, with too few characters that might be of diagnostic use. Much of the problem, however, can be attributed to our relatively poor knowledge of modern microbial eukaryotes, in particular the phylogenetic distribution of preservable characters in those eukaryotes (for exceptions, see Leander et al., 2001, and Popper et al., 2011). This includes not only morphological characters—traditionally the means by which microfossil taxa are diagnosed—but also ultrastructural and chemical characters, which, though promising new sources of phylogenetic information (e.g, Arouri et al., 2000; Javaux et al., 2004; Javaux and Marshal, 2006; Moczydłowska and Willman, 2009), suffer even more from our limited understanding of their distribution among eukaryotes. As a result, even when similarities are identified between Precambrian fossils and modern taxa, it is difficult to know whether such similarities reflect homology or convergence, and if homologous, at what point in the eukaryotic tree they were derived.

This is the case for several of the taxa described here. *Lanulatisphaera laufeldii* (Figs. 9–12) has several similarities with dinoflagellates, including extensive variation in cyst morphology (cf. Lewis and Hallett, 1997) and processes formed by the fusion of several filaments (cf. Hemsley et al., 2004). Many taxa form cysts, however, and many cysts bear spines, and it is possible that similar features may have arisen convergently in a number of clades as a result of the simple mechanisms underlying their formation (e.g., Hemsley et al., 2004). Similarly, the three-dimensional enclosed colonial form of *Palaeastrum dyptocranum* in which the cells are attached to each other by thickened discs

https://doi.org/10.1017/jpa.2016.57 Published online by Cambridge University Press

(Fig. 15) is similar to colonial forms in the Hydrodictyales (Chloroplastida: Chlorococcales; Butterfield, 2009, 2015), but coloniality has been gained and lost many times in eukaryotic algae (Lewis and McCourt, 2004) and these relatively simple characters could have evolved convergently many times. Finally, *Microlepidopalla mira* provides an example of the difficulties that can arise even at the level of domain and even in cases where the phylogenetic distribution of characters is better known. At first glance, the ellipsoidal structures of *M. mira* appear similar to bacteria. However, the size, shape, and arrangement of the ellipsoids, as well as the absence of evidence for fission, warrants closer comparison with scale-bearing protists such as centrohelids, haptophytes, and pompholyxophryids (Porter et al., 2013). Even if the ellipsoids are not homologous with any particular modern group, the widespread convergence of scaly coverings among modern protists suggests that such forms could have evolved convergently in another, now extinct, clade (cf. Cohen and Knoll, 2012).

It might be possible nonetheless to broadly constrain Chuar fossil affinities through inferences about the life habits of these organisms. Some microfossils exhibit medial splits or opercula, suggesting that they may represent cysts, and although the possession of preservable cysts does not by itself indicate any particular eukaryotic affinity or habit, the presence of an outer envelope surrounding a cyst may. Moczydłowska (2010) proposed a model for the interpretation of the Cambrian acritarch *Skiagia* in which the outer envelope surrounding the ornamented vesicle is in fact the wall of a photosynthesizing vegetative cell. If fossilization occurred at this stage, the result would be a simple smooth-walled acritarch (= *Leiosphaeridia*). However, if fossilization occurred after a cyst formed or while it was still forming within the vegetative cell wall, the result would be an acritarch with an outer envelope; if fossilization occurred after release of the cyst, the result would be the same form of acritarch, but without an envelope. In this view, acritarch species that are demonstrably cysts and that include at least some specimens with an outer envelope are the remains of organisms that had cell walls during their vegetative (actively feeding) stage. Because cell walls would prevent acquisition of food via phagocytosis, such an organism would have to have been either a photoautotroph (as in Moczydłowska's [2010] model) and/or an osmotroph. The only Chuar species that definitively falls into this category is the operculum-bearing *Kaibabia gemmulella*; *Lanulastisphaera laufeldii* may also fall into this category, assuming the granulae-bearing structure found on several specimens (Fig. 11.4) is an operculum. It thus makes sense to look for phylogenetic affinities for these taxa among those modern clades in which osmotrophy and photoautotrophy—and not phagotrophy—are common, e.g., fungi and oomycetes (both osmotrophic) and green, red, brown, dinoflagellate, eustigmatophyte, and xanthophyte algae (Graham and Wilcox, 2000; Adl et al., 2012). Several other species exhibit thin outer walls surrounding an ornamented or otherwise complex vesicle (*Cerebrosphaera globosa*, *Culcitulisphaera revelata*, *Galerosphaera walcottii*, and Unnamed Forms A and C), but whether these represent cysts inside vegetative cell walls or are cysts or vegetative cells with multi-layered walls (consisting of both the ornamented layer and the thin outer layer) cannot be determined with the available material.

Stratigraphic patterns in Chuar fossil assemblages.—Organic-walled microfossils are found in fine-grained rocks throughout the Chuar Group, but they are especially diverse in the Tanner and Jupiter members (Fig. 2). Barren intervals are also found throughout the Chuar Group. On a sample-by-sample basis, there is no obvious correlation between the presence, diversity, or preservational quality of fossils and inferred water depth, lithology (shales vs. siltstones), or water column oxygenation (both barren and diverse assemblages occur in samples with FeHR/FeT values ranging from 0.17 to 0.55; data from Johnston et al., 2010, on the same samples in which Chuar fossils were preserved).

More broadly, however, there is a correspondence between the presence, diversity, and preservational quality of organic-walled microfossils in the Chuar Group and the appearance of organic-rich, euxinic conditions within the basin (Nagy et al., 2009; Johnston et al., 2010). Diverse, beautifully preserved fossil assemblages are common in lower Chuar shales, where subsurface waters were intermittently anoxic and ferruginous but never euxinic, whereas barren samples or those with poorly preserved leiosphaerids characterize the upper Awatubi and Walcott shales, where TOC levels are high and Fe-speciation evidence suggests euxinic conditions occurred intermittently. Although ornamented acritarchs are uncommon or absent from upper Awatubi and Walcott rocks, fossils are not. The carbonaceous compression fossil *Chuaria circularis* occurs on bedding planes throughout the Awatubi and lower Walcott members, and vase-shaped microfossils (VSMs) occur in great abundance in upper Awatubi and Walcott mudstones, cherts, and carbonate nodules in shales (Fig. 2; Porter and Knoll, 2000; Porter et al., 2003).

There are several possible explanations for the biostratigraphic pattern recorded in the Chuar Group. One possibility is that the pattern reflects preservational bias. Walcott strata record an overall deepening, so the lack of diverse acritarch taxa may simply reflect the transition to offshore environments, characterized by limited diversity (Butterfield and Chandler, 1992). However, shallow intervals, including microbially laminated silicified carbonates, are present in the upper Awatubi and Walcott members, and those that have been examined for microfossils are either barren or yield only VSMs. Alternatively, high TOC in upper Chuar rocks may have imposed a preservational filter: anecdotal evidence suggests that fossils are uncommon in or absent from organic-rich shales (>1.5 wt% TOC; Butterfield et al., 1994), perhaps because organic-rich waters interfere with flocculation (and thus rapid sinking of phytoplankton cells) or because high TOC may affect the efficacy of clay minerals in adsorbing degradative enzymes (Butterfield, 1990; Butterfield et al., 1994). Consistent with this hypothesis, organic-walled microfossils occur in Chuar samples that range from 0.08 to 1.40 wt% TOC, but none are found in the six samples from the Walcott Member with >1.5 wt% TOC (see Supplemental Data table).

Another possibility is that the pattern may reflect a genuine drop in abundance or the disappearance of acritarch taxa. Nagy et al. (2009) proposed that the Chuar Group records biotic turnover from oligotrophic conditions characterized by diverse eukaryotic phytoplankton to eutrophic conditions in which both prokaryotes and heterotrophic protists proliferated. Although

https://doi.org/10.1017/jpa.2016.57 Published online by Cambridge University Press

the evidence for prokaryote blooms is circumstantial (e.g., Brocks et al., 2016, who call into question the data of Ventura et al., 2005), this model accounts for both the decline of acritarch diversity upsection, as one or a few phytoplankton species monopolize nutrients, as well as the incredible abundance of VSMs and associated high TOC in the upper Chuar, as increased organic matter production drove proliferation of protistan heterotrophs. Johnston et al. (2010) proposed that relative tolerances to sulfide may instead have controlled the paleontological pattern: because cyanobacteria are more sulfide-tolerant than eukaryotes, they would have dominated primary production under euxinic conditions during late Chuar time. The high abundance of VSMs is also consistent with what is observed today in sulfide-rich environments, for example, those of the Santa Barbara Basin, where the abundance and biovolume of heterotrophic protists is an order of magnitude greater than in environments with no detectable sulfide (probably because of symbioses with chemoautotrophic bacteria; Bernhard et al., 2000).

Distinguishing among these hypotheses is not easy because both eutrophication and the conditions leading to the development of sulfidic bottom waters also commonly result in high TOC in the sediments. Thus, the absence of diverse acritarch assemblages in 740–720 Ma rocks (Riedman et al., 2014; Riedman and Sadler, 2015) is consistent with evidence that anoxic and sulfidic conditions were globally expansive during this time (Dahl et al., 2011); however, if these conditions resulted from increased organic carbon export to the seafloor (e.g., Johnston et al., 2010; see 'Geological setting'), then TOC levels may have been high globally as well, perhaps closing a preservational window for acritarchs in shale. (Of course, the absence of diverse acritarchs may also largely reflect the limited sampling and availability of rocks this age.) One approach is to focus on shallow-water successions of late Tonian age that exhibit low TOC content; another is to focus on assemblages preserved in other lithologies, such as silicified carbonates. If these also preserve only simple leiosphaerids and filaments, it would suggest that the absence of diverse acritarchs from coeval, high-TOC shales might be real, rather than an artifact of preservation (cf. Riedman et al., 2014).

Acknowledgments

A. Knoll collected some of the samples studied here and supported SMP's initial involvement in Chuar Group paleontology. The National Park Service gave permission to conduct research and collect samples within the Grand Canyon National Park. Sample collection was supported by the National Science Foundation through grant EAR-9706496 to A. Knoll; subsequent work was supported by NSF grant EAR-0922305 to SMP, by the W. Cole Storrs Memorial Research Award from the Geological Society of America to SMP, and by UCSB's Academic Senate. G. Seward provided help with SEM analyses, and S. Kraemer provided help with FIB-SEM and TEM analyses. This work made use of UCSB's MRL Central Facilities supported by the MRSEC Program of the National Science Foundation under award No. DMR 1121053. C. Cain and R. Nagy helped with data analysis, and C. Dehler, J. Moore, D. Chapman, and two anonymous reviewers provided useful feedback on the manuscript. This paper is dedicated to the memory of Stephen C. Porter, a geologist and father of the first rank.

Accessibility of supplemental data

Data available from the Dryad digital repository: http://datadryad.org/handle/doi:10.5061/dryad.5kv72

References

Adl, S.M., et al., 2012, The revised classification of eukaryotes: Journal of Eukaryotic Microbiology, v. 59, p. 429–493.

Agić, H., Moczydłowska, M., and Yin, L.-M., 2015, Affinity, life cycle, and intracellular complexity of organic-walled microfossils from the Mesoproterozoic of Shanxi, China: Journal of Paleontology, v. 89, p. 28–50.

Arouri, K.R., Greenwood, P.F., and Walter, M.R., 2000, Biological affinities of Neoproterozoic acritarchs from Australia: Microscopic and chemical characterisation: Organic Geochemistry, v. 31, p. 75–89.

Bartley, J.K., 1996, Actualistic taphonomy of Cyanobacteria: Implications for the Precambrian fossil record: Palaios, v. 11, p. 571–586.

Battison, L., and Brasier, M.D., 2012, Remarkably preserved prokaryote and eukaryote microfossils within 1 Ga-old lake phosphates of the Torridon Group, NW Scotland: Precambrian Research, v. 196–197, p. 204–217.

Bernhard, J.M., Buck, K.R., Farmer, M.A., and Bowser, S.S., 2000, The Santa Barbara Basin is a symbiosis oasis: Nature, v. 403, p. 77–80.

Bloeser, B., 1985, *Melanocyrillium*, a new genus of structurally complex Late Proterozoic microfossils from the Kwagunt Formation (Chuar Group), Grand Canyon, Arizona: Journal of Paleontology, v. 59, p. 741–765.

Bloeser, B., Schopf, J.W., Horodyski, R.J., and Breed, W.J., 1977, Chitinozoans from the late Precambrian Chuar Group of the Grand Canyon, Arizona: Science, v. 195, p. 676–679.

Brocks, J.J., Jarrett, A., Sirantoine, E., Kenig, F., Moczydłowska, M., Porter, S.M., and Hope, J., 2016, Early sponges and toxic protists: Possible sources of cryostane, an age diagnostic biomarker antedating Sturtian Snowball Earth: Geobiology, v. 14, p. 129–149 doi:10.1111/gbi.12165.

Buchheim, M., Buchheim, J., Carlson, T., Braband, A., Hepperle, D., Krienitz, L., Wolf, M., and Hegewald, E., 2005, Phylogeny of the Hydrodictyaceae (Chlorophyceae): Inferences from rDNA data: Journal of Phycology, v. 41, p. 1039–1054.

Budd, G.E., and Jensen, S., 2000, A critical reappraisal of the fossil record of the bilaterian phyla: Biological Reviews, v. 75, p. 253–295.

Butterfield, N.J., 1990, Organic preservation of non-mineralizing organisms and the taphonomy of the Burgess Shale: Paleobiology, p. 272–286.

Butterfield, N.J., 2009, Modes of pre-Ediacaran multicellularity: Precambrian Research, v. 173, p. 201–211.

Butterfield, N.J., 2015, Early evolution of the Eukaryota: Palaeontology, v. 58, p. 5–17.

Butterfield, N.J., and Chandler, F.W., 1992, Palaeoenvironmental distribution of Proterozoic microfossils, with an example from the Agu Bay Formation, Baffin Island: Palaeontology, v. 35, p. 943–957.

Butterfield, N.J., Knoll, A.H., and Swett, K., 1994, Paleobiology of the Neoproterozoic Svanbergfjellet Formation, Spitsbergen: Fossils and Strata, v. 34, p. 1–84.

Cohen, P.A., and Knoll, A.H., 2012, Scale microfossils from the mid-Neoproterozoic Fifteenmile Group, Yukon Territory: Journal of Paleontology, v. 86, p. 775–800.

Colbath, G.K., and Grenfell, H.R., 1995, Review of biological affinities of Paleozoic acid-resistant, organic-walled eukaryotic algal microfossils (including "acritarchs"): Review of Palaeobotany and Palynology, v. 86, p. 287–314.

Combaz, A., Lange, F.W., and Pansart, J., 1967, Les "Leiofusidae" Eisenack, 1938: Review of Palaeobotany and Palynology, v. 167, p. 291–307.

Cotter, K.L., 1999, Microfossils from Neoproterozoic Supersequence 1 of the Officer Basin, Western Australia: Alcheringa, v. 23, p. 63–86.

Couëffé, R., and Vecoli, M., 2011, New sedimentological and biostratigraphic data in the Kwahu Group (Meso- to Neo-Proterozoic), southern margin of the Volta Basin, Ghana: Stratigraphic constraints and implications on regional lithostratigraphic correlations: Precambrian Research, v. 189, p. 155–175.

Dahl, T.W., Canfield, D.E., Rosing, M.T., Frei, R.E., Gordon, G.W., Knoll, A.H., and Anbar, A.D., 2011, Molybdenum evidence for expansive sulfidic water masses in ~750 Ma oceans: Earth and Planetary Science Letters, v. 311, p. 264–274.

Deason, T.R., Silva, P.C., Watanabe, S., and Floyd, G.L., 1991, Taxonomic status of the species of the green algal genus *Neochloris*: Plant Systematics and Evolution, v. 177, p. 213–219.

Dehler, C.M., 2014, Advances in Neoproterozoic biostratigraphy spark new correlations and insight in evolution of life: Geology, v. 42, p. 731–732.
Dehler, C.M., Prave, A.R., Crossey, L.J., Karlstrom, K.E., Atudorei, V., and Porter, S.M., 2001a, Linking mid-Neoproterozoic successions in the western U.S.: The Chuar Group-Uinta Mountain Group-Pahrump Group connection (ChUMP): Geological Society of America Abstracts with Programs, v. 33, p. 20.
Dehler, C.M., Elrick, M.E., Karlstrom, K.E., Smith, G.A., Crossey, L.J., and Timmons, M.J., 2001b, Neoproterozoic Chuar Group (~800–742 Ma), Grand Canyon: A record of cyclic marine deposition during global climatic and tectonic transitions: Sedimentary Geology, v. 141–142, p. 465–499.
Dehler, C., Elrick, M., Bloch, J., Crossey, L., Karlstrom, K., and Des Marais, D.J., 2005, High-resolution $\delta^{13}C$ stratigraphy of the Chuar Group (ca. 770–742), Grand Canyon: Implications for mid-Neoproterozoic climate change: Geological Society of America Bulletin, v. 117, p. 32–45.
Dehler, C.M., Porter, S.M., de Grey, L.D., Sprinkel, D.A., and Brehm, A., 2007, The Neoproterozoic Uinta Mountain Group revisited: A synthesis of recent work on the Red Pine Shale and undivided clastic strata, northeastern Utah, U.S.A., *in* Link, P.K., and Lewis, R., eds., Proterozoic Geology of Western North American and Siberia: SEPM Special Publication, v. 86, p. 151–166.
Dehler, C.M., Porter, S.M., and Timmons, J.M., 2012, The Neoproterozoic Earth system revealed from the Chuar Group of Grand Canyon, *in* Timmons, J.M., and Karlstrom, K.E., eds., Grand Canyon Geology: Two Billion Years of Earth's History: Geological Society of America Special Paper 489, p. 49–72.
Dehler, C.M., Gehrels, G., Porter, S.M., Cox, G., Heizler, M.T., Karlstrom, K.E., and Crossey, L.J., 2014, ChUMP (Chuar-Uinta Mountain-Pahrump) strata of the western U.S. record Cretaceous-like ocean anoxia events (OAEs) before Snowball Earth: Geological Society of America Abstracts with Programs, v. 46, p. 627.
Dodge, J.D., 1989, Some revisions of the family Gonyaulacaceae (Dinophyceae) based on a scanning electron microscope study: Botanica Marina, v. 32, p. 275–298.
Downie, C., 1963, 'Hystrichospheres' (acritarchs) and spores of the Wenlock Shales (Silurian) of Wenlock, England: Palaeontology, v. 6, p. 625–652.
Eisenack, A, 1938, Neue Mikrofossilien des baltischen Silurs. IV.: Palaeontologisch Zeitschrift, v. 19(no. 3–4), p. 217–243. pl. 15–16.
Eisenack, A., 1955, Chitinozoen, Hystrichosphären und andere Mikrofossilien aus dem *Beyrichia*-Kalk: Senckenbergiana lethaea, v. 36, p. 157–188.
Eisenack, A., 1958a, Mikrofossilien aus dem Ordovizium des Baltikums: Senckenbergiana lethaea, v. 39, p. 389–405.
Eisenack, A., 1958b, *Tasmanites* Newton 1875 und *Leiosphaeridia* n. g. als Gattungen der Hystrichosphaeridea: Palaeontographica Abteilung A, v. 110, p. 1–19.
Eisenack, A., 1965, Mikrofossilien aus dem Silur Gotlands. Hystrichosphären, Problematika: Neues Jahrbuch für Geologie und Paläontologie Abhandlungen, v. 122, p. 257–274.
Eisenack, A., 1976, Mikrofossilien aus dem Vaginatenkalk von Hälludden, Öland: Palaeontographica Abteilung A, v. 154, p. 181–203.
Ellegaard, M., 2000, Variations in dinoflagellate cyst morphology under conditions of changing salinity during the last 2000 years in the Limfjord, Denmark: Review of Palaeobotany and Palynology, v. 109, p. 65–81.
Elston, D.P., 1989, Middle and late Proterozoic Grand Canyon Supergroup, Arizona, *in* Elston, D.P., Billingsley, G.H., and Young, R.A., eds., Geology of the Grand Canyon, Northern Arizona (with Colorado River Guides): Lee Ferry to Pierce Ferry, Arizona, Washington, D.C., American Geophysical Union, p. 94–105.
Evitt, W.R., 1963, A discussion and proposals concerning fossil dinoflagellates, hystrichospheres, and acritarchs, II: Proceedings of the National Academy of Sciences of the United States of America, v. 49, p. 298.
Fensome, R.A., Williams, G.L., Barss, M.S., Freeman, J.M., and Hill, J.M., 1990, Acritarchs and Fossil Prasinophytes: An Index to Genera, Species and Infraspecific Taxa, Dallas, American Association of Stratigraphic Palynologists Foundation, 771, p.
Foissner, W., Müller, H., and Agatha, S., 2007, A comparative fine structural and phylogenetic analysis of resting cysts in oligotrich and hypotrich Spirotrichea (Ciliophora): European Journal of Protistology, v. 43, p. 295–314.
Ford, T.D., and Breed, W.J., 1969, Preliminary geologic report of the Chuar Group, Grand Canyon, Arizona: Four Corners Geological Society Guidebook, p. 114–122.
Ford, T.D., and Breed, W.J., 1973a, Late Precambrian Chuar Group, Grand Canyon, Arizona: Geological Society of America Bulletin, v. 84, p. 1243–1260.
Ford, T.D., and Breed, W.J., 1973b, The problematical fossil *Chuaria*: Palaeontology, v. 16, p. 535–550.
Gao, L., Xing, Y., and Liu, G., 1995, Neoproterozoic micropalaeoflora from Hunjiang area, Jilin Province and its sedimentary environment: Professional Papers of Stratigraphy and Palaeontology, v. 26, p. 1–27.
Golubic, S., and Campbell, S.E., 1979, Analogous microbial forms in recent subaerial habitats and in Precambrian cherts: *Gloethece coerulea* Geitler and *Eosynechococcus moorei* Hofmann: Precambrian Research, v. 8, p. 201–217.
Graham, L.E., and Wilcox, L.W., 2000, Algae, Upper Saddle River, NJ, Prentice-Hall, 640 p.
Grey, K., 1999, A modified palynological preparation technique for the extraction of large Neoproterozoic acanthomorph acritarchs and other acid-insoluble microfossils: Western Australia Geological Survey, Record 1999/10, 23 p.
Grey, K., and Willman, S., 2009, Taphonomy of Ediacaran acritarchs from Australia: Significance for taxonomy and biostratigraphy: Palaios, v. 24, p. 239–256.
Grey, K., Hill, A.C., and Calver, C., 2011, Biostratigraphy and stratigraphic subdivision of Cryogenian successions of Australia in a global context, *in* Arnaud, E., Halverson, G.P., and Shields-Zhou, G., eds., The Geological Record of Neoproterozoic Glaciations: Geological Society London, Memoirs 36, p. 113–134.
Hemsley, A.R., Lewis, J., and Griffiths, P.C., 2004, Soft and sticky development: Some underlying reasons for microarchitectural pattern convergence: Review of Palaeobotany and Palynology, v. 130, p. 105–119.
Hermann, T.N., 1974, Nakhodki massovykh skoplenii trikhomov v rifee [Findings of mass accumulations of trichomes in the Riphean], *in* Timofeev, B.V., ed., Mikrofitofossilii Proterozoia i rannego Paleozoia SSSR [Microfossils of the Proterozoic and early Paleozoic, USSR], Leningrad, Nauka, p. 6–10 [in Russian].
Hill, A.C., Cotter, K.L., and Grey, K., 2000, Mid-Neoproterozoic biostratigraphy and isotope stratigraphy in Australia: Precambrian Research, v. 100, p. 281–298.
Hofmann, H.J., 1976, Precambrian microflora, Belcher Islands, Canada: Significance and systematics: Journal of Paleontology, v. 50, p. 1040–1073.
Hofmann, H.J., 1999, Global distribution of the Proterozoic sphaeromorph acritarch *Valeria lophostriata* (Jankauskas): Acta Micropalaeontologica Sinica, v. 16, p. 215–224.
Hofmann, H.J., and Jackson, G.D., 1994, Shale-facies microfossils from the Proterozoic Bylot Supergroup, Baffin Island, Canada: Memoir (The Paleontological Society), v. 37, p. 1–39.
Hughes Martiny, J.B., Bohannan, B.J.M., Brown, J.H., Colwell, R.K., Fuhrman, J.A., Green, J.L., Horner-Devine, M.C., Kane, M., Krumins, J.A., and Kuske, C.R., 2006, Microbial biogeography: Putting microorganisms on the map: Nature Reviews Microbiology, v. 4, p. 102–112.
Jankauskas, T.V., 1979a, Nizhnerifeiskie mikrobioty Iuzhnogo Urala (Lower Riphean microbiotas of the southern Urals): Akademii Nauk SSSR, Doklady [Proceedings of the USSR Academy of Sciences], v. 247, p. 1465–1467 [in Russian].
Jankauskas, T.V., 1979b, Srednerifeyski microbiota Yuzhnogo Urala i Bashkirskogo Priural'ya [Middle Riphean microbiota of the southern Urals and the Ural region in Bashkiria]: Akademii Nauk SSSR, Doklady [Proceedings of the USSR Academy of Sciences], v. 248, p. 190–193 [in Russian].
Jankauskas, T.V., 1980, Shisheniakskaia mikrobiota Verkhnego Rifeia Iuzhnogo Urala [Shisheniak microbiota of the upper Riphean of the Southern Urals]: Akademii Nauk SSSR, Doklady [Proceedings of the USSR Academy of Sciences], v. 251, p. 190–192 [in Russian].
Jankauskas, T.V., 1982, Mikrofossilii rifeiia Iuzhnogo Urala [Microfossils of the Riphean of the South Urals], *in* Keller, B.M., ed., Stratotip Rifeya-Paleontologiya paleomagnetizm [Riphean Stratotype: Paleontology and Paleomagnetism]: Akademiya Nauk SSSR Transactions, Volume 368, Moscow, Nauka, p. 84–120. plates, p. 31–48 [in Russian].
Jankauskas, T., Mikhailova, N., and Hermann, T.N., 1989, Mikrofossilii Dokembriia SSSR [Precambrian Microfossils of the USSR], Leningrad, Nauka, 191 p. [in Russian].
Javaux, E.J., 2011, Early eukaryotes in Precambrian oceans, *in* Gargaud, M., Lopez-Garcia, P., and Martin, H., eds., Origins and Evolution of Life: An Astrobiology Perspective, New York, Cambridge University Press, p. 414–449.
Javaux, E.J., and Marshal, C.P., 2006, A new approach in deciphering early protist paleobiology and evolution: Combined microscopy and microchemistry of single Proterozoic acritarchs: Review of Palaeobotany and Palynology, v. 139, p. 1–15.
Javaux, E.J., Knoll, A.H., and Walter, M.R., 2001, Morphological and ecological complexity in early eukaryotic ecosystems: Nature, v. 412, p. 66–69.
Javaux, E.J., Knoll, A.H., and Walter, M.R., 2004, TEM evidence for eukaryotic diversity in mid-Proterozoic oceans: Geobiology, v. 2, p. 121–132.
Johnston, D.T., Poulton, S.W., Dehler, C., Porter, S., Husson, J., Canfield, D.E., and Knoll, A.H., 2010, An emerging picture of Neoproterozoic ocean chemistry: Insights from the Chuar Group, Grand Canyon, USA: Earth and Planetary Science Letters, v. 290, p. 64–73.

https://doi.org/10.1017/jpa.2016.57 Published online by Cambridge University Press

Karlstrom, K.E., et al. 2000, Chuar Group of the Grand Canyon: Record of breakup of Rodinia, associated change in the global carbon cycle, and ecosystem expansion by 740 Ma: Geology, v. 28, p. 619–622.
Knoll, A.H., 1984, Microbiotas of the late Precambrian Hunnberg Formation, Nordaustlandet, Svalbard: Journal of Paleontology, v. 58, 131–162.
Knoll, A.H., 1996, Archean and Proterozoic paleontology, *in* Jansonius, J., and McGregor, D.C., eds., Palynology: Principles and Applications, Volume 1, Dallas, American Association of Stratigraphic Palynologists Foundation, p. 51–80.
Knoll, A.H., 2014, Paleobiological perspectives on early eukaryote evolution: Cold Spring Harbor Perspectives in Biology, v. 6, a016121.
Knoll, A.H., and Calder, S., 1983, Microbiotas of the late Precambrian Ryssö Formation, Nordaustlandet, Svalbard: Palaeontology, v. 26, p. 467–496.
Knoll, A.H., and Swett, K., 1985, Micropalaeontology of the late Proterozoic Veteranen Group, Spitsbergen: Palaeontology, v. 28, p. 451–473.
Knoll, A.H., Swett, K., and Mark, J., 1991, Paleobiology of a Neoproterozoic tidal flat/lagoonal complex: The Draken Conglomerate Formation, Spitsbergen: Journal of Paleontology, v. 65, p. 531–570.
Knoll, A.H., Javaux, E.J., Hewitt, D., and Cohen, P., 2006, Eukaryotic organisms in Proterozoic oceans: Philosophical Transactions of the Royal Society B, v. 361, p. 1023–1038.
Kokinos, J.P., and Anderson, D.M., 1995, Morphological development of resting cysts in cultures of the marine dinoflagellate *Lingulodinium polyedrum* (= *L. machaerophorum*): Palynology, v. 19, p. 143–166.
Leander, B.S., Witek, R.P., and Farmer, M.A., 2001, Trends in the evolution of the euglenid pellicle: Evolution, v. 55, p. 2215–2235.
Lewis, J., and Hallett, R., 1997, *Lingulodinium polyedrum (Gonyaulax polyedra)* a blooming dinoflagellate, *in* Ansell, A.D., Gibson, R.N., and Barnes, M., eds., Oceanography and Marine Biology: An Annual Review, Volume 35, London, UCL Press, p. 97–161.
Lewis, L.A., and McCourt, R.M., 2004, Green algae and the origin of land plants: American Journal of Botany, v. 91, p. 1535–1556.
Li, Z.-X., Evans, D.A.D., and Halverson, G.P., 2013, Neoproterozoic glaciations in a revised global palaeogeography from the breakup of Rodinia to the assembly of Gondwanaland: Sedimentary Geology, v. 294, p. 219–232.
Lindgren, S., 1982, Algal coenobia and leiospheres from the Upper Riphean of the Turukhansk region, eastern Siberia: Stockholm Contributions in Geology, v. 38, p. 35–45.
Logares, R., Bråte, J., Bertilsson, S., Clasen, J.L., Shalchian-Tabrizi, K., and Rengefors, K., 2009, Infrequent marine–freshwater transitions in the microbial world: Trends in Microbiology, v. 17, p. 414–422.
Marchant, H.J., 1977, Cell division and colony formation in the green alga *Coelastrum* (Chlorococcales): Journal of Phycology, v. 13, p. 102–110.
McManus, H.A., and Lewis, L.A., 2011, Molecular phylogenetic relationships in the freshwater family Hydrodictyaceae (Sphaeropleales, Chlorophyceae), with an emphasis on *Pediastrum duplex*: Journal of Phycology, v. 47, p. 152–163.
Mertens, K.N., et al., 2009, Process length variation in cysts of a dinoflagellate, *Lingulodinium machaerophorum*, in surface sediments: Investigating its potential as salinity proxy: Marine Micropaleontology, v. 70, p. 54–69.
Moczydłowska, M., 2010, Life cycle of early Cambrian microalgae from the *Skiagia*-plexus acritarchs: Journal of Paleontology, v. 84, p. 216–230.
Moczydłowska, M., and Willman, S., 2009, Ultrastructure of cell walls in ancient microfossils as a proxy to their biological affinities: Precambrian Research, v. 173, p. 27–38.
Nagovitsin, K., 2009, *Tappania*-bearing association of the Siberian platform: Biodiversity, stratigraphic position and geochronological constraints: Precambrian Research, v. 173, p. 137–145.
Nagy, R.M., and Porter, S.M., 2005, Paleontology of the Neorproterozoic Uinta Mountain Group, *in* Dehler, C.M., Pederson, J.L., Sprinkel, D.A., and Kowallis, B.J., eds., Uinta Mountain Geology: Utah Geological Association Publication 33, p. 49–62.
Nagy, R.M., Porter, S.M., Dehler, C.M., and Shen, Y., 2009, Biotic turnover driven by eutrophication before the Sturtian low-latitude glaciation: Nature Geoscience, v. 2, p. 415–418.
Naumova, S.N., 1949, Spory nizhnego Kembriia [Spores of the lower Cambrian]: Izvestiia Akademii Nauka, Seriia Geologicheskaia [Bulletin of the Academy of Sciences of the USSR, Geologic Series], v. 1949, no. 4, p. 49–56 [in Russian].
Naumova, S.N., 1950, Spory nizhnego Silura [Spores of the lower Silurian): Trudy Konferentsii po Sporovo-Pyltsevomu Analizu, 1948 Goda, Geografischeskii Facultet, Izdatelstvo Moskovskogo Universita [Proceedings from the Conference on Pollen Analysis, 1948], Moscow, Moscow University Press, p. 165–190 [in Russian].
Ogurtsova, R.N., and Sergeev, V.N., 1989, Megasferomorfidy Chichkanskoi svity verkhnego Dokembriia iuzhnogo Kazakhstana [Megaspheromorphids from the upper Precambrian Chichkan Formation, southern Kazakhstan]: Paleontologicheskii Zhurnal [Paleontological Journal], v. 1989, no. 2, p. 119–122 [in Russian].
Pang, K., Tang, Q., Schiffbauer, J.D., Yao, J., Yuan, X., Wan, B., Chen, L., Ou, Z., and Xiao, S., 2013, The nature and origin of nucleus-like intracellular inclusions in Paleoproterozoic eukaryote microfossils: Geobiology, v. 11, p. 499–510.
Peat, C.J., Muir, M.D., Plumb, K.A., McKirdy, D.M., and Norvick, M.S., 1978, Proterozoic microfossils from the Roper Group, Northern Territory, Australia: BMR Journal of Australian Geology & Geophysics, v. 3, p. 1–17.
Peng, Y., Bao, H., and Yuan, X., 2009, New morphological observations for Paleoproterozoic acritarchs from the Chuanlinggou Formation, North China: Precambrian Research, v. 168, p. 223–232.
Popper, Z.A., Michel, G., Hervé, C., Domozych, D.S., Willats, W.G.T., Tuohy, M.G., Kloareg, B., and Stengel, D.B., 2011, Evolution and diversity of plant cell walls: From algae to flowering plants: Annual Review of Plant Biology, v. 62, p. 567–590.
Porter, S.M., 2004, The fossil record of early eukaryotic diversification: Paleontological Society Papers, v. 10, p. 35–50.
Porter, S.M., and Knoll, A.H., 2000, Testate amoebae in the Neoproterozoic Era: Evidence from vase-shaped microfossils in the Chuar Group, Grand Canyon: Paleobiology, v. 26, p. 360–385.
Porter, S.M., Meisterfeld, R., and Knoll, A.H., 2003, Vase-shaped microfossils from the Neoproterozoic Chuar Group, Grand Canyon: A classification guided by modern testate amoebae: Journal of Paleontology, v. 77, p. 409–429.
Porter, S.M., Dehler, C.M., Moore, J.L., Riedman, L.A., and Wang, S.C., 2013, Possible scale-bearing protists in the mid-Neoproterozoic Chuar Group, Grand Canyon, and Uinta Mountain Group, Utah: Geological Society of America Abstracts with Programs, v. 45, p. 693.
Pyatiletov, V.G., 1980, O nakhodkakh mikrofossilii roda N*avifusa* v Lakhandinskoi Svite [On the discovery of microfossils in the genus *Navifusa* in the Lakhanda Formation]: Paleontologicheskii Zhurnal [Paleontological Journal], v. 1980, no. 3, p. 143–145 [in Russian].
Riedman, L.A., and Porter, S.M., 2016, High morphological diversity of organic-walled microfossils from the Neoproterozoic Alinya Formation, Officer Basin, Australia: Journal of Paleontology, p. 854–887.
Riedman, L.A., and Sadler, P.M., 2015, Global species richness record and biostratigraphic potential of early to middle Neoproterozoic eukaryote fossils: Geological Society of America Abstracts with Programs, v. 47, p. 212.
Riedman, L.A., Porter, S.M., Halverson, G.P., Hurtgen, M.T., and Junium, C.K., 2014, Organic-walled microfossil assemblages from glacial and interglacial Neoproterozoic units of Australia and Svalbard: Geology, v. 42, p. 1011–1014.
Samuelsson, J., 1997, Biostratigraphy and palaeobiology of early Neoproterozoic strata of the Kola Peninsula, Northwest Russia: Norsk Geologisk Tidsskrift, v. 77, p. 165–192.
Samuelsson, J., and Butterfield, N.J., 2001, Neoproterozoic fossils from the Franklin Mountains, northwestern Canada: Stratigraphic and paleobiological implications: Precambrian Research, v. 107, p. 235–251.
Samuelsson, J., Dawes, P.R., and Vidal, G., 1999, Organic-walled microfossils from the Proterozoic Thule Supergroup, Northwest Greenland: Precambrian Research, v. 96, p. 1–23.
Schiffbauer, J.D., and Xiao, S., 2009, Novel application of focused ion beam electron microscopy (FIB-EM) in preparation and analysis of microfossil ultrastructures: A new view of complexity in early eukaryotic organisms: Palaios, v. 24, p. 616–626.
Schopf, J.W., 1968, Microflora of the Bitter Springs Formation, late Precambrian, central Australia: Journal of Paleontology, v. 42, p. 651–688.
Schopf, J.W., 1992, Atlas of representative Proterozoic microfossils, *in* Schopf, J.W., and Klein, C., eds., The Proterozoic Biosphere, Cambridge, Cambridge University Press, p. 1057–1117.
Schopf, J.W., Ford, T.D., and Breed, W.J., 1973, Microorganisms from the late Precambrian of the Grand Canyon, Arizona: Science, v. 179, p. 1319–1321.
Semikhatov, M.A., Ovchinnikova, G.V., Gorokhov, I.M., Kuznetsov, A.B., Vasil eva, I.M., Gorokhovskii, B.M., and Podkovyrov, V.N., 2000, Isotope age of the middle-upper Riphean boundary: Pb-Pb geochronology of the Lakhanda Group carbonates, eastern Siberia: Doklady Earth Science, v. 372, p. 625–629.
Sergeev, V.N., 2006, Okremnennye mikrofossilii Dokembriia: Priroda, klassifikatsiia I biostratigraficheskoe znachenie [Precambrian Microfossils in Cherts: Their Paleobiology, Classification, and Biostratigraphic Usefulness], Moscow, Geos, 280 p. [in Russian].
Sergeev, V.N., and Schopf, J.W., 2010, Taxonomy, paleoecology and biostratigraphy of the late Neoproterozoic Chichkan microbiota of South Kazakhstan: The marine biosphere on the eve of metazoan radiation: Journal of Paleontology, v. 84, p. 363–401.
Shields-Zhou, G., Porter, S.M., and Halverson, G.P., 2016, A new rock-based definition for the Cryogenian Period: Episodes, v. 39, p. 3–8.
Simonetti, C., and Fairchild, T.R., 2000, Proterozoic microfossils from subsurface siliciclastic rocks of the São Francisco Craton, south-central Brazil: Precambrian Research, v. 103, p. 1–29.

https://doi.org/10.1017/jpa.2016.57 Published online by Cambridge University Press

Stein, F.V., 1883, Der Organismus der Infusionthiere. III. Abtheilung. II. Hälfte. Die Naturgeschichte der Arthrodelen Flagellaten, Leipzig, Wilhelm Engelmann, 81 p.

Strauss, J.V., Rooney, A.D., Macdonald, F.A., Brandon, A.D., and Knoll, A.H., 2014, 740 Ma vase-shaped microfossils from Yukon, Canada: Implications for Neoproterozoic chronology and biostratigraphy: Geology, v. 42, p. 659–662.

Summons, R.E., Brassell, S.C., Eglinton, G., Evans, E., Horodyski, R.J., Robinson, N., and Ward, D.M., 1988, Distinctive hydrocarbon biomarkers from fossiliferous sediment of the late Proterozoic Walcott Member, Chuar Group, Grand Canyon, Arizona: Geochimica et Cosmochimica Acta, v. 52, p. 2625–2637.

Tang, Q., Pang, K., Xiao, S., Yuan, X., Ou, Z., and Wan, B., 2013, Organic-walled microfossils from the early Neoproterozoic Liulaobei Formation in the Huainan region of North China and their biostratigraphic significance: Precambrian Research, v. 236, p. 157–181.

Tang, Q., Pang, K., Yuan, X., Wan, B., and Xiao, S., 2015, Organic-walled microfossils from the Tonian Gouhou Formation, Huaibei region, North China Craton, and their biostratigraphic implications: Precambrian Research, v. 266, p. 296–318.

Timmons, J.M., Karlstrom, K.E., Dehler, C.M., Geissman, J.W., and Heizler, M.T., 2001, Proterozoic multistage (~1.1 and ~0.8 Ga) extension in the Grand Canyon Supergroup and establishment of northwest and north-south tectonic grains in the southwestern United States: Geological Society of America Bulletin, v. 113, p. 163–180.

Timofeev, B.V., 1959, Drevneishaia flora Pribaltiki i ee stratigraficheskoe znachenie [Ancient flora of the Baltic states and its stratigraphic significance]: Vseoyuznyi Neftyanoi Naucho-Issledovatelskii Geologor-azvedochnyi [Proceedings of the Union Petroleum Research Exploration Institute], Leningrad, VNIGRI, 129, p. 1–136, pl. 1–24 [in Russian].

Timofeev, B.V., 1966, Mikropaleofitologicheskoe Issledovanie Drevnikh Svit [Micropaleophytological research into ancient strata], Moscow, Nauka [USSR Academy of Sciences], 89 pl. 126 p. [in Russian].

Timofeev, B.V., and Hermann, T.N., 1979, Dokembriiskaia mikrobiota Lakhandinskoi svity [Precambrian Microbiota of the Lakhanda Formation], *in* Sokolov, B.S., ed., Paleontologiia Dokembriia i Rannego Kembriia [Paleontology of the Precambrian and early Cambrian], Leningrad, Nauka, p. 137–147 [in Russian].

Timofeev, B.V., Hermann, T.N., and Mikhailova, N.S., 1976, Mikrofitofossilii Dokembriia, Kembriia i Ordovika [Plant Microfossils of the Precambrian, Cambrian, and Ordovician], Leningrad, Scientific Institute of Precambrian Geology and Geochronology, 106 p. [in Russian].

Tippery, N.P., Fučiková, K., Lewis, P.O., and Lewis, L.A., 2012, Probing the monophyly of the Sphaeropleales (Chlorophyceae) using data from five genes: Journal of Phycology, v. 48, p. 1482–1493.

Tynni, R., and Donner, J., 1980, A microfossil and sedimentation study of the late Precambrian formation of Hailuoto, Finland: Geological Survey of Finland, Bulletin 311, 27 p, 8 pl.

Tynni, R., and Uutela, A., 1984, Microfossils from the Precambrian Muhos Formation in Western Finland: Geological Survey of Finland, Bulletin 330, 38 p, 20 pl.

Ventura, G.T., Kenig, F., Grosjean, E., and Summons, R.E., 2005, Biomarker analysis of solvent extractable organic matter from the Neoproterozoic Kwagunt formation, Chuar group (~800–742 Ma), Grand Canyon, 22nd International Meeting on Organic Geochemistry, Volume 2: Seville, p. Abstr. PB 2–19.

Vidal, G., 1976a, Late Precambrian acritarchs from the Eleonore Bay Group and Tillite Group in East Greenland: Grønlands Geologiske Undersøgelse, v. 78, p. 1–19.

Vidal, G., 1976b, Late Precambrian microfossils from the Visingsö Beds in southern Sweden: Fossils and Strata, v. 9, p. 1–57.

Vidal, G., 1979, Acritarchs from the upper Proterozoic and lower Cambrian of East Greenland: Grønlands Geologiske Undersøgelse Bulletin, v. 134, p. 1–55.

Vidal, G., 1981, Micropalaeontology and biostratigraphy of the upper Proterozoic and lower Cambrian sequence in East Finnmark, northern Norway: Norges Geologiske Undersøkelse Bulletin, v. 362, p. 1–53.

Vidal, G., and Ford, T.D., 1985, Microbiotas from the late Proterozoic Chuar Group (Northern Arizona) and Uinta Mountain Group (Utah) and their chronostratigraphic implications: Precambrian Research, v. 28, p. 349–389.

Vidal, G., and Siedlecka, A., 1983, Planktonic, acid-resistant microfossils from the upper Proterozoic strata of the Barents Sea region of Varanger Peninsula, East Finnmark, northern Norway: Norges Geologiske Undersøkelse Bulletin, v. 382, p. 45–79.

Vorob'eva, N.G., Sergeev, V.N., and Knoll, A.H., 2009, Neoproterozoic microfossils from the northeastern margin of the East European platform: Journal of Paleontology, v. 83, p. 161–196.

Vorob'eva, N.G., Sergeev, V.N., and Petrov, P.Yu., 2015, Kotuikan Formation assemblage: A diverse organic-walled microbiota in the Mesoproterozoic Anabar succession, northern Siberia: Precambrian Research, v. 256, p. 201–222.

Walcott, C.D., 1899, Precambrian fossiliferous formations: Geological Society of America Bulletin, v. 10, p. 199–244.

Weil, A.B., Geissman, J.W., and Van der Voo, R., 2004, Paleomagnetism of the Neoproterozoic Chuar Group, Grand Canyon Supergroup, Arizona: Implications for Laurentia's Neoproterozoic APWP and Rodinia breakup: Precambrian Research, v. 129, p. 71–92.

Yin, L., and Guan, B., 1999, Organic-walled microfossils of Neoproterozoic Dongjia Formation, Lushan County, Henan Province, North China: Precambrian Research, v. 94, p. 121–137.

Yin, L., and Sun, W., 1994, Microbiota from the Neoproterozoic Liulaobei Formation in the Huainan region, northern Anhui, China: Precambrian Research, v. 65, p. 95–114.

Zang, W.L., 1995, Early Neoproterozoic sequence stratigraphy and acritarch biostratigraphy, eastern Officer Basin, South Australia: Precambrian Research, v. 74, p. 119–175.

Zang, W.L., and Walter, M.R., 1992a, Late Proterozoic and Cambrian microfossils and biostratigraphy, Amadeus Basin, central Australia: Memoirs of the Association of Australasian Palaeontologists, v. 12, p. 1–132.

Zang, W.L., and Walter, M.R., 1992b, Late Proterozoic and early Cambrian microfossils and biostratigraphy, northern Anhui and Jiangsu, central-eastern China: Precambrian Research, v. 57, p. 243–323.

Zhang, Y., 1988, Proterozoic stromatolitic micro-organisms from Hebei, North China: Cell preservation and cell division: Precambrian Research, v. 38, p. 165–175.

Accepted 20 November 2015